

# DESIGN OF A BENCHTOP NMR/MRI SYSTEM

Daniel Fonseca

Bachelor of Engineering and a Degree of Bachelors of Business Administration  
Electronics Engineering Major



Department of Electronic Engineering  
Macquarie University

June 6, 2016

Supervisor: Dr. Yves De Deene



## **ACKNOWLEDGMENTS**

I sincerely would like to thank my supervisor Dr. Yves De Deene for his patience, understanding and guidance throughout my thesis at Macquarie University. I appreciate his vast knowledge within the area of medical imaging and giving me the opportunity to work on such an exciting project.

I would also like to thank my parents for their support throughout my time at University. Without your constant care and understanding, this thesis would not have been possible.



## STATEMENT OF CANDIDATE

I, Daniel Fonseca, declare that this report, submitted as part of the requirement for the award of Bachelor of Engineering in the Department of Electronic Engineering, Macquarie University, is entirely my own work unless otherwise referenced or acknowledged. This document has not been submitted for qualification or assessment at any academic institution.

Student's Name: Daniel Fonseca

Student's Signature: D. Fonseca

Date: 6th June 2016



## ABSTRACT

Nuclear Magnetic Resonance (NMR) provides us with ways to look at objects in a very intricate and detailed manner. A major advantage of these systems is their non-destructive nature and them not requiring any contact with the samples. Current systems are quite often exorbitant and complex in nature, making them unfeasible for teaching and research purposes. There has been a demand for low-cost systems making its application possibilities endless. With the advances in the consumer electronics industry, products such as the PC MRI solution by Spincore Technologies, discussed as part of this project, provide great alternatives.

The ultimate goal of the project was to deliver a design that would bring together different elements to create a benchtop NMR system. An NMR probe has been developed to function within an existing Halbach magnet array which is used to transmit an excitation pulse and also receive the NMR signal. The remaining elements make use of commercially available products and where required programmed using MATLAB. Utilising the Spincore MRI system reduced the need for additional equipment and can be expanded to incorporate gradient magnetic field coils.



# Contents

<b>Acknowledgments</b>	<b>iii</b>
<b>Abstract</b>	<b>vii</b>
<b>Table of Contents</b>	<b>ix</b>
<b>List of Figures</b>	<b>xi</b>
<b>List of Tables</b>	<b>xiii</b>
<b>1 Introduction</b>	<b>1</b>
1.1 Project Overview . . . . .	2
1.1.1 Project Objectives . . . . .	2
1.1.2 Document Overview . . . . .	3
1.1.3 Time Budget Review . . . . .	3
1.1.4 Financial Budget Review . . . . .	4
<b>2 Background and Related Work</b>	<b>5</b>
2.1 Principles of NMR/MRI . . . . .	5
2.1.1 A Protons Magnetic Field . . . . .	5
2.1.2 RF Pulse . . . . .	6
2.1.3 Signal to Noise Ratio . . . . .	7
2.1.4 Halbach Magnet . . . . .	7
2.1.5 Helmholtz coils . . . . .	8
2.1.6 Resonant Coil (LC circuit) . . . . .	9
<b>3 Literature Review</b>	<b>11</b>
3.1 Magnet Design . . . . .	11
3.2 Probe Circuit Designs . . . . .	12
3.3 Additional Hardware . . . . .	12
3.4 Software . . . . .	14
3.5 One-sided Access . . . . .	14

<b>4</b>	<b>Calculations</b>	<b>17</b>
4.1	Magnetic field strength of Halbach Magnet . . . . .	17
4.2	Larmor's Frequency . . . . .	17
4.3	Pulse Width . . . . .	18
4.4	NMR Probe Design . . . . .	18
4.4.1	Probe Magnetic Field Strength . . . . .	18
4.4.2	Required current . . . . .	19
4.4.3	Inductance of coil . . . . .	19
4.4.4	Resistance and Q factor of coil . . . . .	19
4.4.5	Skin Depth . . . . .	19
4.4.6	Wire Resistance . . . . .	20
4.4.7	Section of thin sheet current . . . . .	20
4.4.8	Resistance of Coil . . . . .	20
4.4.9	Tuning Capacitance . . . . .	20
4.4.10	Matching Capacitance . . . . .	21
4.4.11	Required transmitter power . . . . .	21
4.4.12	Peak Voltage across the Coil . . . . .	22
4.4.13	Power dissipated through inductor . . . . .	22
4.5	Power amplifier . . . . .	22
4.5.1	Output peak voltage . . . . .	22
4.5.2	Amplifier Input Voltage . . . . .	22
4.6	Preamplifier . . . . .	23
4.7	Chapter Summary . . . . .	24
<b>5</b>	<b>Experimental Results</b>	<b>25</b>
5.1	Introduction . . . . .	25
5.2	External Halbach Magnet . . . . .	26
5.3	NMR Probe . . . . .	28
5.3.1	LC Resonant Circuit . . . . .	28
5.3.2	Coil . . . . .	29
5.3.3	Q-factor . . . . .	30
5.3.4	Impedance Matching . . . . .	31
5.3.5	Tuning and Matching Capacitors . . . . .	31
5.3.6	Construction and Testing . . . . .	32
5.3.7	Power Requirements . . . . .	35
5.4	Transmit/Receive System . . . . .	35
5.4.1	Spincore RadioProcessor G . . . . .	35
5.4.2	Utilising the Board . . . . .	36
5.4.3	Pulse Duration . . . . .	37
5.4.4	Acquisition Time . . . . .	38
5.4.5	Number of Points . . . . .	38
5.4.6	Spectral Width . . . . .	39
5.4.7	Power . . . . .	39

---

5.5	Amplification Stages . . . . .	41
5.5.1	Transmit Power Amplifier . . . . .	41
5.5.2	Receive Preamplifier . . . . .	41
5.6	Passive Transmit/Receive Switch . . . . .	44
5.6.1	Crossed Diodes . . . . .	45
5.6.2	$\lambda/4$ wavelength cable . . . . .	45
5.6.3	How it functions . . . . .	46
<b>6</b>	<b>Conclusions and Future Work</b>	<b>47</b>
6.1	Ideal Design . . . . .	47
6.2	Conclusions . . . . .	50
<b>7</b>	<b>Abbreviations</b>	<b>53</b>
<b>A</b>	<b>Circuit Analysis</b>	<b>55</b>
A.1	LC Resonant Circuit Analysis . . . . .	55
<b>B</b>	<b>Hallbach Magnetic field table</b>	<b>57</b>
<b>C</b>	<b>Project Deliverables</b>	<b>63</b>
C.1	Thesis Preparation Report . . . . .	63
C.2	Meeting Records . . . . .	69
<b>D</b>	<b>Datasheets</b>	<b>71</b>
D.1	Honeywell Hall Sensor . . . . .	71
D.2	RadioProcessor G Specifications . . . . .	73
D.3	Ophir Power Amplifier Specifications . . . . .	75
D.4	Linear Technologies 626810f Operational Amplifier Datasheet . . . . .	77
	<b>Bibliography</b>	<b>100</b>



# List of Figures

2.1	Protons with and without and external Magnetic field [8]	6
2.2	Protons precessing in phase after applying an RF pulse [22]	6
2.3	Halbach Magnet [9]	7
2.4	Halbach Magnet placement [7]	8
2.5	Helmholtz coil pair [6]	8
2.6	Ideal Resonant Circuit [2]	9
3.1	H-shape permanent magnet design [11]	11
3.2	Typical Probe Circuit [17]	12
3.3	H-shape permanent magnet design [17]	13
3.4	One-sided magnet arrangement [14]	15
3.5	Figure 8 coil [14]	15
5.1	Hall Sensor	26
5.2	Halbach Magnet	27
5.3	Parallel Resonant Circuit	28
5.4	Halbach Magnet	29
5.5	Skin and Proximity effects on electrons	30
5.6	NMR Probe Circuit	31
5.7	Initial NMR Probe	33
5.8	Final NMR Probe	34
5.9	Spectrum Analyser Magnitude readout	34
5.10	Impedance readout	35
5.11	RadioProcessor PC Card [24]	36
5.12	Initial RadioProcessor Output	40
5.13	RadioProcessor Voltage Output	40
5.14	Ophir Amplifier [3]	41
5.15	Bandpass Filter Design	44
5.16	Passive Switch Circuit	45
6.1	Helmholz Coil Design	48



# List of Tables

1.1	Time Budget Review . . . . .	4
4.1	Time Budget Review . . . . .	23
5.1	Parameters within the program [24] . . . . .	37
5.2	Initial test Parameters . . . . .	39
6.1	Helmholtz Coil Probe Parameters . . . . .	49



# Chapter 1

## Introduction

Nuclear Magnetic Resonance (NMR) is a technique that is implemented in many industries and has numerous applications. It is a process wherein the nucleus of certain elements can absorb and emit electromagnetic radiation. A specific radio frequency is utilised in order to transmit the energy to the nuclei within a strong magnetic field. Uses include the identifying of structures and the kinetic studies of proteins, lipids and carbohydrates. It is also used to aid in the exploration of petroleum and gas where the rock needs to be analysed for fluids and porosity.

Since the 1950s, NMR has been the term used to describe the process. As time progressed and NMR imaging methods were being used for medical purposes, patients became concerned with the term nuclear. There were misconceptions around NMR with patients associating it with nuclear radioactivity and nuclear energy. [18] Over time, the word nuclear was removed and Magnetic Resonance Imaging was favored.

Magnetic Resonance Imaging systems use the same technique as NMR and is used on a regular basis for the study of animals, plants and humans. Systems that are currently employed within the medical industry cost millions of dollars and create images of many different parts of the human body to aid in the detection of possible abnormalities. The latest MRI scanners use strong magnetic fields, radio, gradient and shimming coils to develop an image. These systems provide high quality images and create images in relatively little time.

Unfortunately it is not possible to use these kind of systems for research purposes as they are quite large and expensive. There have been many groups that have created smaller and more inexpensive units for laboratory and teaching purposes. With using smaller systems, comes with an obvious trade-off where the images received will not be as detailed and the imaging size will be significantly smaller.

There has been a need for NMR systems which can be placed on surfaces, where the article to be imaged does not have to go through a specified space. This creates a limitation on the article size and reduces the number of applications on which NMR imaging techniques can be used.

## 1.1 Project Overview

The project first starts of by examining the existing Halbach magnet that is available. Using a hall sensor, the variation in magnetic field is measured and mapped out. The area where we expect to place the sample is of key importance as the variation in field strength must be known. From this field strength, the precessional frequency is calculated for hydrogen.

A probe is then designed and constructed with a coil that has a diameter of 1cm. This allows for a test tube with a sample to be placed within it. A tuning capacitor was used to tune the coil to the precessional frequency and a matching capacitor to ensure the probe circuit has an impedance of  $50\Omega$ . Although the tuning and matching capacitors were calculated, during construction it was found that the real values were different when testing it with a spectrum analyser.

The idea of the probe was for it to be connected to the Spincore RadioProcessor excitation and acquisition system which is controlled by a computer. The computer had multiple MATLAB GUIs that were available and MS DOS programs that could be run. Within the MS DOS program, parameters such as frequency, pulse duration and output power can be controlled. The outputs were observed on an oscilloscope. It was important to see that the output voltage amplitude can be varied due the power amplifier being used as part of the design.

It was calculated that approximately 6W of power needed to be delivered to the probe. This required the use of a powerful amplifier that can amplify the output from the RadioProcessor. The Ophir power amplifier available in the lab was incorporated as part of the design. The amplifier had a minimum gain of 50dB which meant that the input needed to be varied in order to receive our output.

A passive switch was investigated. A switch is required as there is only one line going to and from the probe. A transmitter and receiver both need to be connected to it but not at the same time. While the transmit pulses are being delivered, the preamplifier needs to be decoupled from the circuit. If the powerful transmit pulses enter the preamplifier stage, it could be destroyed. Also, when the probe receives a signal, it needs to be routed to the preamplifier input and not to the power amplifier output.

### 1.1.1 Project Objectives

- Understand why magnetic resonance imaging is used.
- Understand and research electromagnetism and other required knowledge needed to complete the project.
- Research further into benchtop NMR/MRI Systems.
- Look into the information on electronics required in relation to AC current, amplifiers, filters.

- Identify the equipment that is currently available and may need to be used in the lab.
- Develop an appropriate resonant coil.
- Carry out necessary calculations to design a transmit/receive system.
- Incorporate an existing power amplifier into the design.
- Research a preamplifier for the receive stage.
- Design an appropriate switch.

### 1.1.2 Document Overview

This section provides an introduction to the project and the objectives hoped to be achieved. A plan for the project, in the form of a Gantt chart can be found in Appendix C.1. The supervisor for the project is Dr. Yves De Deene, a Biomedical Engineering lecturer within the Department of Engineering. There have been regular meetings with the supervisor over the course of the project to ensure that the project remains on track, dates of which can also be found in Appendix C.2.

Chapter 2 provides background information on topics related to the project such how an external magnetic field and a RF pulse affect protons, the Halbach magnet array, Helmholtz coil configuration and resonant coils.

A literature review is conducted in the following chapter. Different designs are looked at based on what has been done through research in the past. This section is separated into sections based on previous magnet designs, Probe Circuit Designs, the hardware that has been implemented and if software was used. Another area that is also examined are systems that have one sided access.

Chapter 4 goes through the calculations step by step in order to look at how different components were chosen.

Chapter 5 justifies the design chosen in a qualitative manner and how the system was constructed. It also considers other approaches that could have been used to solve the problem.

Chapter 6 covers how the system was tested, the results it produced and where it worked as expected. The final chapter provides a conclusion and other potential work that could be carried out in the future.

### 1.1.3 Time Budget Review

Table 4.1 summarizes the time spent conducting the project. It also provides a percentage of its total completion. Specific time was allotted to certain activities which were followed as closely as possible. Some of the activities required extra time which was unforeseen. Due to this, the project was not completed as expected.

Estimated Work	84 days
Realised Work	98 days
Percentage Completion	80%

**Table 1.1:** Time Budget Review

#### 1.1.4 Financial Budget Review

The project was initially allocated a budget of \$300. The project did not require any purchases to be made. The components required were already available in the lab. If a specific component was not available, multiple components were put together to achieve the desired value. The additional elements required such as the external magnet and the excitation/receive system, was also readily available in the lab. MATLAB was also required, but the computer being used had a copy installed on it. Therefore, no further purchasing was done.

# Chapter 2

## Background and Related Work

### 2.1 Principles of NMR/MRI

There are many elements that can be used to conduct NMR, but hydrogen is chosen specifically due to its number of protons within the nucleus. Elements such as Oxygen16 and Carbon12 have an even number of protons and neutrons, hence no magnetic spin and no way of exciting the spin system. Whereas Hydrogen and Carbon13 do possess a spin and at the same time is naturally occurring. Carbon13 is usually found in cellulose in small amounts and hydrogen exists in plenty within the human body as the human body is around 70% water.

#### 2.1.1 A Protons Magnetic Field

Quite often we look at exciting a spin system of an element with an odd number of protons and neutrons in the nucleus, such as hydrogen. The proton within hydrogen is a positive electrical charge that is constantly moving, possessing a spin. It is essentially an electrical charge that is constantly moving, therefore inducing a magnetic field. Each proton can be observed such that it is a magnet with its own North and South Pole. Without any external magnetic field, they all face in different directions, cancelling out each other with a net magnetic field of 0. When an external magnetic field is applied to the protons, slightly more than half the protons line up in the direction of the external field and the remainder in the opposite direction. [10] Consequently, the net magnetic force is in the direction of the magnetic field, with it increasing exponentially over time.

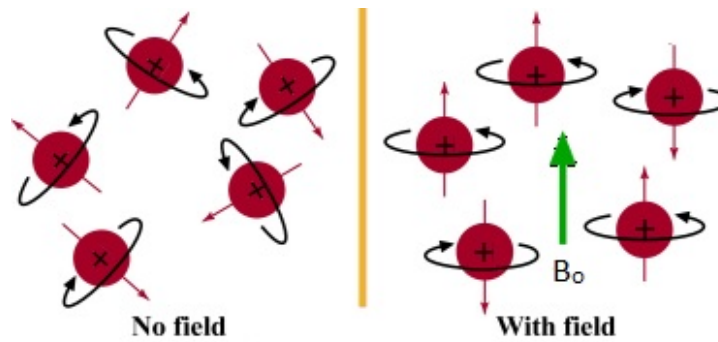


**Figure 2.1:** Protons with and without and external Magnetic field [8]

### 2.1.2 RF Pulse

We know that the protons spin at a certain frequency and this depends on the environment that they are in, known as its precession frequency. This concept can be demonstrated through Larmors Frequency which relates the precession frequency to the strength of the external magnetic field that the protons are in. The stronger the magnetic field, the higher the precession frequency.

Given the precession frequency, it is possible for a radio frequency pulse to exchange energy with the protons, that is if they both have the same frequency. Previously to the RF pulse, the protons precess randomly within the external magnetic field. Once applied, they all precess in the same direction at the same time, therefore moving in sync. The net magnetic vectors of the individual protons add up to form a transversal magnetic vector which moves in phase with the precessing protons.



**Figure 2.2:** Protons precessing in phase after applying an RF pulse [22]

The RF pulse once applied, is quickly switched off, causing the protons to go back to its original state, with a net magnetic vector in the longitudinal direction. As it is going back to its original state, the net magnetic vector of the proton performs a spiral motion as the transversal component of the vector decreases. This changing magnetic force induces an electrical current, which is the signal received.

### 2.1.3 Signal to Noise Ratio

It is very challenging to detect a signal from the proton because it is an issue of signal to noise ratio. Signal-to-noise ratio (abbreviated to SNR) is a measure that compares the level of a desired signal to the level of background noise. It is defined as the ratio of signal power to the noise power, often expressed in decibels.

There is noise from all the other electronics that detect the signal on one hand, and from the preamplifier as well. A relatively low voltage is induced in those coils, so if there is any noise, it could be hidden within it. What it comes down to is that a frequency filter needs to be added in order to get rid of the noise. An active filter may be used with a chosen input voltage. This filter can help reduce the noise more efficiently. Depending on how large the voltage that is to be detected in terms of the noise, needs to be looked at more quantitatively. Calculations can be done to find out how much voltage can be induced in these coils and then test measurements need to be carried out to compare as such.

Natural occurrence is an issue as well as its sensitivity. The signal comes from the nucleus of the atom, from the proton which have a magnetic dipole. When it comes to the human body, there are plenty of hydrogen atoms, some of which align with the magnetic field. Usually around 1/100000 that will be preferentially aligned when placed in a strong magnetic field of around 3T. With a lower field strength of say 0.3T, possibly what will be expected during the project, only about 1/1,000,000 will actually be aligned. This is due to all the other protons counteracting each other therefore making the signal extremely small.

### 2.1.4 Halbach Magnet

Permanent magnets placed in the form of a Halbach array allows the magnetic field on one side to be stronger, while the field on the other side is close to zero. With one magnet, the magnetic field on each side is equal. In our case, the magnets are placed in a cylinder where the magnetic field remains homogeneous on the inside and almost zero on the outside.

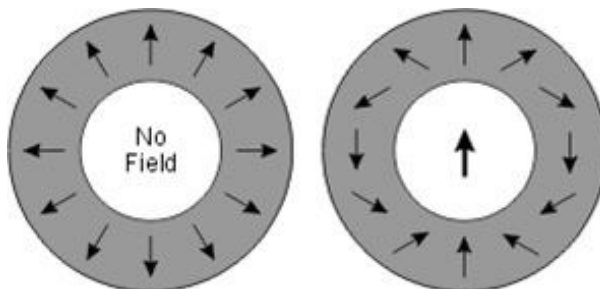


Figure 2.3: Halbach Magnet [9]

An ideal Halbach magnet utilises bar magnets with equal magnetic fields that are positioned so that its centre has the same distance from the origin as the other magnets.

The angle at which the magnet is placed is calculated using the equation  $\gamma = 2\beta$ . The number of magnets used affects how homogeneous the field is, with more magnets also resulting in a stronger field. Other benefits include the fact that it is fairly cheap to produce and quite compact in nature.

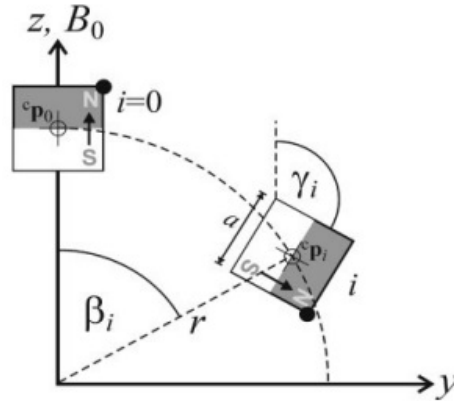


Figure 2.4: Halbach Magnet placement [7]

### 2.1.5 Helmholtz coils

A Helmholtz coil is a pair of coils that are placed parallel to each other. This phenomena was discovered by a German physicist by the name of Hermann von Helmholtz. The distance at which the coils are placed apart is the same as both the coils radius. The idea is that an area of nearly uniform magnetic field is produced at the centre along the x-axis. Two factors that are proportional to the intensity of the magnetic field produced are the number of turns of each coil and the current through both the coils, both of which must be equivalent. In order to actually determine the magnetic field homogeneity, requires the use of elliptical integral calculus.

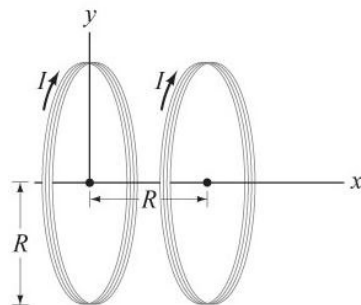
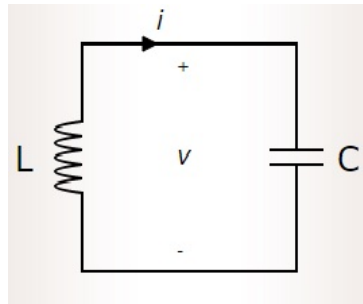


Figure 2.5: Helmholtz coil pair [6]

### 2.1.6 Resonant Coil (LC circuit)

A resonant coil is where an inductor and capacitor are placed in parallel with no resistors. The capacitor has an initial charge which is stored in its electric field. As it discharges, current flows through the inductor, which is changing, causing the inductor to induce a magnetic field. Once fully discharged, the capacitor cannot supply anymore energy. All the energy is now stored within the inductors magnetic field. As the inductor is discharging, the strength of the magnetic field decreases, at that moment, there is a changing magnetic field yet again. The inductor releases its energy by inducing a current through the circuit onto the other side of the capacitor, charging the capacitor again. Assuming both the components are ideal, the charge will flow back and forth between the 2 components. The frequency at which the circuit resonant can be found by using the formula  $\omega = \sqrt{\frac{1}{LC}}$



**Figure 2.6:** Ideal Resonant Circuit [2]



# Chapter 3

## Literature Review

### 3.1 Magnet Design

Depending on the way the magnet is to be used affects the design of the magnet. A majority of designs involve two permanent magnets that are placed opposite each other, such as the one by Shen et al. [11] The design is known as an H-shape design, with a magnetic field of  $0.3T$ . These magnets provide a large homogeneous field area of about  $2100cm^3$  and a gap of  $22cm$  between the magnets. Creating a homogeneous field using this design is probably one of the easiest as it only requires 2 large permanent magnets. Due to their low cost these designs are great for research purposes or for use in labs. As mentioned by Sahakian et al.. [21] although the magnets used provide a high magnetic field strength, the section that is actually uniform is quite weak. In their case, two  $0.6T$  magnets 1 inch thick and 5 inches in diameter only had a uniform field the size of  $1cm^3$  with a field strength of  $0.08T$ .

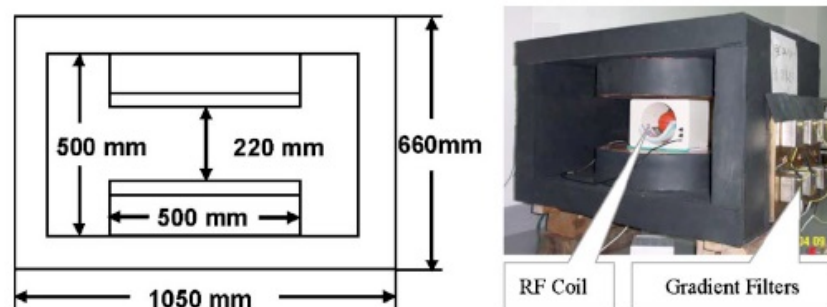
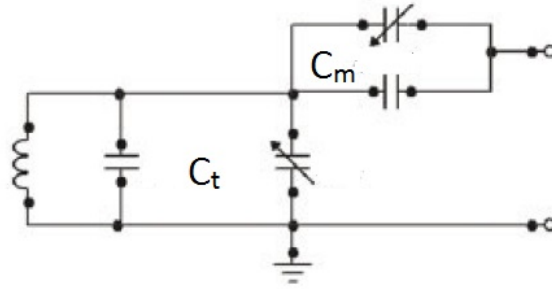


Figure 3.1: H-shape permanent magnet design [11]

Another design that was prevalent was that of the Halbach Magnet system. Moresi and Magin [17] put together 8 cylindrical magnets in an aluminium frame to form a Halbach array. The magnets had to be carefully inserted into the frame without it breaking and were then screwed in place. They were able to achieve a uniform field within a  $3x3x5mm$  area with a field strength of  $0.596T$ .

## 3.2 Probe Circuit Designs

Shen et al. [11] made use of a single coil with many loops and also a copper film coil that had 4 loops. Different coils were used due to the nature of the objects to be imaged having various sizes. The copper film coil was tuned and matched with capacitors, each in parallel with a variable capacitor. A plexiglass skeleton in the shape of a tube with a diameter of 15cm helped in keeping the copper film in place.



**Figure 3.2:** Typical Probe Circuit [17]

A different coil was used by Moresi in that they chose to wrap a wire around a glass tube with a diameter of 4mm and a length of 5mm. The coil was tuned and matched in the same way as Shen [11] by utilising variable capacitors in parallel with set values of tuning and matching capacitors. They ensured that the capacitors were soldered as close as possible to the coil and no gradient or shimming coils were used. The sample was placed within the tube on which the coil was wrapped around.

Billeter [5] made a good point of ensuring that the quality factor of the coil is high enough. It needs to be taken into consideration when designing a coil as it allows for a more reasonable SNR value. It can be calculated using the following formula:

$$Q = \frac{\omega L}{R} = \frac{2\pi f L}{R} \quad (3.1)$$

This also meant the inductance of the coil needed to be high enough.

$$Q = \frac{n^2 a^2}{23a + 25b} \quad (3.2)$$

Where  $a$  is the coil diameter in cm,  $b$  is the length of the coil in cm and  $n$  the number of turns.

## 3.3 Additional Hardware

The spectrometer requires the use of a pulse generator, rf waveform generator, a digital receiver and a gradient waveform generator. The one used by Shen et al. had 16 independent channels which were used to control the rf signal applied, how the acquisition will

be triggered and the way the rf signal is switched. A table of events was set up on the computer with an FPGA chip reading each element and then outputting the necessary pulse. On the analogue side, the transmit system consisted of a class A amplifier of which the signal was fed into a transmit /receive switch.

Kirsch [12] on the other hand utilised a slightly different set-up without the use of a computer. An oscillator sent an RF sinewave to a power splitter which allowed the impedances to remain matched. One side of the power splitter was connected to the RF port of a Double balance mixer and the other connected to a phase detector so that it can be used as a reference signal. A current controlled switch was connected in series with the power amplifier. The pulse generator utilises five NE555N timer chips which have a manual and repeated mode. Potentiometers connected to the chips controlled the widths of the pulses. An amplifier was required at the receive stage as the signal received was usually in the order of  $-100dBm$  before the signal could be seen on the oscilloscope.

The excitation and detection system that was designed by Moresi [17] (seen in Fig. 3.4) was similar to Kirschs. The signal generator generates a signal that is at the Larmor frequency which is then modulated by a pulse generator. A switch and Schottky diodes are used to keep the transmit signal from entering the receive amplifier. The signal received is amplified and then passed through a filter before entering an acquisition card. The signal processing was carried out by a PCI conversion card manufactured by Labview. A fairly wide pulse width was used of about  $20\mu s$  with a power of  $1dBm$ . To detect the signal required a  $20ms$  acquisition time where 500 averages were plotted.

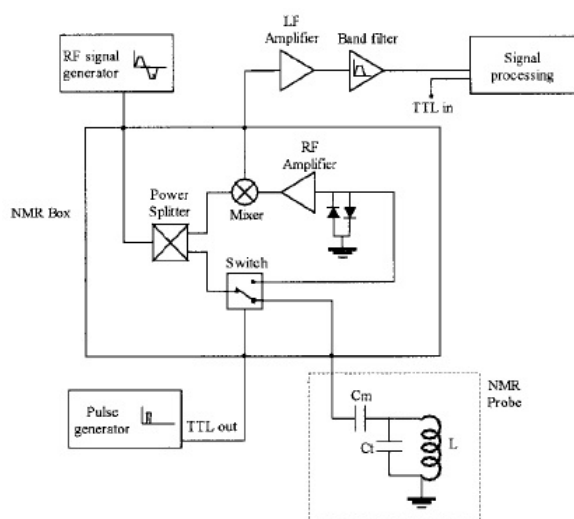


**Figure 3.3:** H-shape permanent magnet design [17]

A team at Northwestern University (Billeter [5]) made use of a 16-bit Texas Instruments ultra-low power Microprocessor which is responsible for the pulse generation and A/D conversion of the receive signal. This meant the use of C++ was required to program it. For someone with a background in programming or with knowledge would have lot less of an issue implementing a similar design to this. Two amplifiers were placed in

series with the first one raising the signal to 1W and then the second one to 10W. An amplifier with a 50dB gain and a noise figure of 3.5dB was used which seems sensible when considering the signal to noise ratio.

### 3.4 Software

WinMRI was a type of software used that was developed in-house by Shen et al [11] which consisted of an operating command, a graphical pulse sequence editor, parameter editor and a 1D/2D display. MRI pulse sequences are set individually as events by the user. The display window provides a 1D view in real time of the signal during acquisition. After the signal had been acquired, the data can be viewed in 2D. There was no mention of the type of software used in the Moresi system but it is assumed that one would be required in order to use the LabVIEW A/D conversion card. Wright [25] also discusses the use of LabVIEW as being the software that controlled their system. The user would input parameters such as number of averages, number of samples and how often the pulse is emitted. The software then displayed the pulse and any echoes that may have followed which the user can then analyse.

Also mentioned below, Billeter [5] and team used C++ to control their RF pulse processor. MATLAB was used in conjunction with the C++ code required for the processor, which was able to send timing parameters to the processor and process the signal received.

### 3.5 One-sided Access

Portable NMR systems that have one sided access have a different set of applications that are not normally possible with standard NMR systems. This particular design has many additional uses such as where it may be important to measure moisture content in samples that cannot be moved or large samples of liquids. The system can be placed on top of the sample rather than the sample having to fit in between magnets.

One successful group in this area was Manz [14] and his team who successfully designed a complete one-sided NMR sensor. Their magnet design is based on 8 cylindrical magnets and a disc magnet which are positioned in such a way that the magnetic field in the middle is uniform FIGURE. The magnets are spaced equally and are all tilted at the same angle. Adjusting the angle affects the magnetic field homogeneity and its position.

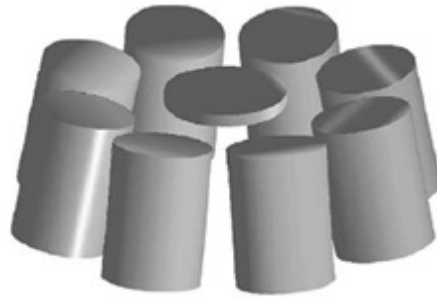


**Figure 3.4:** One-sided magnet arrangement [14]

The magnetic field produced by the magnets is orthogonal to its surface. The coils that have been designed, needed to create a magnetic field parallel to the surface. This was achieved using a figure 8 coil where 2 separate coils of wires of a certain length are separated by a distance  $d$ . When calculating the length and distance, there needed to be a compromise between the required field strength and the uniformity of the field. This is something that may need to be considered when carrying out the design of the transmit/receive coils within the project. If the number of turns are increased, so can the sensitivity of the coil.

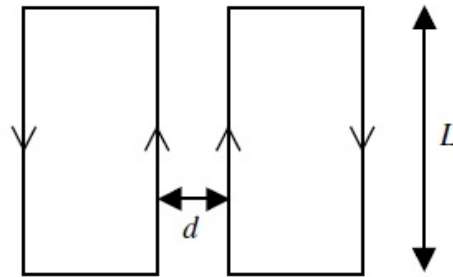


**Figure 3.5:** Figure 8 coil [14]

To reduce dielectric coupling and improve sensitivity, the coil was placed in a circuit with tuning capacitors of equal size on both sides [14]. The tuning and matching capacitors determine the resonance frequency ( $\nu_0$ ) of the circuit, bandwidth ( $V$ ) and quality factor ( $Q = \nu_0 / V$ ) which can be used to work out the Signal to Noise Ratio.



# Chapter 4

## Calculations

### 4.1 Magnetic field strength of Halbach Magnet

Given the output voltage of 6.4928V, the magnetic field strength could be calculated as follows:

$$V_{out} - V_{in} = V_{diff}$$
$$6.4928 - 4 = 2.4928V$$

Given that  $1mV = 1G$

$$2.4928V = 2492G$$

Given that  $1G = 0.01T$

$$2470G = 0.24928T$$

### 4.2 Larmor's Frequency

In order to find the frequency of the rf pulse that is to be applied to the protons, the precessional frequency of the protons within the external magnetic field needs to be observed. The calculation is:

$$f = \gamma B_o \quad (4.1)$$

Where  $f$  is the precession frequency,  $\gamma$  is the gyromagnetic ratio and  $B_o$  is the strength of the external magnetic field in Tesla.

Given that the gyromagnetic ratio of Hydrogen is  $42.5MHz$  and the strength of the magnetic field is  $0.24928T$ :

$$= 42.5 \times 0.24928T$$
$$= 10.5944MHz$$

The resonant frequency is  $10.5944MHz$ , when converted to angular frequency:

$$\begin{aligned}
 \omega &= 2\pi f \\
 &= 2 \times \pi \times 10.5944 \times 10^6 \\
 &= 66566578.42
 \end{aligned}$$

### 4.3 Pulse Width

For the purposes of this experiment a pulse width of  $9.43\mu s$  was chosen. We see that this would be an appropriate choice as it accounts for the variation in magnetic field within the coil. If the pulse width was unknown and was required to be calculated, the following would be done in reverse.

$$\begin{aligned}
 PW &= \frac{1}{BW} \\
 BW &= 10.5944 \times 10^6 \times 1\% \\
 BW &= 105944Hz \\
 PW &= \frac{1}{105944} \\
 PW &= 9.4389\mu s
 \end{aligned}$$

## 4.4 NMR Probe Design

### 4.4.1 Probe Magnetic Field Strength

The following equation is used to calculate the probe magnetic field strength:

$$\theta = \gamma \times B_1 \times t \quad (4.2)$$

Where  $\gamma$  is the gyromagnetic ration of hydrogen in radians,  $B_1$  is the magnetic field required to be produced by the coil and  $t$  being the duration of the pulse. If the pulse-width had a duration of  $9.4389\mu s$ , the magnetic field would be:

$$\begin{aligned}
 B_1 &= \frac{\theta}{\gamma t} \\
 &= \frac{0.5\pi}{267035375.6 \times 9.4389 \times 10^{-6}} \\
 &= 0.6232mT
 \end{aligned}$$

### 4.4.2 Required current

As there is already a requirement for the magnetic field strength to be produced by the coil and limitations on its size, the current required can therefore be calculated using:

$$B = \frac{\mu_o n I}{L} \quad (4.3)$$

$$I = \frac{BL}{\mu_o n}$$

where  $B$  is the magnetic field induced within the coil,  $\mu_o$  is the permeability constant,  $I$  is the current through the coil and  $n$  is the number of turns. The size of the coil was specified to be 1cm in diameter with the wire having a thickness of 1mm.

$$I = \frac{0.6232mT \times 0.01}{4\pi \times 10^{-7} \times 10}$$

$$= 0.4959A$$

### 4.4.3 Inductance of coil

The inductance of the coil can be calculated as:

$$L = \left( \frac{\mu_o n^2 A}{l} \right) \quad (4.4)$$

$L$  is the coil inductance,  $\mu_o$  is the permeability of free space,  $l$  is the length of the coil and  $A$  is the area of the coil.

$$L = \left( \frac{4\pi \times 10^{-6} \times 10^2 \times 0.00007853981}{0.01} \right)$$

$$= 0.987\mu H$$

### 4.4.4 Resistance and Q factor of coil

In order to calculate the resistance of the coil, skin effects need to be taken under consideration. The following 3 equations are used and amalgamated to calculate the resistance.

### 4.4.5 Skin Depth

$$\delta = \sqrt{\frac{2\rho}{\mu\omega_o}} \quad (4.5)$$

where  $\rho$  is the resistivity of copper,  $\mu$  is the permeability and  $\omega$  is the angular frequency.

#### 4.4.6 Wire Resistance

$$r = \rho \frac{l_w}{\sigma} \quad (4.6)$$

where  $l_w$  is the length of straight isolated conductor,  $\rho$  is the resistivity of copper and  $\sigma$  is the section of thin sheet current.

#### 4.4.7 Section of thin sheet current

$$\sigma = \pi \phi \delta \quad (4.7)$$

where  $\phi$  is the diameter of the wire used for the coil and  $\delta$  is the skin depth.

#### 4.4.8 Resistance of Coil

$$r = \rho \frac{nd_m}{\phi \delta} \quad (4.8)$$

$$\begin{aligned} r &= \frac{1.7 \times 10^{-8} \times 10 \times 0.01}{0.001 \times 20.25 \times 10^{-6}} \\ &= 0.0839 \text{ Ohm} \end{aligned}$$

#### 4.4.9 Tuning Capacitance

In order to create a resonant circuit, an appropriate tuning capacitor is to be placed in parallel with the inductor. It is calculated using:

$$C_t w_s = \frac{Q \pm A}{B} \quad (4.9)$$

$$r = \frac{\omega_s L}{Q_L} \quad (4.10)$$

$$Q_L = \frac{\omega_s L}{r}$$

$$\begin{aligned} Q_L &= \frac{66566578.42 \times 1.3 \mu H}{0.0839} \\ &= 1030.995 \end{aligned}$$

$$B = r(1 + Q^2) \quad (4.11)$$

$$\begin{aligned} B &= 0.0839(1 + 1030.995) \\ &= 89218.823 \end{aligned}$$

$$A = \sqrt{\frac{B}{Z_o} - 1} \quad (4.12)$$

$$\begin{aligned} A &= \frac{89218.823}{50\Omega} - 1 \\ &= 42.23 \end{aligned}$$

$$C_t = \frac{Q - A}{B\omega_s} \quad (4.13)$$

$$\begin{aligned} C_t &= \frac{1030.995 - 42.23}{89218.823 \times 66566578.42} \\ &= 1.665 \times 10^{-10} \\ &= 166pF \end{aligned}$$

#### 4.4.10 Matching Capacitance

The resistance is calculated in the previous step and used to work out the Q factor of the inductor. The matching capacitance can be calculated using:

$$C_m = \frac{1}{\omega_s Z_o A} \quad (4.14)$$

$$\begin{aligned} C_m &= \frac{1}{66566578.42 \times 50\Omega \times 42.23} \\ &= 7.11 \times 10^{-12} \\ &= 7.11pF \end{aligned}$$

#### 4.4.11 Required transmitter power

The power required to be delivered to the probe circuit can be calculated using the standard power formula:

$$P = I_{RMS}^2 \times Z_o \quad (4.15)$$

where P is power in watts, I is the average current delivered to the coil and  $Z_o$  is the matching impedance of the circuit.

$$\begin{aligned} I_{RMS} &= \frac{0.4959}{\sqrt{2}} \\ P &= 0.3507^2 \times 50\Omega \\ &= 6.1486W \end{aligned}$$

#### 4.4.12 Peak Voltage across the Coil

$$\begin{aligned}
 V_p &= \omega L \times I_p & (4.16) \\
 &= 86.536 \times 0.4959A \\
 &= 42.9157V
 \end{aligned}$$

#### 4.4.13 Power dissipated through inductor

As with any inductor, the power that is dissipated through heat can be calculated using the above power formula:

$$\begin{aligned}
 P &= I_{RMS}^2 \times R & (4.17) \\
 I_{RMS} &= \frac{0.4959}{\sqrt{2}} \\
 P &= 0.3507^2 \times 50\Omega \\
 &= 10.303mW
 \end{aligned}$$

### 4.5 Power amplifier

#### 4.5.1 Output peak voltage

The peak voltage that the amplifier needs to deliver at the output can be calculated as:

$$V_p = \sqrt{2PZ_0} \quad (4.18)$$

$$\begin{aligned}
 V_p &= \sqrt{2 \times 6.1486 \times 50\Omega} \\
 &= 24.7963V
 \end{aligned}$$

#### 4.5.2 Amplifier Input Voltage

The input voltage for the amplifier needs to be calculated due to the minimum 50dB gain requirement. The peak output amplifier voltage is known to be 24.79V so the output RMS voltage is therefore 17.53V. The voltage gain formula is used here, but the power gain formula can also be used, using a resistance of 50Ω. Here  $V_{in}$  is the voltage output of the RadioProcessor and  $V_{out}$  being the output voltage of the power amplifier.

$$A_v = 20 \log_{10} \left( \frac{V_{out}}{V_{in}} \right) \quad (4.19)$$

$$50 = 20 \log \left( \frac{17.5326}{V_{in}} \right)$$

$$V_{in} = 0.05544V$$

$$= 55.44mV$$

## 4.6 Preamplifier

### Expected Input Voltage

The voltage induced by the sample within the coil can be calculated using the following formula:

$$\epsilon(t) = \frac{B_1}{I_0} \times \eta_0 \times \frac{I(I+1)\gamma^3 \hbar^2 B^2 \sin\theta}{3kT_{sample}} \times \delta V \quad (4.20)$$

Where  $\frac{B_1}{I_0}$  is the magnetic field generated by the coil with 1 amp of current, I is the spin quantum number, k is Boltzmanns constant, h bar is Plancks constant over 2pi, B is the strength of the external magnetic field, T is the temperature of the sample in Kelvin,  $\sin\theta$  is the angle the coil makes with respect to the B1 field generated and  $n_0\delta V$  is the number of hydrogen atoms within the sample volume.

$\gamma$	$42.5^6 \times 2\pi$
$I$	$\frac{1}{2}$
$k$	$1.38 \times 10^{23}$
$\hbar$	$\frac{h}{2\pi=1.05 \times 10^{-34}}$
T	293.15
B	0.24928T
$\frac{B_1}{I_0}$	1.2567mT

**Table 4.1:** Time Budget Review

In order to calculate  $\eta_0\delta V$  meant that we needed to find the number of hydrogen atoms in the sample within the coil. Given that he coil is shaped like a cylinder and accounting for the 1mm thickness of glass, there would be 0.64ml of water. Therefore this equates to 0.64g of  $H_2O$ . Since the total atomic mass of  $H_2O$  is 18.015g/mol, there is 0.0355mol  $H_2O$  within the coil. Using Avogadro's constant the number of water molecules within the sample is:  $0.0355 \times 6.022 \times 10^{23} = 2.13 \times 10^{22}$ . As each molecule of  $H_2O$  has 2 Hydrogen atoms and 1 Oxygen atoms there would be:  $2.13 \times 10^{22} \times 2 = 4.27 \times 10^{22}$ Hydrogen atoms.

The voltage of the signal that we expect to receive is 43.677 $\mu$  V.

## 4.7 Chapter Summary

In this chapter, we break down the different elements of the NMR Probe and calculate the values of each component. This demonstrates the relationships between the different components and shows how each formula relies on another.

# Chapter 5

## Experimental Results

### 5.1 Introduction

The aim of this design is to bring together existing components that are already available to ensure that the overall cost is kept to a minimum. Certain elements, such as the probe and preamplifier cannot be acquired due to their specific requirements and have to be designed to suit the system. A system such as this is especially useful in teaching applications as it allows for different concepts of NMR application to be demonstrated and explained.

- We identify the limitations of the Halbach Magnet.
- We propose and build a suitable coil design that can excite the protons within a sample.
- We incorporate an existing power amplifier into the design
- We discuss the use of a passive switch to separate the transmit stage from the receive stage
- We discuss a preamplifier for the receive stage

This chapter is organised as follows. Section 5.2 examines an existing Halbach magnet and its suitability as part of the design. The magnetic field is measured and analysed to ensure that the power delivered to the probe is acceptable. Section 5.3 looks at how size, skin effect and proximity effect played a role in the design of the probe. The way in which it was constructed and the final results are also presented. In section 5.4 the use of the Spincore RadioProcessor G is discussed along with the software needed to control it. The input and output power requirements play a large role in our choice of power amplifier for the transmit stage and preamplifiers for the receive stage. Which lead us to section 5.5 where an existing amplifier is considered for the transmit stage. Section 5.5.2 goes on further to examine a proposed preamplifier that would be suitable for the system. Key factors include gain, voltage input, the voltage output range and voltage noise. In the

final section the use of an active or passive switch is debated with the passive method being favoured.

## 5.2 External Halbach Magnet

As there was an existing Halbach magnet with an unknown magnetic field, there needed to be a way of measuring its intensity and homogeneity. There were two available Hall sensors that could be used to measure the magnetic field, both manufactured by Honeywell. These were the SS94A1F and the SS94A2D, details of which are provided in appendix D.1.

The probe, which requires 4 volts at the input, was connected to a power supply. The output was connected to a multimeter which shows the voltage at a specific point. Measurements were first carried out using the SS94A1F Hall sensor. There was an issue where the voltage at the output was constantly showing 7.35 volts. This was due to the sensors limitations which could only measure up to 100G. The SS94A2D sensor had a much larger range with measurements of up to 2500G. After carrying out a few test measurements, the sensor did not reach saturation at any point therefore making it the more appropriate sensor.

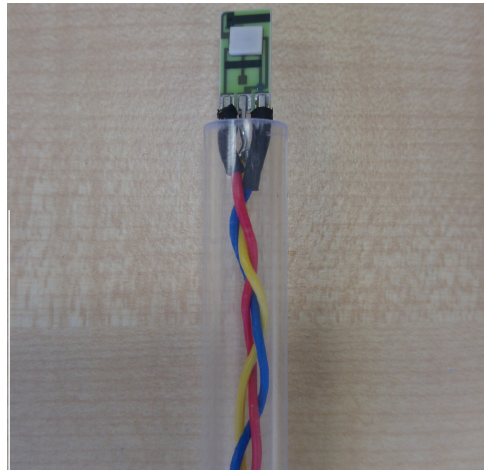


**Figure 5.1:** Hall Sensor

Given that the centre of the Halbach magnet is considered to have a uniform field, that area was measured first. It could be seen that there was an area of about 2cm, not necessarily in the shape of a cube that had a constant voltage of 6.47V. It is important to note here that there is a limitation when it comes to these measurements as the multimeter only provides a reading of up to 2 decimal places. It was possible that there were minute changes in voltage within that area, but that is something that could not be initially seen.



**Figure 5.2:** Halbach Magnet

A more accurate voltmeter was then made available at a later stage and the magnetic field was measured again. The multimeter, manufactured by Isotech provided a reading of upto 4 decimal places. The measurements were set up so that the field was measured in layers from bottom to top. The area within the magnet was divided up into  $1\text{cm}$  increments. At the bottom, it was possible to only measure the middle, providing one row of measurements. Loose leaf paper was put together so that it had a thickness of  $1\text{cm}$  and was added to the measurement platform to increase the height as we moved from layer to layer.  $1\text{cm}$  grid paper was used to ensure that the Hall sensor was moved in accurate  $1\text{cm}$  increments across the magnet. As we got to the middle, it was possible to measure completely across the magnet.

Surface contour graphs were created with the data that was collected. The data can be found in the appendix (B). The voltages measured had to be converted to Tesla before the graphs were plotted. The contour scale ranges from  $0.10\text{T}$  to  $0.25\text{T}$  allowing us to observe the difference in field strength at different points. Just through observation, it can be seen that there is quite a variation in field strength as we move around the magnet. Choosing a pulse width has a direct correlation with this variation as a larger variation results in a larger bandwidth and a higher amount of current being delivered to the probe. The y-axis from all the graphs represents the position of the hall sensor from 1 being the leftmost point of the magnet and 7 being the rightmost. The 1 on the y-axis is the front of the magnet with 12 being the back. There are 7 graphs which are provided, with the 1st providing measurements of the base of the magnet, with the 7th one being the top.

The most important measurement was the one right in the centre of the magnet. This was where the sample would be placed and this in turn aligns with the  $2\text{cm}$  square hole

at the top from which the sample would be put through. It was important to ensure that the hall sensor was right in the centre and aligned with this hole. In general, any slight movement in the sensor would affect the measurement or if it was on a slight angle. A measurement was eventually collected and was 0.24928. This would be the value used to calculate the precessional frequency of the hydrogen protons within that particular area of the magnetic field.

## 5.3 NMR Probe

Given the magnetic field strength of the Halbach magnet, it is possible to calculate the corresponding bandwidth, which is then converted to the pulse width. These calculations are then used to work out the strength of the coils magnetic field that is to be applied. This gives an idea of the protons that will be excited, depending on where they are within the external magnetic field.

### 5.3.1 LC Resonant Circuit

Going into more detail of what a resonant circuit is and the effects of a Q factor on the circuit. When looking at resonant circuits, it is usually always observed in the case where the components are ideal. The impedance across these components becomes infinite at resonance and looks more like an open circuit. There would be no current flow at this point as the lossless components do not allow current to enter into the resonant circuit. However in a practical circuit, there are all sorts of factors that contribute to the overall resistance of the circuit right from component leads, the coil itself, skin and proximity effects.

The impedance of the circuit can actually be calculated assuming the resistance of the inductor is close to 0 due to them being lossless using [4]:  $Z = L/CRL = RL(1 + Q^2)$

Notice that these equations later on are used to calculate the matching capacitor so that the circuit is matched to  $50/\Omega$ .

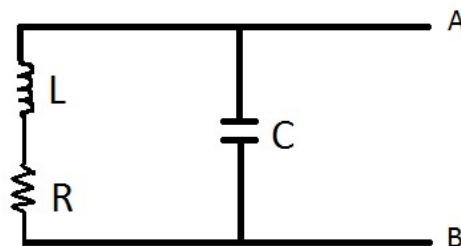
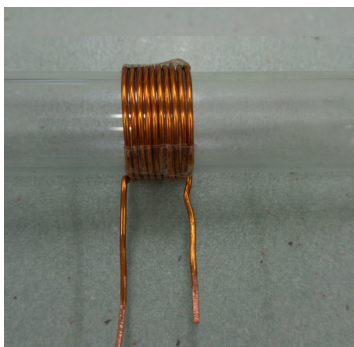


Figure 5.3: Parallel Resonant Circuit

### 5.3.2 Coil

Copper wire was wrapped around a test tube that was 1cm in diameter for 10 turns. Once wrapped, the coil was held together with tape to stop it from expanding. Under normal circumstances, some form of epoxy glue would be used as a more studier alternative. A diameter of 1cm was chosen so that it would be possible to place a test tube with a sample of water within the coil.



**Figure 5.4:** Halbach Magnet

It was important to take into consideration the thickness of the wire used as they each have a maximum amount of current they can carry. The wire used had a thickness of about 1mm, which could be converted to AWG18 therefore rated to carry a maximum current of 2.9Amps. The calculated peak current through the coil was 0.0496 Amps for which this particular wire would suffice.

#### Skin Effect

When considering coil resistance at high frequencies when applying alternating current, it is imperative that skin effects are taken into consideration. It is where the current tends to travel near the surface of the solid conductor rather than through the centre. The available cross-sectional area of the conductor is then limited, therefore increasing its resistance as when compared to direct current. This is due to the changing magnetic field which induced opposing eddy currents within the conductor. At higher frequencies, the skin depth decreases and the resistance increases. The resistance is then calculated as a function of skin depth, for our case, the skin depth was  $20.25\mu m$ , resulting in a resistance of  $0.0839\Omega$ .

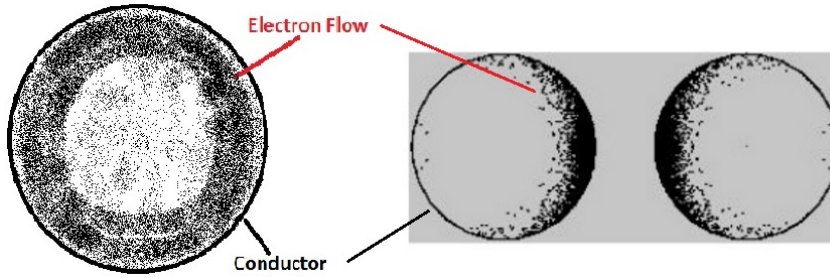


Figure 5.5: Skin and Proximity effects on electrons

### Proximity Effect

As the probe consists of a coil of wire, the conductors are placed in close proximity to each other which contributes to an increased resistance. This occurs when alternating current is used and the resistance therefore increases at higher frequencies. Once again, eddy current are induced in neighbouring conductors due to the alternating magnetic field. There is more current within the wire in the areas further away from adjacent wires with current moving in the same direction. Although not calculated, the matching capacitor chosen will have a range large enough to account for the added resistance.

### 5.3.3 Q-factor

The Q-factor of the probe being designed, plays a major role in the capacitor values chosen for the circuit. The 'Q' stands for quality of a resonant circuit which is a measure for how 'good' the circuit is [15]. For certain applications it is important to have a high Q-factor in certain applications such as in telecommunications. More specifically, it is a ratio of power stored to the power dissipated and can be viewed as:

$$Q = \frac{P_{stored}}{P_{dissipated}} \quad (5.1)$$

$$= \frac{I^2 X_L}{I^2 R} \quad (5.2)$$

$$= \frac{X_L}{R} \quad (5.3)$$

$$= \frac{\omega L}{R} \quad (5.4)$$

As we are observing the Q factor of the inductor, we would expect to look at the magnetic energy stored. Typically, NMR coils have Q factors that range from 50 – 500 therefor with a resistance of  $1\Omega$  or less. The capacitors within the circuit are generally ignored as they usually have Q factors over 10,000 making their resistance negligible for frequencies around 1MHz. The Q factor at frequencies around 500MHz range from 250 – 1000 [16]. In our case, we are working with a frequency of about 10MHz, so even

if the capacitors exhibited a small resistance, this would be accounted for when varying the capacitors during the tuning and matching process.

Taking into account the skin depth calculation as a function of frequency, the resistance was calculated to be approximately  $0.08\Omega$ . It wouldnt have been appropriate to use the measured resistance value of  $0.024\Omega$  as it is measured at a frequency of  $1000Hz$  which is nowhere near the frequency at which it is being implemented. For this calculation the inductance value that was calculated was close to  $1/\mu H$  but when measured with an RLC meter, it was  $1.3\mu H$ . The measured value was used for all calculations requiring the inductance value of the coil, including the Q-factor.

### 5.3.4 Impedance Matching

With impedance matching, the general idea is to allow for maximum transfer of power from the source to the load. This would mean that the source impedance and the load impedance need to be equal to each other. As we are dealing with impedances, the real parts need to be equal to  $50\Omega$  in our case as the amplifier has a load impedance of  $50\Omega$ . Not having equal impedances results in part of the wave being reflected back to the source. Therefore some of the energy gets lost in transmission and does not end up being delivered to the load.  $C_T$  and  $C_M$  are chosen such that the load is matched to  $50\Omega$

### 5.3.5 Tuning and Matching Capacitors

We are able to match the coil to  $50\Omega$  by having a tuning capacitor in parallel to the coil and a matching capacitor in series.  $C_t$  and  $C_m$  are chosen such that the load is matched to a real  $50\Omega$ .

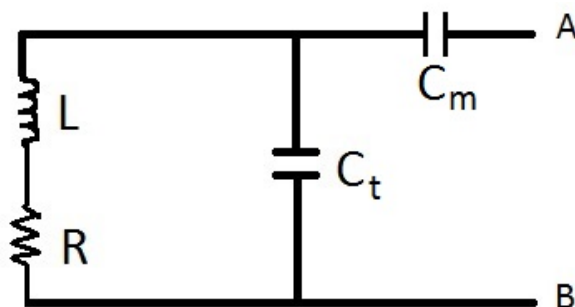


Figure 5.6: NMR Probe Circuit

In a parallel configuration, the circuit impedance which has a real part and imaginary part is given by:

$$Z_{AB} = R + j\omega L \parallel \frac{1}{j\omega C_T} \quad (5.5)$$

Ignoring the matching capacitor at this point, after some algebra (can be found in appendix A), the real part of the impedance is equal to:

$$Z = \frac{R}{(1 - w^2LC_T)^2 - (wRC_T)^2} \quad (5.6)$$

To achieve a real impedance of  $50\Omega$ , the tuning capacitor is first adjusted while maintaining the spectrometer frequency. Equation 5.6 can further be simplified as demonstrated by Mispelter et. al [16] to the following equation where:

$$C_t w_s = \frac{Q \pm A}{B} \quad (5.7)$$

$$Q_L = \frac{\omega_s L}{r}$$

$$A = \sqrt{\frac{B}{Z_o} - 1}$$

$$B = r(1 + Q^2)$$

To ensure the circuit is matched,  $A$  needs to be a real value, this will occur when  $B > Z_o$ . When calculating  $C_t$ , the negative sign is chosen allowing the resonant frequency to be lower than the resonant frequency.

Now when taking into account the matching capacitance and its effect on the imaginary part of the circuit impedance, results in:

$$Z_{Im}(w_s) = \pm Z_o A \quad (5.8)$$

Since the negative sign was chosen before, the positive sign is now chosen due to their correspondence with each other. Therefore the matching capacitance can be calculated as:

$$C_m = \frac{1}{w_s Z_o A} \quad (5.9)$$

It was determined that the tuning capacitor had a value of 166pF and the matching capacitor was 7.11pF. Being that the actual Q factor is unknown, it is expected that these values will vary when it comes to testing the probe circuit using the spectrum analyser.

### 5.3.6 Construction and Testing

Once the capacitor values were calculated, they were soldered to a circuit board. The capacitors used initially were standard fixed value capacitors which were already available in the lab. Appropriate values needed to be put together to get the desired capacitor values. To get the 165pF tuning capacitor, a 150pF cap and a 15 pF cap were put together in parallel. To achieve the 7pF matching cap, two 15pF caps were placed in series. Calculating the total capacitance whether in series or parallel is opposite to when

calculating resistors in series or parallel. The outer layer of the coil at both ends needed to be removed in order for there to be an electrical contact with the board. A BNC connector required 2 wires to be soldered to it before it could also be attached to the board. The first iteration of the probe can be seen below:

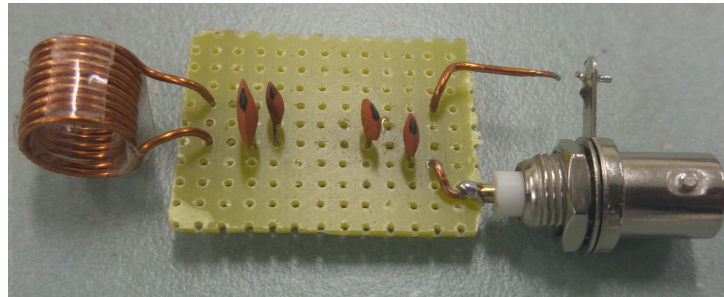


**Figure 5.7:** Initial NMR Probe

Using a spectrum analyser allows us to get direct readings of the reflection coefficient, among other parameters. The magnitude graph was observed to look at  $S_{11}$  and the Smith Chart to ensure the probe was matched to  $50\Omega$ . The marker was set to the desired frequency which then corresponded to the readouts. Initially testing this circuit with the spectrum analyser, the frequency was around 14Mhz which was not close to the frequency that was required. The board used was quite small and there wasn't enough room to add more capacitors, so a solderless breadboard was utilised before moving to a larger board. Using a solderless breadboard saved time from not having to constantly solder and desolder components. Once we reached closer to the targeted values, a larger board was used which can be viewed below. It could be seen that the tuning capacitor needed to be increased in value to decrease the frequency. An extra 125pf had to be added to get a frequency close to 10.59Mhz. It was now appropriate to add a variable capacitor in parallel so that the right frequency can be achieved. A similar task was carried out to achieve the correct matching capacitance. Ideally, the output of the detector equal to 0 at the required frequency for a perfect match. There were some cases where the trough was quite wide which would mean that it was over-coupled resulting in the frequency response being too wide. On the other hand, the output was higher at frequencies higher than what was required, resulting in the circuit being under-coupled.

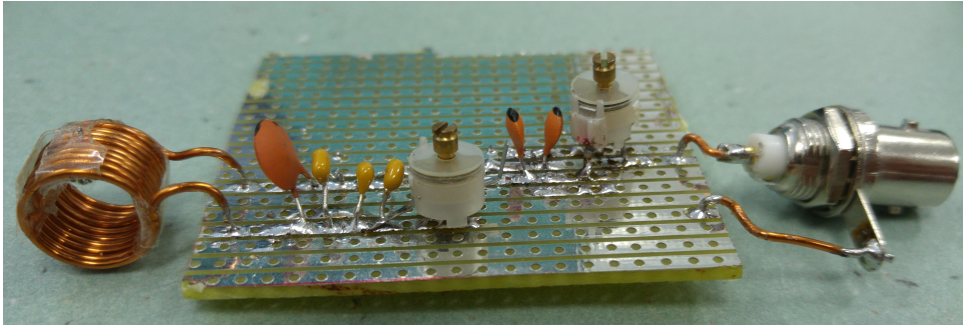


**Figure 5.8:** Final NMR Probe

The initial 7pF cap value was too low and needed to be increased to match the probe to 50Ω. Eventually two 33pF capacitors were put in series to get a value of 16.5pF and a variable capacitor in parallel. Both the variable capacitors used had a range from 1.3 7.2pF. Finally the variable capacitors were adjusted to obtain the correct frequency and resistance.

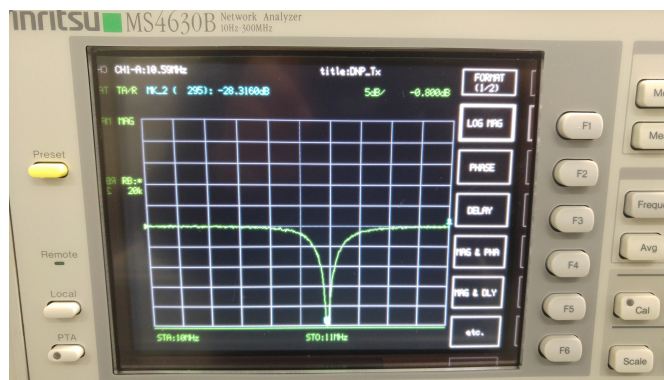


**Figure 5.9:** Spectrum Analyser Magnitude readout

Once tuned and matched, the output at 10.59Mhz was about -28dB with the resistance being approximately 50Ω. There was some noise present within the circuit which affected the final values in that it was fluctuating slightly. There are a few factors that may have an effect on the coils stability, firstly with the coil being held together with glue rather than tape. Within the tape, the coil had a small amount of room in which it could move. Not being held together rigidly, can result in the frequency shifting. Also, having gaps in between the conductor affects the tuning and matching values. Other minute factors could be that there were a multitude of capacitors used and the leads of those components can contribute slightly to the unexpected change in values. A graph was plotted of what the tuning and matching capacitor values would be if the resistance of the coil was to increase. This would result in a decrease in Q-factor and decrease the tuning capacitance which increases the matching capacitance. Our matching capacitor value of 33pF was on the graph and could suggest that that the Q-factor of the circuit was much lower than

initially calculated. On the other hand, the tuning capacitance was nowhere near the expected plot and was more of an outlier.



**Figure 5.10:** Impedance readout

### 5.3.7 Power Requirements

Given that the size of the coil and the magnetic field required has already been established, the current required by the coil can be calculated using Amperes Law. This gives us a required peak current of 0.4959A through the coil using equation 4.3. From this, the peak voltage across the coil can be calculated from equation 4.16 to be 42.91V. The voltage is not too high here, but in some circumstances for more powerful systems, this value can go into the kilovolts range. Then this would be where components that are chosen for the circuit have a high voltage rating.

The peak current is converted to its effective counterpart and from that the required transmitted power can be calculated, see in equation 4.15. This is calculated to be about 6.15W which is important when looking at an amplifier that can actually deliver that. Given the required power, the amplifier needs to have a peak output voltage of 24.79V.

The power supplied by the amplifier and the amount dissipated through the inductor is about 10.3mW, assuming the calculated resistance value. The power dissipated value will in fact be slightly higher than this, resulting in the power dissipated being higher than the calculated 10.3mW. This also assumes negligible capacitor losses as a majority of the time, capacitors have a very high Q-factor contributing minimally to the overall resistance of the circuit. The remainder of the power is transferred to the protons allowing its magnetisation to rotate  $90^\circ$ .

## 5.4 Transmit/Receive System

### 5.4.1 Spincore RadioProcessor G

The RadioProcessor is a radio frequency excitation and acquisition system created by a company called Spincore in Florida, USA. This whole system is built onto a PCI card

and is placed inside one of the computers in the lab. It has 2 inputs, one being digital and the other analogue and 2 outputs, 1 being digital and the other analogue. The card can form RF excitation pulses and stores the acquired data in multiple formats all while maintaining signal coherence between them. Having a system such as this means that separate signal generators and pulse controllers are not required.



**Figure 5.11:** RadioProcessor PC Card [24]

Looking more closely at the board, there are 3 major components which are the excitation core, data acquisition core and a timing engine which controls the system through a high resolution timing control. The incoming RF signal is captured using an Analogue to Digital converter which is then demodulated and filtered to a baseband signal [24].

### 5.4.2 Utilising the Board

There are multiple ways in which the board can be used. Two of the main options include using one of the MATLAB interface programs or through a C program which are provided. A user is not limited to using what is available, and can write their own program or edit one of the available ones.

There was an issue where the required MATLAB program was not working initially when attempting to use it. It would have been a better option as it is much easier to preview the data after scanning. The different MATLAB programs would have been able to automatically find the spectrometer resonant frequency and the 90 degree pulse width instead of having to calculate it or carry out CPMG experiments to calculate T2 relaxation times.

The file where the parameters are established is a separate file to the file where the actual file where the code is. The parameters that can be changed can be seen in the following table.

Some of them are quite familiar and we come across them in the calculations. Some are new and are important when looking at the system as a whole. The blanking delay is used to allow the power amplifier to warm up if needed and then the pulse is applied. After than a transient time can be set so that the coil can ring down due the high voltage

Board Number	Selects which board to program if multiple SpinCore boards are connected to the computer
ADC Frequency	Clock frequency of the board. Always 75MHz, unless a custom clock is being used as input to the RadioProcessor
Enable TX	A 1 enables the transmitter, a 0 disables the transmitter
Enable RX	A 1 enables the receiver, a 0 disables the receiver
Repetition Delay	Repetition delay in seconds between scans
Number of Scans	Number of times to repeat the scan and average the results together
Number of Points	Number of complex points to be captured
Spectrometer Frequency	Spectrometer frequency in MHz
Spectral Width	Desired base band spectral width in kHz
Pulse Time	Duration of Transmitter excitation pulse in $\mu s$
TX Phase	Phase of the Transmitter output channel in degrees
Amplitude	TX output amplitude scaling factor (between 0.0 and 1.0).
Shaped Pulse	Uses a 'sinc' shaped pulse for the Transmitter output
Bypass FIR	RA 1 bypasses the FIR filter, 0 enables it
Fname	File name to save the acquired data in. Data will be saved in ASCII, Felix, and JCAMP formats
Verbose	A 1 enables normal output, a 0 disables normal output and the program outputs nothing
Blanking Bit	Specifies which TTL Flags to use for blanking
Blanking Delay	Delay needed to warm-up the SpinCore RF Power Amplifier prior to the RF pulse

**Table 5.1:** Parameters within the program [24]

previously induced. Then we would expect to set an acquisition time where the FID signal would be acquired. Lastly a repetition delay is required to allow the sample to relax before the next pulse.

Once the program is run, it is expected that multiple output files are produced which can be opened up in programs such as Felix or Jcamp.

### 5.4.3 Pulse Duration

Applying a short frequency pulse for a certain period of time at a specific frequency rotates the net magnetization of the proton. The width of the pulse and its power affects the amount at which it rotates and at 90 degrees the maximum signal can be obtained. For most experiments the pulse width is quite often set between  $8 - 13\mu s$  [1]. It was decided that a pulse width of about  $10\mu s$  would be appropriate as the power requirements are achievable. From this the magnetic field that needs to be created of the coil will have

a strength of 0.6232mT. Given that the coil has dimensions that are known, the peak current through the coil will be 0.4951A.

By applying a resonant frequency of 10.5944Mhz for a duration of 9.4388 $\mu$ s we allow for an external magnetic field coverage of approximately 1%. This means that if the magnetic field inside the magnet varies +/- 0.5%, the protons within the 0.249T field and the field surrounding it (to +/- 0.5%) will become excited. Within the magnet, this will cover an area of slightly more than 1cm (not necessarily in the shape of a cube). The sample will need to remain within the confines of that area only, as the signal received will only be from that volume. The noise expected to be received will be the same as what is transmitted which will depend on the electronics used. Additional noise would be expected if the sample was larger than the imaging area, lowering the signal to noise ratio.

If a larger sample needs to be imaged, a shorter pulse width with a stronger magnetic field will need to be applied to compensate. Or we can have a weaker RF pulse over a longer period of time. The SNR is also affected by the bandwidth which is equal to  $\frac{1}{\sqrt{\text{bandwidth}}}$ . If the bandwidth increases, the SNR decreases implying there is a trade-off. The pulse width duration can be calculated on the basis of SNR and where it will be optimised affecting how big the volume of the sample can be to have the optimum SNR. This assumes that the deviation within that magnet is well known.

To increase the sample imaging area to 3cm,  $B_1$  was required to be stronger. The external magnetic field within that area ranged from 0.246T to 0.252T. This was a deviation of about +/- 1.203%, with the bandwidth therefore equal to 127500Hz. The pulse width is 7.84 $\mu$ s and  $B_1$  is 0.75mT as a result. A design looking at a larger imaging area along with a larger coil is discussed in Chapter 6.

#### 5.4.4 Acquisition Time

At this stage the pulse has caused the magnetisation of the sample to flip 90°. The time specified to acquire the FID signal is known as the acquisition time. The acquisition time depends on the time taken for the proton to reach equilibrium. It would not be appropriate to set it to be as long as possible as it is only useful up to a point and the signal acquired will not be maximised any further. Having a long acquisition time can result in additional unwanted noise and if too short, the complete signal will not be acquired.

#### 5.4.5 Number of Points

The analogue signal which is picked up by the coil needs to be converted to a digital signal. The ADC captures points along the FID curve. For a higher resolution, a higher number of points is required to be set. The RadioProcessor can capture around 16000 points [24].

### 5.4.6 Spectral Width

When it comes the FID signal that is captured, it is not in fact the signal we want, as it is captured in the time domain. The signal is Fourier transformed so that a spectrum can be observed within the frequency domain. This allows us to observe the different levels of intensity depending on the frequency. The spectrometer frequency is at 10.59Mhz so a spectral width of about 100Hz is required to scan 10 ppm. If required, there is room for extending the spectral width to over 1000Hz so that more can be observed. Although, at the same time, may result in excessive noise which could interfere with what needs to be observed.

The number of points, spectral width and the acquisition time are all in fact related by the following equation:

$$AcquisitionTime = \frac{No.ofPoints}{2 \times SpectralWidth} \quad (5.10)$$

If we were to choose the maximum number of points being 16384 every time and chose a spectral width, we are then able to calculate the acquisition time required.

### 5.4.7 Power

The output from the board is generally quite weak and is normally used in conjunction with an external amplifier. Looking at the specifications sheet, we see that the peak-peak output voltage has a maximum of 1.2V. This is only if there is no 50Ω voltage termination, but since there is, the output voltage drops to about half. Given that the input of the external amplifier can handle a maximum of 0dBm, the output RadioProcessor voltage should not be a problem. 0dBm when converted to peak-peak voltage becomes approximately 0.632V. However, when testing the output voltage of the Radio Processor board, the output voltage was not what was expected .

An initial test was carried out where an oscilloscope was connected to the analogue output. The following parameters were set:

Spectrometer frequency (MHz)	10.59
Pulse Time ( $\mu s$ )	94.389
Transmitter	1
Receiver	0

**Table 5.2:** Initial test Parameters

At the output, the pulse could be observed. The oscilloscope was set with the voltage scale being  $\pm 1V$  and the timing scale being  $20\mu s/div$ . Looking at the image below, we notice that the peak voltage is higher than expected and comes in about 0.7V. This meant that the board was in working order and followed the parameters.

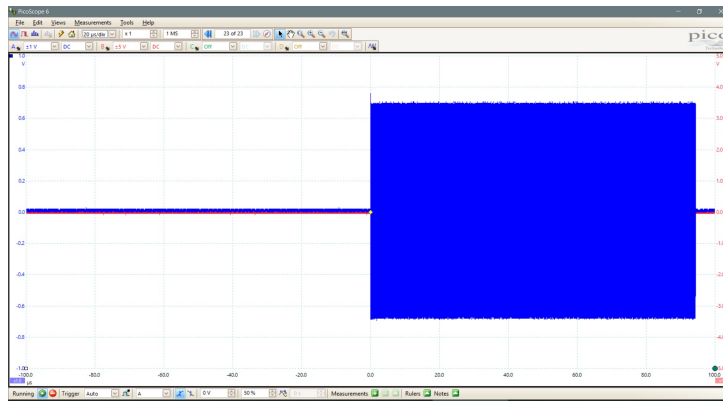


**Figure 5.12:** Initial RadioProcessor Output

It is possible to reduce the amplitude output level. The output was measured using an oscilloscope at regular intervals and a graph was plotted in figure 5.13. Both the peak to peak voltage and RMS voltage was measured using a 50Ω load. What was interesting was that the RMS voltage is significantly lower that what is expected if it were to be calculated from the peak to peak voltage. For the highest level of output, we would expect the RMS voltage closer to 300mV if the peak voltage was 393mV rather than 191mV.

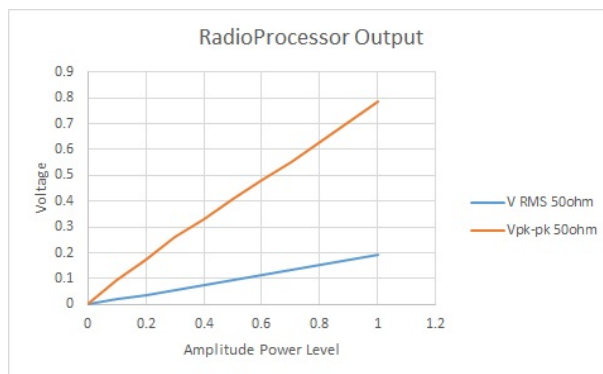


**Figure 5.13:** RadioProcessor Voltage Output

The input power amplifier voltage was calculated earlier from equation 4.6 to be 55.44mV. So by looking at the graph and the table used to create it, the output level should be around 0.293. When measured with an oscilloscope at that output, it was lower than expected. To reach the desired output, it had to be set to 0.299. When using the RadioProcessor, it is imperative that the output is measured previously as what is expected does not actually occur.

## 5.5 Amplification Stages

### 5.5.1 Transmit Power Amplifier

An amplifier at the transmit stage is required because the signal provided by the Spincore RadioProcessor is not powerful enough to excite the protons within the sample by itself. It has a maximum voltage output of 191mV and can be converted to 0.732mW, assuming an impedance of  $50\Omega$ . The RadioProcessor output voltage can be varied which is important due to the input requirements of the power amplifier.

An Ophir RF power amplifier was available in the lab, and has been incorporated into the design of the NMR system. It is a Class AB amplifier that can deliver a maximum of 100W at the output. At the input, no more than 1mW can be applied, which is where the variation in output voltage from the RadioProcessor comes in. Also, it amplifies the input by a minimum of 50dB [19], so if 1mW was applied at the input, would result in the max output power. The NMR probe used, needs to be matched to  $50\Omega$ , otherwise the amplifier shuts down if the impedance varies too much.



Figure 5.14: Ophir Amplifier [3]

Given that we need 6.14W at the output and there is minimum 50dB gain, the power at the input will need to be  $61.47\mu W$ . So at  $50\Omega$ , the voltage will have to be regulated to  $0.05544V_{RMS}$  as seen in equation 4.6. The amplifier output will be connected to the probe which was previously matched to  $50\Omega$  and the input, to the RadioProcessor.

### 5.5.2 Receive Preamplifier

It was decided that a preamplifier would need researched as there were no available amplifiers in the lab. When searching for preamplifiers for this stage, there are a lot more variables that needed to be considered, especially noise. There were amplifiers by Advanced Receiver and Minicircuits that were available, which are discussed briefly. They were not chosen, due to having an inappropriate noise figure or the frequency at which they amplified was different to what was required.

Considering the size of our sample, the voltage of the signal that is expected to be received was calculated to be  $43.677\mu V$  4.20. This voltage is so low, that the RadioProcessor will not be able to pick it up.

When looking at RF receivers, the signal that comes from the probe, has to first pass through a Low Noise Amplifier which then amplifies the signal. Noise Figure (in dB) characterises the degradation in Signal to Noise Ratio by the receiver. Noise Factor of an amplifier is the ratio of the SNR at the input and at the SNR at the output. [20] It is imperative that a preamplifier has a low noise figure, as we know from the Friis equation, plays a large role in the overall noise at the output. Whereas slightly higher noise figures of further amplifier stages do not affect the total noise figure as much.

$$F_N = F_1 + \frac{F_2 - 1}{G_1} + \frac{F_3 - 1}{G_1 G_2} + \dots + \frac{F_n - 1}{G_1 G_2 \dots G_N} \quad (5.11)$$

where  $F_N$  is the total noise factor,  $F$  is the noise factor of each stage and  $G$  is the gain of each stage.

### Voltage gain required

The induced signal was calculated to be around  $43.677\mu V$  which means that an appropriate gain is required. There was no minimum input signal voltage that was given, but the RadioProcessor manual does mention the used of an amplifier that had a gain between 45-60dB. The preamplifiers output voltage was chosen to be 10mV from which the gain required could be calculated. This meant the gain was calculated to be approximately 47.19dB which matches what is said in the manual. This also assumes that the RadioProcessor is able to pick up the signal with minimal noise. If say a preamplifier was chosen and it had a higher gain than 50dB, it shouldnt be a problem as the RadioProcessor can handle a maximum input voltage of 1.2Vpp.

### Minicircuits LNA

The Minicircuits LNA is quite a simple LNA, in that it has an input and output BNC connectors and all thats required is for it to be powered up. Looking at the gain specifications as a result of the voltage supply, it is possible to achieve a gain of 29dB with a 16V power supply. This is at the 10.59Mhz frequenc, which is part of this amplifiers bandwidth. It has already been matched to  $50\Omega$  and has a noise figure of 2.8dB which is considered fairly low. The only issue is that the gain may not be enough resulting in the amplified signal not be received by the RadioProcessor. It does have quite a large bandwidth, so a filter will need to be placed before it to ensure the frequencies being amplified is what is required.

### Linear Technologies LTC6268-10 4Ghz Operational Amplifier

Another option that was available for an amplifier, was to go with an operational amplifier. Choosing an operational amplifier requires going through the datasheet and ensuring that

the parameters given will suit our needs. Not only that, the operational amp requires to be powered by an external power supply and requires other 3<sup>rd</sup> party components to allow it to work. The operational amplifier chosen was the LTC6268-10 model manufactured by Linear Technologies. It was chosen as it satisfied quite a few requirements which meant that it had a very low noise input, low bias current and is was able to amplifier at a frequency of 10.59Mhz.

### Gain Bandwidth Product

Under ideal conditions, an operational amplifier generally has infinite gain and can amplify any frequency. When looking at real op-amps, the first thing to note is the gain bandwidth frequency as they are all limited by such a value. The Gain-Bandwidth Product is the frequency at where the gain of the amplifier is at unity. This particular op amp has a GDP of 4Ghz, so at approximately 10.59Mhz, we would expect a gain of about 50dB which is in fact slightly better that what we initially required. The GBP is quite high, the reason being, op amps with lower GBPs have a much lower gain. The amplifier will require a filter to be added to it so that it only amplifies around the 10.59Mhz frequency. Either one can be designed and placed before the op amp or otherwise BNC filters are available by companies such as Minicircuits.

### Voltage Noise

Looking at the level of voltage noise the amplifier adds to the input was another key requirement. Given that we are working with microvolts, any such noise will affect our output signal. It is also important to consider that the other components connected to the amplifier such as resistors and capacitors will also add to the overall noise of the system. There were quite a few low noise amplifiers that had an input voltage noise of under  $1nV/\sqrt{Hz}$  but their gain levels were quite low and so was their GDP. The LTC6268-10 had a very low input noise of  $4nV/\sqrt{Hz}$  at 1Mhz. We would expect that this value remain the same at 10.59Mhz as the graph which compares the voltage noise density to frequency has a large scale increasing by 100Mhz.

### Common Mode Voltage

The common mode voltage is the average of the two inputs of the amplifier. This amplifier has a range of -0.1V to 2.8V. Our expected input is around  $43\mu A$  which is within the  $V_{CM}$  range. If it was outside the range, the amplifier output would not be within the linear operating region.

### Supply Voltage/Output Voltage

The values discussed, applies to the op amp being connected to a voltage supply of 3.3V. The output voltage swing range can then be determined by the power supply. The rail to rail voltage output is specified to be 80mV with a load resistance of 1000ohms. As our

output is expected to be around 10mV, this should satisfy the LTC6268s voltage output range.

### Bandpass Filter

A simple band pass filter was designed to remove all the unnecessary frequencies that may be amplified otherwise. The filter can be built simply using 2 capacitors calculated using  $C = 1/\omega f$  and 2 resistors. It was assumed that the resistor values would be fixed to  $1000\Omega$ . For the high pass stage, the frequency was set to 9.5944Mhz which resulted in  $C_1$  being 16.5pF. For the low pass stage, the frequency was set to 11.59Mhz which meant  $C_2$  would become 13.7pF. The circuit would essentially be set out as Figure 5.15. Choosing these specific upper and lower cut-off points allows for the center frequency to be 10.59Mhz which is our spectrometer frequency.

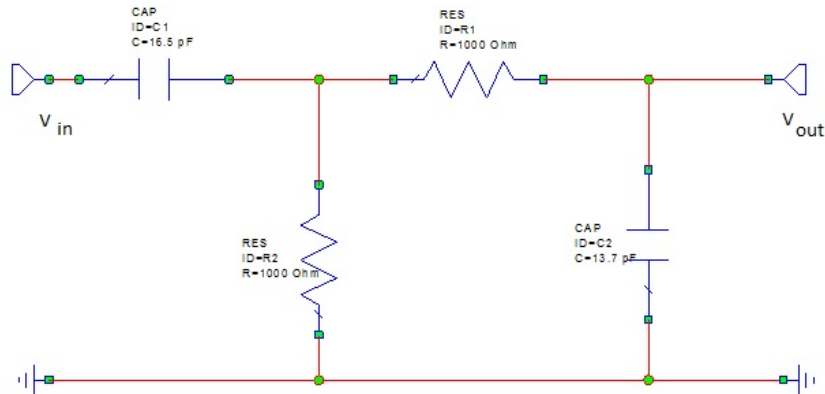


Figure 5.15: Bandpass Filter Design

## 5.6 Passive Transmit/Receive Switch

A switch within the circuit plays a vital role in ensuring that the system performs as expected and eliminates any sort of damage that may occur within the circuit. It is generally used when there is only one coaxial cable connecting the probe to the system, through which the excitation pulse and the acquisition signal travel through. The switch works by connecting the probe to the power amplifier when an excitation pulse is being delivered. At other times, the probe is connected to the preamplifier so that the acquisition signal is routed to it, from the probe. What it not wanted is a situation where the transmit pulse enters the preamplifier, possibly destroying it. This is due to the high power pulses that the preamplifier input cannot handle.

There are two options in this case, one of them being an active switch where a mosfet is used. The gate voltage can be controlled by a computer to turn the mosfet on or off depending on when the pulse is applied. The other option is a passive switch, which consists of crossed diodes and a quarter wavelength cable. The passive design, originates

initially from Lowe and Tarr [13] and has been discussed by Mispelter et. al [16] and Sleator [23].

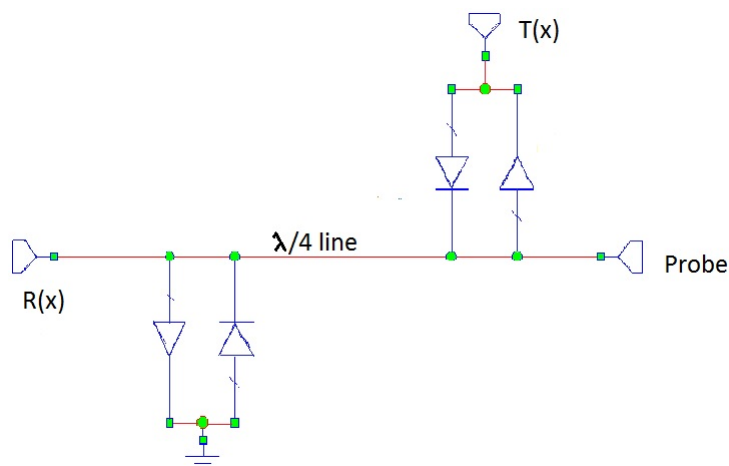


**Figure 5.16:** Passive Switch Circuit

### 5.6.1 Crossed Diodes

Crossed diodes are where 2 diodes are placed in parallel and are pointing in different directions. When observing the characteristics of a diode, it is known that when it is forward biased and the voltage across it is less than 0.6V, no current will pass through the diode. For current to pass through the diode, the voltage across the diode needs to be greater than 0.6V, which is known as the bias voltage. For the purposes of our system, one set of crossed diodes will be placed in series at the power amplifier output. Another set will be placed just before the preamplifier input with the other side connected to ground.

### 5.6.2 $\lambda/4$ wavelength cable

A  $\lambda/4$  wavelength cable is used to connect the two sets of diodes together. The reason it is used is due to a very specific property that it exhibits. If a component with an impedance  $Z_{output}$  is attached to one side of the cable, then the impedance at the other end ( $Z_{input}$ ) is given by:

$$Z_{input} = \frac{Z_0^2}{Z_{output}} \quad (5.12)$$

where  $Z_0$  is the impedance of the coaxial cable (usually  $50\Omega$ ). So for example, one end has an impedance of 0, the other end will exhibit an infinite impedance.

### 5.6.3 How it functions

During the transmit pulses, the diodes before the preamplifier act as a short due to it being connected to ground. Therefore, the  $\lambda/4$  line that is connected to that side exhibits an impedance equal to zero. This means that the other side of the line has an infinite impedance ensuring the preamplifier is not connected to the circuit during this time. The diodes in series with the preamplifier have a very low impedance as the voltage is high enough for the diodes to be forward biased.

When the transmitter is off, the transmitter diodes show a high series impedance as if like an open circuit. This means that the transmitter and any other noise that may be delivered, is isolated from the probe circuit.

When the excitation signals are being routed to the preamplifier, the signal observes a cable impedance of  $50\Omega$ . This causes the side of the cable connected to the diodes and preamplifier to have an infinite impedance. The signal goes through the cable and not through to the transmit amplifier as those diodes show an infinite impedance, as the signal voltage is much lower than the forward bias voltage.

# Chapter 6

## Conclusions and Future Work

### 6.1 Ideal Design

The ideal design put forward in this chapter can be implemented if there were no restrictions of funds required to create it. Essentially having a larger imaging area is more beneficial, but at the same time requires more powerful equipment. This can be seen further down in regards to the power requirements in order to transmit a signal. Powerful amplifiers capable of delivering such power will end up costing tens of thousands of dollars. We see from table 6.1 that the amount of power required is about 140W.

#### Helmholtz Coil Design

The coil will be wrapped around a perspex or acrylic tube that is 5cm in diameter. Assuming the inductor wire has a thickness of 1mm, the coil will be tightly wound 10 times and then a gap of 1.5 cm, then again for another 10 turns. This ensures the radius and the distance between the coils are identical. This size was specifically chosen, as the diameter of the interior of the Halbach magnet was 7cm. If the coil radius and distance between the coils were slightly larger, the magnet would not be able to accommodate a tube 4cm long and a diameter of 6cm.

#### Probe Magnetic Field Strength

Given the magnetic field strength of the Halbach magnet, it is possible to calculate the corresponding bandwidth, which is then converted to the pulse width. These calculations are then used to work out the strength of the coils magnetic field that is to be applied. This gives an idea off the protons that will be excited, depending on where they are within the external magnetic field. To allow for a sample imaging area of approximately 2cm, the magnetic field required to be generated, needs to be quite strong.

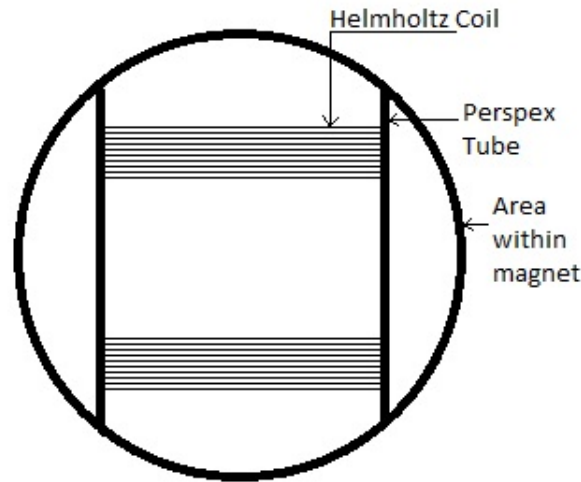


**Figure 6.1:** Helmholtz Coil Design

The following equation is used to calculate the probe magnetic field strength:

$$\theta = \omega \times B_1 \times t \quad (6.1)$$

If the pulse-width had a duration of  $3.45\mu s$ , the magnetic field would be:

$$\begin{aligned} B_1 &= \frac{\theta}{\gamma t} \\ &= \frac{0.5\pi}{(42.5MHz \times 2 \times \pi) \times 3.45\mu s} \\ &= 1.704mT \end{aligned}$$

The external magnetic field within that area ranged from 0.24644T 0.25337T. The bandwidth is therefore equal to 289,770Hz and the pulse width being  $3.45\mu s$ . By applying a resonant frequency of 10.5944Mhz for a duration of  $3.45\mu s$  we allow for a variance in external magnetic field coverage of approximately 2.73%. This means that if the magnetic field inside the magnet varies +/- 1.36%, the protons within the 0.24928T field and the field surrounding it (to +/- 1.36%) will become excited. Within the magnet, this will cover an area of about 2cm (not necessarily in the shape of a cube). The sample will need to remain within the confines of that area only, as the signal received will only be from that volume. The noise expected to be received will be the same as what is transmitted which will depend on the electronics used. Additional noise would be expected if the sample was larger than the imaging area, lowering the signal to noise ratio.

If a larger sample needs to be imaged, a shorter pulse width with a stronger magnetic field will need to be applied to compensate. Or we can have a weaker RF pulse over a longer period of time.

### Inductance of coil

The inductance of the coil can be calculated as:

$$L = \left( \frac{\mu_n n^2 A}{l} \right) \quad (6.2)$$

L is the coil inductance,  $\mu_o$  is the permeability of free space,  $l$  is the length of the coil and A is the area of the coil. Note that the value of inductance calculated is to be multiplied by 2 as there are 2 identical coils in series.

$$\begin{aligned} L &= \left( \frac{4\pi \times 10^{-6} \times 10^2 \times 0.00196}{0.01} \right) \\ &= 24.674\mu H \end{aligned}$$

$$\begin{aligned} L_T &= 24.674\mu H \times 2 \\ &= 49.348\mu H \end{aligned}$$

The remainder of the values can be calculated, similarly to the calculations in Chapter 3. This can be seen below in the following table:

Peak Current through Coil	2.369
Skin Depth	$20.16 \times 10^{-6}$
Coil Resistance	$0.843\Omega$
Q factor	3895.680
$C_m$	1.4pF
$C_t$	24.3pF
RMS Current	1.6751A
Required Transmitter Power	140.304W

**Table 6.1:** Helmholtz Coil Probe Parameters

### Preamplifier

The op amp chosen was not put into a circuit and was discussed on the basis of what was given in the datasheet. The next step would be to build and test the preamplifier ensuring that it can handle the low voltage input. Changes may need to be made incase the output voltage is not high enough where an option would be to add a second stage.

### Switch

An active switch could be a better option rather than the passive method. By having a pulse that turns on and off almost instantly as opposed to the sine wave from the rf

pulse would minimise noise leakage. The passive switch relies on the transmitter being switched off or on when switching from open to closed.

## 6.2 Conclusions

The main goal of the project was to provide an appropriate design for a benchtop MRI system that could eventually be constructed. An important factor was being able to utilise components available within the lab to keep costs to a minimum. Having a system such as this available, can provide for a great teaching resource which helps in demonstrating the principles of NMR. The project involved investigating the different components individually and if they were to be put together that it functions as expected.

### Halbach Magnet

The magnetic field encompassing the area where the sample was to be placed was not very uniform and that was something that needed to be taken into consideration. This meant that after measuring the magnetic field with a Hall sensor, an appropriate amount of power would have to be calculated and then be delivered. Magnetic field graphs are provided in the appendix (Section B).

### RadioProcessor/Power Amplifier

Components such as the transmit/receive system and the power amplifier were already available. Time needed to be spent examining how they worked individually and whether it would be suitable as part of the system. The RadioProcessor output could be varied and set depending on the output required from the power amplifier.

### NMR Probe

A probe was a key requirement and had to be built, as there aren't probes that are commercially available. It heavily depends on the external magnet being used and the size of the sample to be imaged. A probe was successfully constructed and tuned to 10.59MHz and matched to 50Ω which allowed for optimum power transfer.

### Passive Switch

A passive switch design was researched and discussed. The switch in its entirety is quite simple in nature and makes use of 2 sets of crossed diodes and a  $\lambda/4$  line. This cable, for a specific frequency, has a property where if the impedance on one side is 0, the other side becomes infinite. This ensures that the receive circuit remains disconnected to the circuit while the excitation pulses are being transmitted.

**Preamplifier**

The induced voltage in the sample to be imaged is expected to be quite small, usually in the microvolts range. This voltage isn't something that can be picked up easily by the RadioProcessor, which is why a preamplifier is required. The amplifier chosen was an op amp manufactured by Linear Technologies which had a gain of about 50dB at our spectrometer frequency.



# Chapter 7

## Abbreviations

dB	Decibels
dBm	Decibels milliWatts
FID	Free Induction Decay
GBP	Gain Bandwidth Product
Ghz	Gigahertz
MRI	Magnetic Resonance Imaging
NMR	Nuclear Magnetic Resonance
RMS	Root Mean Square
RF	Radio Frequency
RX	Receiver
SNR	Signal to Noise Ratio
SINR	Signal to Interference plus Noise Ratio
TX	Transmitter



# Appendix A

## Circuit Analysis

### A.1 LC Resonant Circuit Analysis

$$\begin{aligned} Z_0 &= R + j\omega L \parallel \frac{1}{j\omega C_T} \\ &= \left[ \frac{1}{R + j\omega L} + \frac{1}{\frac{1}{j\omega C_T}} \right]^{-1} \\ &= \frac{1}{R + j\omega L} + j\omega C_T \\ &= \frac{1 + j\omega C_T(R + j\omega L)}{R + j\omega L} \\ &= \frac{R + j\omega L}{1 + j\omega C_T(R + j\omega L)} \\ &= \frac{R + j\omega L}{1 + Rj\omega C_T + j^2\omega^2 C_T L} \\ &= \frac{R + j\omega L}{1 + Rj\omega C_T - \omega^2 C_T L} \\ &= \frac{R + j\omega L}{(1 - \omega^2 C_T L) + Rj\omega C_T} \end{aligned}$$

the conjugate would be

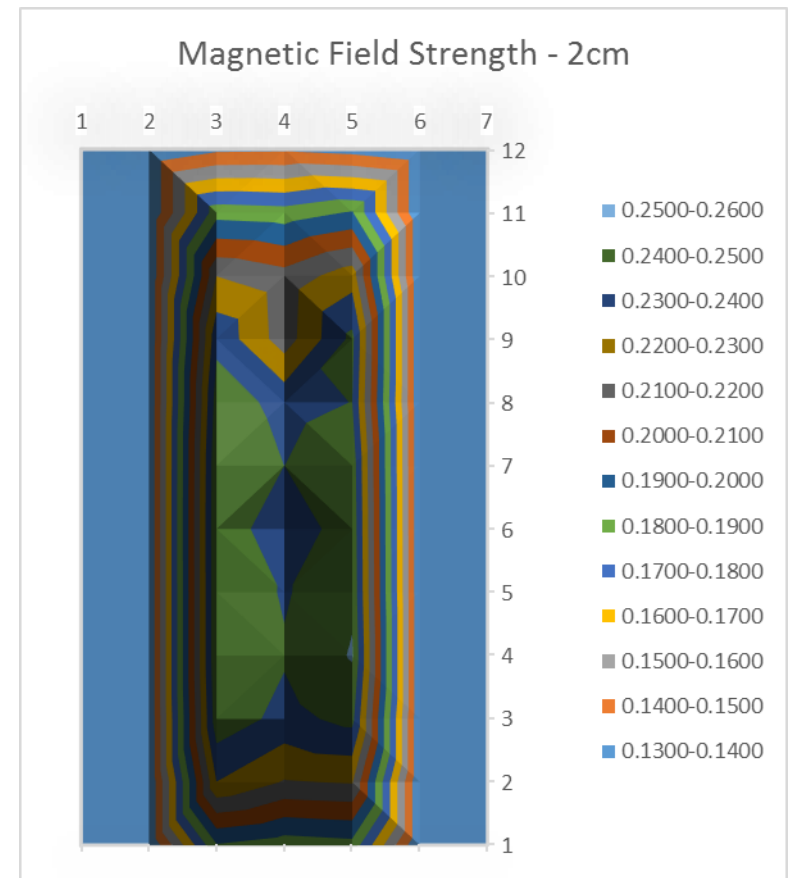
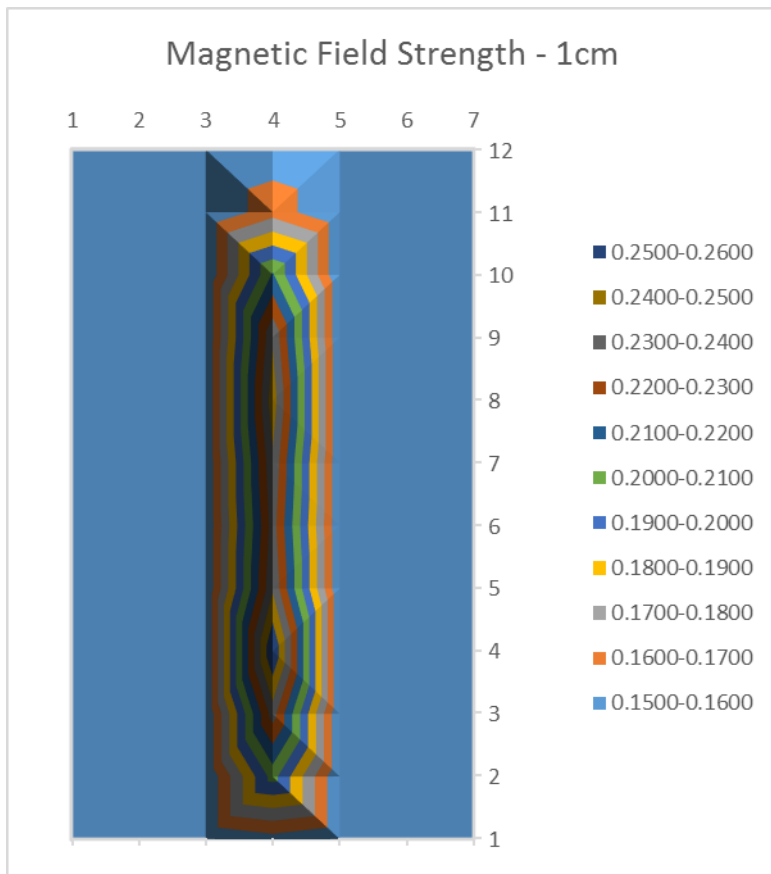
$$\begin{aligned}
 &= \frac{(R + j\omega L)((1 - \omega^2 LC_T) - j\omega RC_T)}{(1 - \omega^2 LC_T)^2 - (\omega RC_T)^2} \\
 &= \frac{(R + j\omega L)(1 - \omega^2 LC_T) - (R + j\omega L)(j\omega RC_T)}{(1 - \omega^2 LC_T)^2 - (\omega RC_T)^2} \\
 &= \frac{R(1 - \omega^2 LC_T) + \omega^2 LC_T + j(-\omega R^2 C_T + \omega L(1 - \omega^2 LC_T)^2)}{(1 - \omega^2 LC_T)^2 - (\omega RC_T)^2} \\
 &= \frac{R - R\omega^2 LC_T + \omega^2 RLC_T + j(-\omega R^2 C_T + \omega L(1 - \omega^2 LC_T)^2)}{(1 - \omega^2 LC_T)^2 - (\omega RC_T)^2} \\
 &= \frac{R + j(-\omega R^2 C_T + \omega L(1 - \omega^2 LC_T)^2)}{(1 - \omega^2 LC_T)^2 - (\omega RC_T)^2} \\
 &= \frac{R}{(1 - \omega^2 LC_T)^2 - (\omega RC_T)^2} + \frac{j(-\omega R^2 C_T + \omega L(1 - \omega^2 LC_T)^2)}{(1 - \omega^2 LC_T)^2 - (\omega RC_T)^2}
 \end{aligned}$$

# Appendix B

## Hallbach Magnetic field table

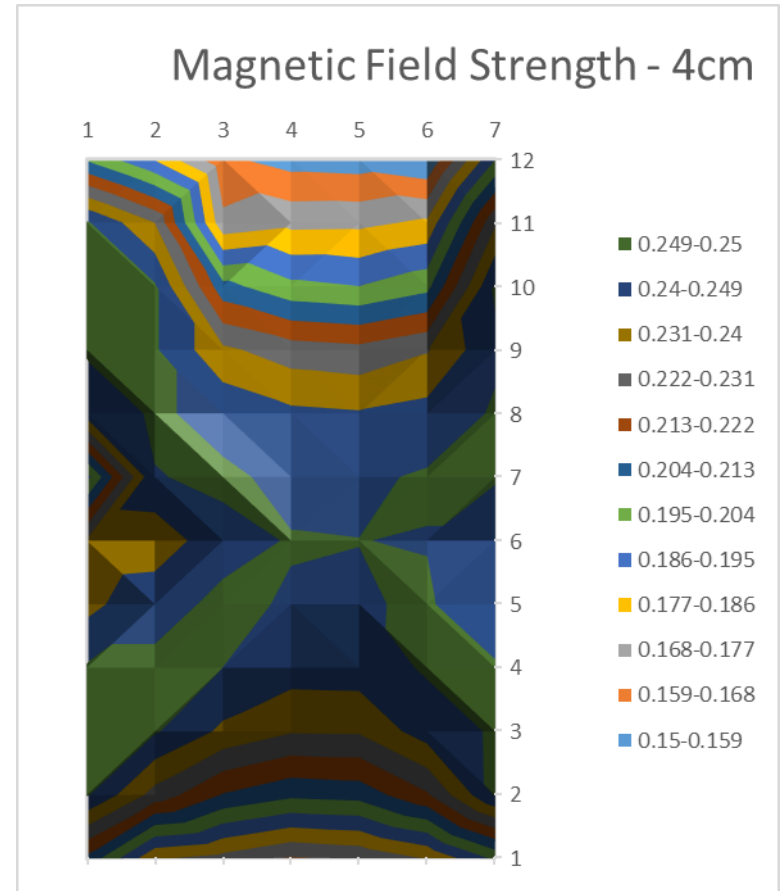
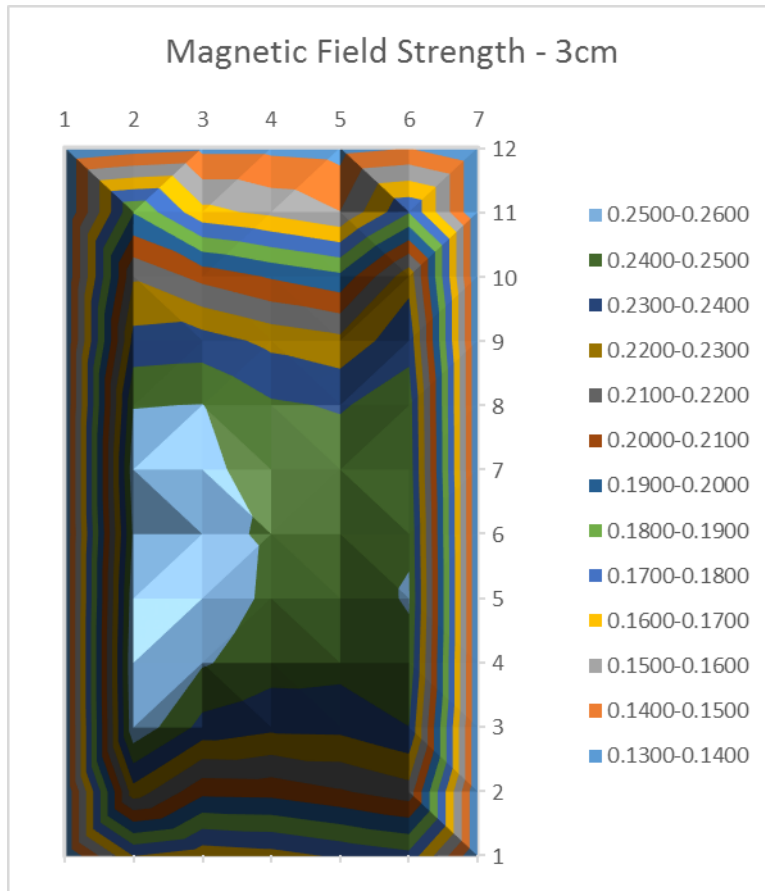
1cm (Base)	1	2	3	4	5	6	7
1				0.1559			
2				0.20408			
3				0.23462			
4				0.26272			
5				0.23862			
6				0.23467			
7				0.23833			
8				0.24544			
9				0.23877			
10				0.2112			
11				0.1659			
12				0.15428			

2cm	1	2	3	4	5	6	7
1			0.18907	0.18442	0.18645		
2			0.22985	0.21921	0.22069		
3			0.24638	0.23674	0.243		
4			0.2492	0.24113	0.2508		
5			0.24913	0.2389	0.24839		
6			0.24946	0.23069	0.24763		
7			0.2488	0.23996	0.24631		
8			0.24504	0.23698	0.24015		
9			0.23751	0.21491	0.24264		
10			0.21982	0.21386	0.22553		
11			0.18612	0.18453	0.19089		
12			0.13809	0.13849	0.13587		



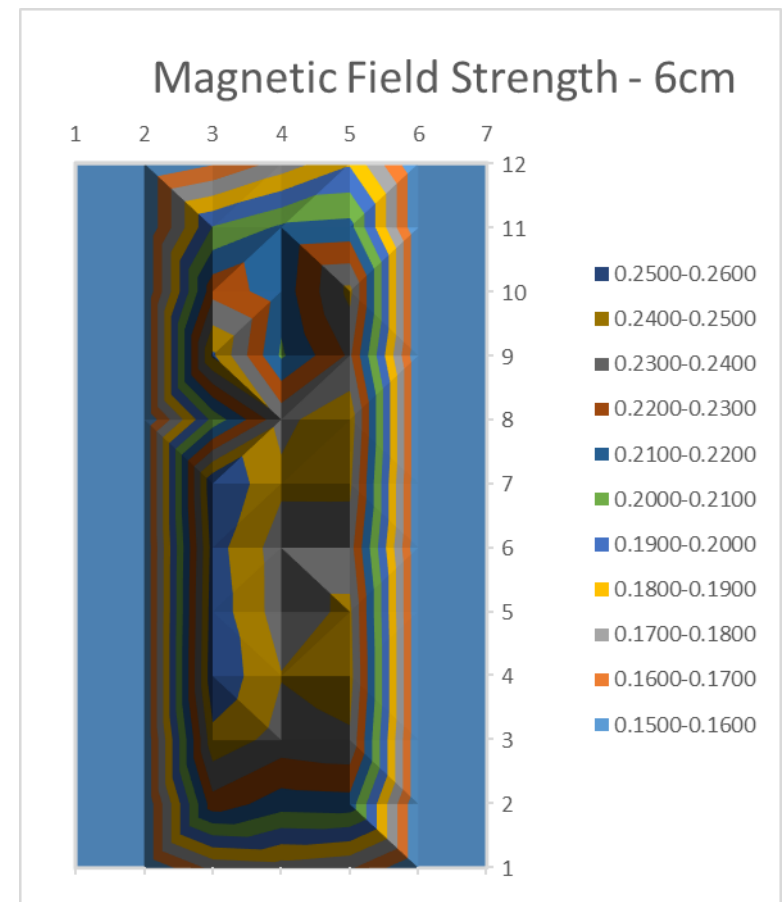
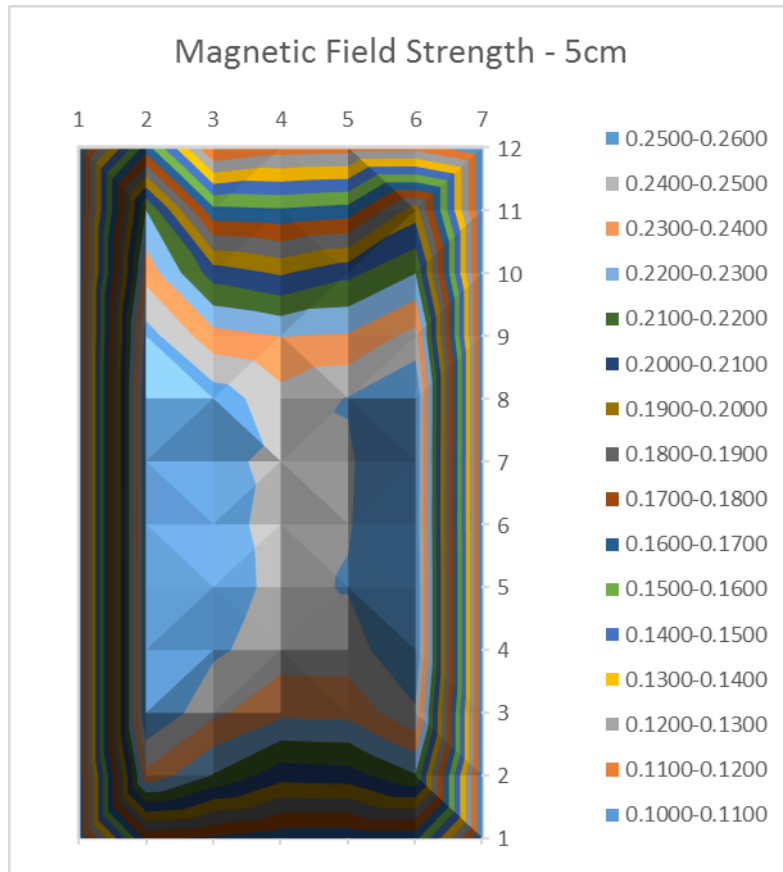
3cm	1	2	3	4	5	6	7
1		0.17006	0.16342	0.16584	0.17141	0.17659	
2		0.22587	0.20273	0.20347	0.20886	0.21567	
3		0.2578	0.23665	0.23223	0.23273	0.23985	
4		0.26187	0.25098	0.24483	0.24356	0.24795	
5		0.25712	0.25337	0.24892	0.24635	0.25065	
6		0.25168	0.25153	0.24927	0.24644	0.24911	
7		0.25636	0.25198	0.24651	0.24538	0.2462	
8		0.2496	0.25022	0.24139	0.2391	0.24484	
9		0.23334	0.23469	0.22737	0.22296	0.23673	
10		0.218777	0.20667	0.19875	0.19223	0.22662	
11		0.18915	0.16291	0.15748	0.1502	0.17922	
12		0.12482	0.12755	0.12754	0.12608	0.12971	

4cm	1	2	3	4	5	6	7
1	0.21078	0.1781	0.17381	0.16706	0.16955	0.17761	0.19682
2	0.26516	0.2275	0.21243	0.20607	0.20752	0.22089	0.24989
3	0.28917	0.25463	0.23815	0.23175	0.23205	0.24462	0.27333
4	0.28138	0.26411	0.24899	0.2442	0.24456	0.2506	0.26566
5	0.23712	0.24732	0.25001	0.24858	0.24837	0.24992	0.24242
6	0.23175	0.23308	0.24749	0.24928	0.24907	0.2487	0.24171
7	0.19182	0.24875	0.25003	0.24763	0.24752	0.25074	0.25342
8	0.24408	0.26493	0.24689	0.24191	0.24073	0.24329	0.26282
9	0.28196	0.26345	0.23281	0.22638	0.22452	0.23019	0.24757
10	0.28522	0.25963	0.20699	0.19731	0.19506	0.20111	0.25229
11	0.26819	0.23078	0.17036	0.17451	0.17486	0.17866	0.22971
12	0.20256	0.18504	0.16069	0.15524	0.15418	0.15002	0.19461

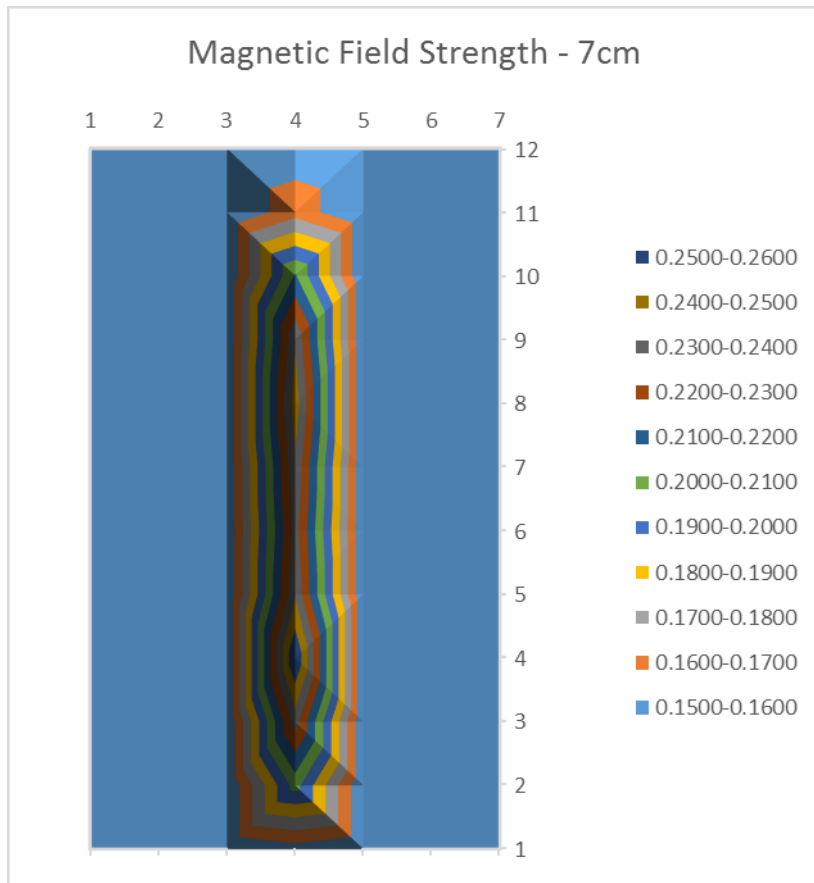


5cm	1	2	3	4	5	6	7
1		0.1722	0.1680	0.1632	0.1626	0.1632	
2		0.2373	0.2192	0.2043	0.2055	0.2192	
3		0.2683	0.2422	0.2323	0.2330	0.2484	
4		0.2760	0.2518	0.2449	0.2450	0.2609	
5		0.2705	0.2546	0.2474	0.2507	0.2635	
6		0.2597	0.2532	0.2471	0.2494	0.2586	
7		0.2673	0.2520	0.2481	0.2490	0.2590	
8		0.2696	0.2558	0.2436	0.2505	0.2605	
9		0.2543	0.2337	0.2296	0.2309	0.2435	
10		0.2363	0.2051	0.1987	0.2072	0.2197	
11		0.2200	0.1627	0.1612	0.1642	0.1950	
12		0.1642	0.1080	0.1143	0.1155	0.1159	

6cm	1	2	3	4	5	6	7
1			0.17275	0.17528	0.17128		
2			0.22587	0.21471	0.21576		
3			0.24696	0.23578	0.23875		
4			0.25793	0.24045	0.24415		
5			0.25638	0.2347	0.24215		
6			0.25448	0.2346	0.23448		
7			0.25945	0.24205	0.24211		
8			0.20309	0.2375	0.24677		
9			0.25159	0.2084	0.23175		
10			0.2269	0.2142	0.2427		
11			0.2006	0.2117	0.2135		
12			0.1589	0.1736	0.1886		



7cm (Top)	1	2	3	4	5	6	7
1				0.1559			
2				0.20408			
3				0.23462			
4				0.26272			
5				0.23862			
6				0.23467			
7				0.23833			
8				0.24544			
9				0.23877			
10				0.2112			
11				0.1659			
12				0.15428			





# Appendix C

## Project Deliverables

### C.1 Thesis Preparation Report

# Development of Electronics for a Benchtop NMR/MRI system

Daniel Fonseca - 42446309

ENGG411 – Engineering Research Thesis  
Department of Engineering  
Macquarie University NSW 2019 Australia  
E-mail: daniel.fonseca@students.mq.edu.au  
10<sup>th</sup> March, 2016

**Abstract**— this report looks at preparing for a Thesis project. The project revolves around researching and building a system that can transmit and receive signals from a benchtop NMR/MRI system and its applications. Included, is a Project plan looking at how the project will be carried out and its approximate scheduling.

## I. INTRODUCTION

Magnetic Resonance Imaging systems are used on a regular basis for the study of animals, plants and humans. Currently there exist systems that cost millions of dollars which are used to create images of many different parts of the human body to aid in the detection of possible abnormalities. These systems provide high quality images and do not require a lot of time to create an image.

Unfortunately it is not possible to use these sort of systems for research purposes as they are also quite large and expensive. There have been many groups that have created smaller and more inexpensive units for laboratory and teaching purposes.

## II. PROJECT SPECIFICATIONS

### A. Thesis Challenge to be solved

Currently there is a need for a transmit/receive system that is able to be integrated into an existing Halbach cylinder. This will depend on the uniformity of the cylinder and whether it will be appropriate to use to look at the magnetic resonance of small droplets of water.

### B. Hydrogen

The project will be focusing on Hydrogen atoms due to it having an odd number of protons within the nucleus. Since the proton is a positive electrical charge that is constantly spinning, a magnetic field is induced as a result. The frequency at which a proton precesses depends on the magnetic field which it is in. This can be calculated using the Larmors equation given that the gyromagnetic ratio for hydrogen is 42.5 MHz/T.

A majority of the protons cancel each other out as they point in all sorts of directions. But when placed in an external magnetic field, about half of the protons line up in the

opposite direction of the magnetic field and slightly more than half of the electronics line up in the direction of the magnetic field. This results in the net magnetization of the protons in the direction of the external magnetic field.

### C. Apparatus to be used

A Halbach magnet has already been previously constructed by my supervisor Yves De Deene.

It is possible to have a magnetic field that is homogeneous by utilizing the Halbach magnet design. Many magnets are placed in a cylindrical manner allowing the very center of the cylinder to have a uniform magnetic field. The orientation of the magnetic field is transverse to the cylindrical axis [3].

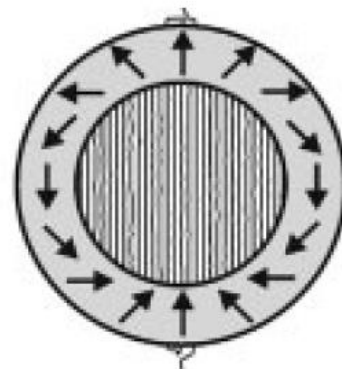


Fig. 1 Ideal Halbach magnet design

### D. Electronics Component

Items that will need to be used include a signal and pulse generator at the input. A switch will be needed to ensure the receive circuit is isolated from the transmit circuit.

It is very challenging in order to detect a signal from there because it is an issue of signal to noise ratio. Signal-to-noise ratio (abbreviated SNR) is a measure that compares the level of a desired signal to the level of background noise. It is defined as the ratio of signal power to the noise power, often expressed in decibels.

There is noise from all the other electronics that detect the signal on one hand, and from the preamplifier as well. A relatively low voltage is induced in those coils, so if there is any noise, it could be hidden within it. What it comes down to is that a frequency filter needs to be added to get rid of the noise. An active filter may be used with a chosen input voltage. This filter can help reduce the noise more efficiently. We need to look more quantitatively as to how large the voltage is to be detected in terms of the noise that will also be picked up. Calculations can be done to find out how much voltage can be induced in these coils and then we can work out with some test measurements.

### III. LITERATURE REVIEW

#### A. A mobile one-sided NMR sensor with a homogeneous magnetic field: The NMR Mole[1]

This journal article provides an explanation of a design of a one-sided NMR sensor. This particular design has many applications where it may be important to measure moisture content in samples that cannot be moved or large samples of liquids. The system can be placed on top of the sample rather than the sample having to fit in between magnets.

The magnet that they have designed is based on 8 cylindrical magnets and a disc magnet which are position in such a way that the magnetic field in the middle is uniform (Fig. 2). The magnets are spaced equally and are all tilted at the same angle. Adjusting the angle affects the magnetic field homogeneity and its position.

The magnetic field that is produced by the magnets is orthogonal to its surface. The coils that have been designed needs to create a magnetic field parallel to the surface. This was achieved using a figure 8 coil where 2 separate coils of wires of a certain length are separated by a distance (Fig. 3). When calculating the length and distance, there will need to be a compromise between the required field strength and the uniformity of the field. This is something I will need to consider with my design of the transmit/receive coils. If the number of turns are increased, so can the sensitivity of the coil.

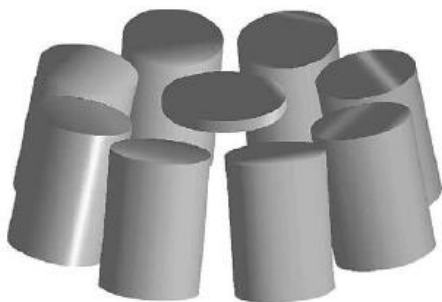


Fig. 2: Magnet arrangement

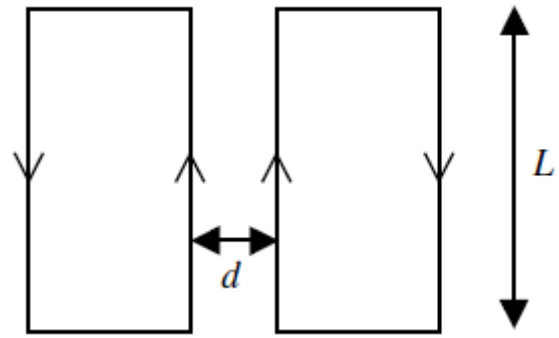


Fig. 3 Figure 8 coil

To reduce dielectric coupling and improve sensitivity, the coil was placed in a circuit with “tuning capacitors of equal size in both sides”. The tuning and matching capacitors determine the resonance frequency ( $\nu_0$ ) of the circuit, bandwidth ( $\Delta V$ ) and quality factor ( $Q = \nu_0 / \Delta V$ ) which can be used to work out the Signal to noise ratio.

#### B. Miniature Permanent Magnet for Table-top NMR[2]

The magnet structure that was used consisted of 8 cylindrical magnets that were placed in an aluminum cylinder utilizing the Halbach design. The magnetic field that was measured was 0.5964 T so the coil was tuned and matched to the Larmor frequency of 25.406 MHz. The schematic of the coil circuit can be seen in Fig. 4 where tuning and matching capacitors are used to achieve the Larmor Frequency. The coil had an inner diameter of 4mm, 8 turns and a length of 5mm.

The excitation and detection system that was designed is shown in Fig. 5. The signal generator generates a signal that is at the Larmor frequency which is then modulated by a pulse generator. A switch and Schottky diodes are used to keep the transmit signal from entering the receive amplifier. The signal received is amplified and passed through a filter before entering an acquisition card.

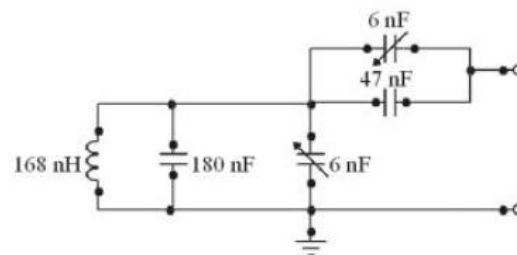


Fig. 4 Schematic of Coil Circuit

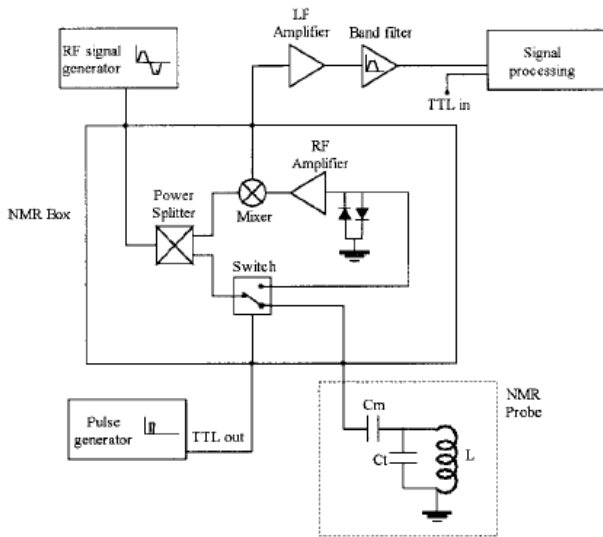


Fig. 5 Transmit/Receive System

### C. Filters

When it comes to designing a filter it is important to know four things before starting out [4]:

- Power supply available
- The frequencies to be passed or rejected
- A transmission/center frequency
- An initial capacitor value which depends on the frequencies that are being used

It is not known yet what type of filter will be used as part of the project, so that will be decided at the time in conjunction with the supervisor.

### D. Inductance of a coil

$$L = \frac{\mu_0 n^2 A}{l}$$

$\mu_0$  > Magnetic permeability of free space ( $4\pi \times 10^{-7}$ )

$n$  > No. of turns

$A$  > Area of one of the wire loops

$L$  > Length of the coil, measured from 1<sup>st</sup> to last turn

### E. Larmor's Frequency

The precession frequency is important as a pulse at the same frequency can be applied to the proton allowing for energy to be transferred from the RF pulse.

$$\omega_o = \gamma B_o \quad (2)$$

$\omega_o$  > Precession frequency in Hz

$\gamma$  > Gyromagnetic ratio of the material

$B_o$  > Strength of the external magnetic field

### F. Magnetic Momentum

Nuclear Magnetic Resonance is where nuclei in a magnetic field absorb and re-emit electromagnetic radiation at a specific resonance frequency [5]. To measure the magnetic momentum of a particle with a net spin the formula:

$$\mu = \gamma S = \gamma m_s h \quad (3)$$

$\gamma$  = gyromagnetic ratio of particle

$S$  = spin angular momentum

$m_s$  = magnetic quantum number

$h$  = Planck's constant

When the nuclei is in a uniform magnetic field in the direction z, it will align in parallel or anti parallel in the direction of the field.

### G. Biot Savart's Law

When testing the detection system within the project, a copper loop will be used.

In order to find the magnetic field that is produced at a point by a current in a curved wire, equation (4) is used. It is important to note that the equation only finds us the magnetic field at the center of a full circle of current [5]. An arc requires a modification in the formula.

$$B = \frac{\mu_0 i}{2R} \quad (4)$$

$\mu_0$  = permeability constant

$R$  = radius of the loop

$I$  = current

### H. Spin Magnetic Dipole Moment

An electron within an atom has a spin angular momentum also known as 'spin' [5]. The spin itself cannot be measured but there is a component with relation to direction which can. Therefore the electron has a spin-up state and a spin-down state.

$$S_z = m_s \frac{h}{2\pi}$$

Where  $m_s = \pm 1/2$

$m_s$  = spin magnetic quantum number

$h$  = Planck's constant

## IV. PROJECT PLAN

This project will hopefully take around 15 weeks to accomplish which include the process of research, design, assembly and testing. It will begin with me brushing up on all the required

physics and electronics knowledge I'll need. Using this knowledge I will be able to complete the project successfully with the guidance of the project supervisor.

*A. Project Goals*

The goals for the project:

- Understand why magnetic resonance imaging is used
- Understand and research electromagnetism and other required knowledge needed to complete the project
- Research further into benchtop NMR/MRI Systems
- Look into the knowledge of electronics required in relation to amplifiers and filters.
- Understand the equipment being used that is currently in the lab
- Observe that the transmit and receiving coils are working by simulating a magnetic field using a copper wire
- Design the necessary filter

The project will be broken down into different stages in conjunction with the project goals:

- Planning and Documenting
- In depth Researching
- Design Analysis
- Construction of the system
- Testing

*B. Roles & Responsibilities*

My role and responsibility will be to conduct the project in an efficient manner. The supervisor will be there to assist where necessary.

*C. Project Schedule*

My thesis project will commence semester 1, 2016. Documenting everything that is done during the project will be imperative. The expected start and finish time is given in table 1 Gantt chart below. The amount of hours I expect to put in per weekday is between 6-8 hours during the period of the project.

*D. Resources*

The resources that are required to carry out the project are:

- Textbooks
- Journal Articles
- Supervisor
- Apparatus is provided in the laboratory
- Possibly other academics

Research	1/03/2016	90
Design	1/04/2016	30
Construction	15/04/2016	50
Testing	15/05/2016	20
Documenting	1/03/2016	95
Report Due Date	6/06/2016	1
Seminar title/extract	6/06/2016	6
Poster	6/06/2016	14
Presentation	6/06/2016	16

Table1: Expected start dates

V. CONCLUSION

Hopefully though this project, a way will be found in which a signal from the protons in water can be detected therefore making the project successful. This project will be carried out in the Biomedical Engineering Labs in conjunction with Yves DeDeene as a supervisor.

Goal	Start Date	Duration(days)
Planning	1/3/16	30

REFERENCES

- [1] B. Manz, A. Coy, R. Dykstra, C.D. Eccles, M.W. Hunter, B.J. Parkinson, P.T. Callaghan, "A mobile one-sided NMR sensor with a homogeneous magnetic field: The NMR Mole", *Journal of Magnetic Resonance*, Vol. 183, pp. 25-31, 2006
- [2] G. Moresi, R. Magin, "Miniature Permanent Magnet for Table-top NMR", *Concepts in Magnetic Resonance Part B: Magnetic Resonance Engineering*, Vol.19(1), pp. 35-43, 2003
- [3] N. Dogan, R. Topkaya, H. Subasi, Y. Terli, B. Rameev, "Development of Halback magnet for portable NMR device", *International Conference of Superconductivity and Magnetism: Journal of Physics: Conference Series 153*, IOP Publishing, 2009
- [4] B. Carter, "Filter Design in Thirty Seconds", Application Report, Texas Instruments, 2001
- [5] Bio-Savarts Law, [Online], Available: [http://en.wikipedia.org/wiki/Biot%E2%80%93Savart\\_law](http://en.wikipedia.org/wiki/Biot%E2%80%93Savart_law)
- [6] Walker, J. *Fundamentals of Physics*, 9<sup>th</sup> Ed. John Wiley & Sons 9, 2011

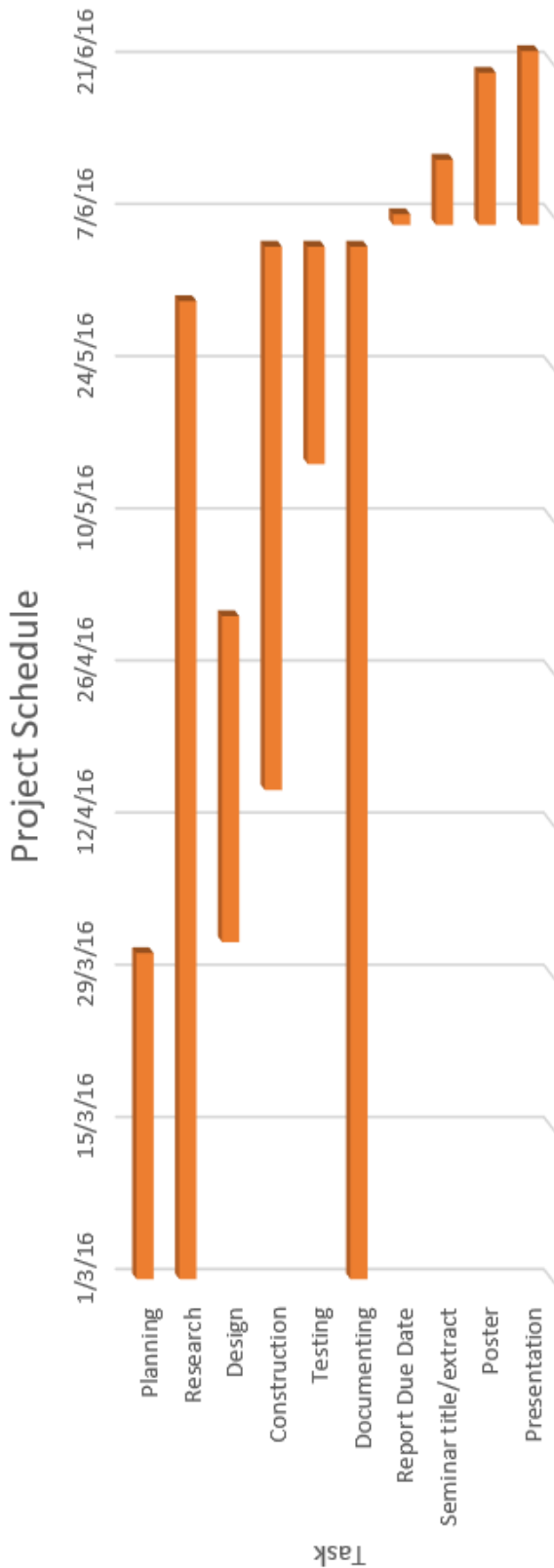
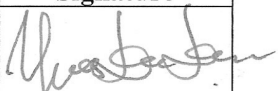
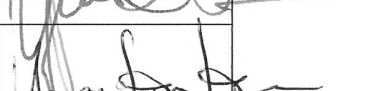
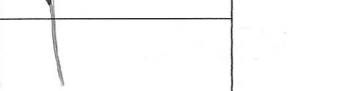


Fig. 6 Gantt chart

## **C.2 Meeting Records**

### Consultation Meetings Attendance Form

Week	Date	Comments (if applicable)	Student's Signature	Supervisor's Signature
1	3/3/16	Discuss which magnet to use, Hall sensors		
3	16/3/16	Coils - size, type		
5	1/4/16	General thesis, concept discussion		
7	13/4/16	values decided on are ideal, too expensive, need a smaller coil that uses less power		
Mid sem break	27/4/16	Spectrum analyser walk through		
8	6/5/16	Probe design & tuning		
10	19/5/16	use of Radio Processor		
11	27/5/16	Preamp design, overall concepts		

# Appendix D

## Datasheets

### D.1 Honeywell Hall Sensor

# Solid State Sensors

## Analog Position Sensors

SS94A Series



### FEATURES

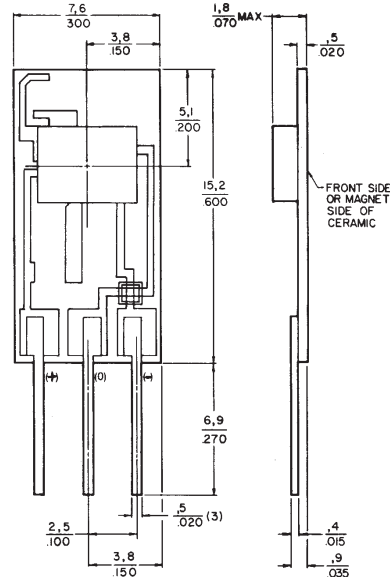
- Single current sinking or current sourcing linear output
- Improved temperature stability
- Three pin in-line printed circuit board terminals
- Standard .100" mounting centers
- Laser trimmed thin film and thick film resistors minimize sensitivity variations and compensate for temperature variations
- Flux range of  $\pm 100$  to  $\pm 2500$  gauss

### OPERATION

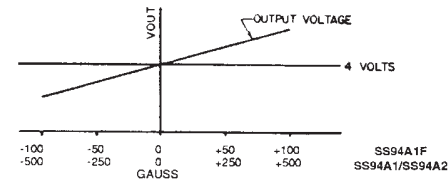
The SS9 utilizes a Hall effect integrated circuit chip which provides increased temperature stability and performance. Laser trimmed thick film resistors on the ceramic substrate and thin film resistors on the integrated circuit reduce null and gain shifts over temperature which results in consistent sensitivity from one device to the next.

### MOUNTING DIMENSIONS (For reference only)

#### SS9



### TYPICAL TRANSFER CHARACTERISTICS



Analog

### SS9 ORDER GUIDE

Catalog Listing	SS94A1	SS94A1B	SS94A1E	SS94A1F	SS94A2	SS94A2C	SS94A2D
Main Feature	Gen. purpose	5 VDC operation	Low drift	High sensitivity	Noise shielded††	Noise shielded††	Noise shielded††
Supply Voltage (VDC)*	6.6 to 12.6	4.5 to 8.0	6.6 to 12.6				
Supply Current (mA)**	13 typ. 30 max.	8 typ. 17.5 max.	13 typ. 30 max.	13 typ. 30 max.	13 typ. 30 max.	13 typ. 30 max.	13 typ. 30 max.
Output Current (mA) Sinking or Sourcing	1 max.						
Response Time ( $\mu$ sec.)	3 typ.						
Magnetic Characteristics*** Span*	.625 $V_s$	.375 $V_s$	.625 $V_s$				
Range (gauss)*	-500 to +500	-500 to +500	-500 to +500	-100 to +100	-500 to +500	-1000 to +1000	-2500 to +2500
Sensitivity (mV/gauss @ 25°C)	5.0 $\pm$ .1	1.875 $\pm$ .100	5.0 $\pm$ .1	25.0 $\pm$ .5	5.0 $\pm$ .1	2.50 $\pm$ .05	1.00 $\pm$ .02
Linearity† (% span)	-0.8 typ. -1.5 max.						
Vout (0 gauss @ 25°C)***	4.00 $\pm$ .04V	2.50 $\pm$ .05V	4.00 $\pm$ .04V	4.00 $\pm$ .08V	4.00 $\pm$ .04V	4.00 $\pm$ .04V	4.00 $\pm$ .04V
Temperature Error (all %s reference 25°C value)* Null (%/°C)	$\pm$ .02	$\pm$ .025	$\pm$ .01	$\pm$ .10	$\pm$ .02	$\pm$ .0125	$\pm$ .007
Gain (%/°C)	$\pm$ .02	$\pm$ .025	$\pm$ .02	+0.2 -0.055	$\pm$ .02	$\pm$ .02	$\pm$ .02

\* -40° to 125°C.

MilliTesla = Gauss  $10^{-3}$

\*\* Excludes load. Typical at 25°C/Maximum at -40°C.

\*\*\* @  $V_s = 5$  VDC for SS94A1B only/@  $V_s = 8$  VDC for all others.

† Derived from straight line between end points.

†† Silver coating on back of ceramic is electrically connected to - terminal. Specified using a 2.2K $\Omega$  resistor unless otherwise noted.

Null voltage (Vout at 0 gauss) and sensitivity are ratiometric to supply voltage.

**Magnets page 25.**

Application consideration: The output is clamped at the high end. Clamping voltage may be as low as 9VDC. The output will not exceed the clamping voltage regardless of field strength or supply voltage.

## **D.2 RadioProcessor G Specifications**

## Specifications

**Table 1: Product Specifications.**

<b>Parameter</b>		<b>Min</b>	<b>Typ</b>	<b>Max</b>	<b>Units</b>
Analog Input	Input Frequency Range	0		100	MHz
	A/D Sampling Precision			14	bits
	Input Voltage Range (peak-peak)			1.13	V
	A/D Sampling Frequency		75 <sup>(1)</sup>		MHz
RF Analog Output	D/A Sampling Rate		300		MHz
	D/A Sampling Precision			14	bits
	Output Voltage Range (peak-peak)			1.2 <sup>(2)</sup>	V
	Phase resolution			0.09	deg.
	Frequency resolution		0.28		Hz
Gradient Analog Output	Output Voltage (1 kOhm load)	-3.3		3.3	V
	Update rate	66.6			ns
	Resolution		16		bits
Digital Output	Number of Digital Outputs		4		
	Logical 1 output voltage		3.3 <sup>(2)</sup>		V
	Logical 0 output voltage		0		V
	Output drive current			25	mA
	Rise/Fall time			< 5	ns
Digital Input (HW_Trig, HW_Reset)	Logical 1 Input voltage	1.7		4.1	V
	Logical 0 Input voltage	-0.5		0.7	V
Data acquisition	Spectral width (SW) of acquired data	72 Hz		9.4 MHz	
	# Complex points	1		16k	
Pulse Program	# of Instruction words			2048	words
	Pulse resolution <sup>(3)</sup>		13.3		ns
	Pulse length <sup>(4)</sup>	66.6 ns		693 days	

**Notes**

(1): If the signal to be detected is very close to ¼ of the sampling rate, there will be aliasing during the detection process. To alleviate this, a slightly higher or lower clock speed can be used.

(2): This is the value seen without using termination. When the line is terminated with 50Ω, the output voltage will be reduced by as much as half.

(3): Pulse resolution equals one clock period of the PulseBlaster Timing Core clock oscillator.

(4): Minimum pulse width is five clock periods of the PulseBlaster clock oscillator. Maximum pulse width is 2<sup>52</sup> clock periods of the PulseBlaster clock oscillator.

## **D.3 Ophir Power Amplifier Specifications**

## Equipment Specifications

---

Table 1-1. Specifications @ 25° C

Class of Operation:	AB
Frequency Range:	.01 – 200 MHz
Output Power @ Saturation:	100 Watts CW Typical
Output Power @ 1 dB Compression:	60 Watts CW minimum
Small Signal Gain:	+50 dB minimum
Small Signal Gain Flatness:	± 1.5 dB maximum
Input/Output Impedance:	50 ohms nominal
Input VSWR:	2:1 maximum
<b>Max. RF Input</b>	<b>0 dBm</b>
Operating Temperature Range:	0° C to 50° C
Operating Humidity Range:	95%, Non-condensing
Temp. Protection:	Shut down @ 80° C minimum
Cooling system:	Internal Forced Air
AC Input:	100 - 240 VAC, 50/60 Hz, 1Ø
AC Input Power:	600 Watts maximum
Dimensions:	19" W x 8.75" H x 20" D
Weight:	80 Pounds maximum

Option(s) included:

- Type-N Connectors on Rear Panel
- RS-232 Interface Connector on Rear Panel
- IEEE Interface Connector on Rear Panel
- Ethernet Port on Rear Panel
- Front Panel Digital Display

**\*NOTE – Specifications subject to change without notice**

## **D.4 Linear Technologies 626810f Operational Amplifier Datasheet**

## FEATURES

- **Gain Bandwidth Product: 4GHz**
- **Low Input Bias Current:**
  - $\pm 3\text{fA}$  Typ. Room Temperature
  - $4\text{pA}$  Max at  $125^\circ\text{C}$
- **Current Noise (100kHz):  $7\text{fA}/\sqrt{\text{Hz}}$**
- **Voltage Noise (1MHz):  $4.0\text{nV}/\sqrt{\text{Hz}}$**
- **Extremely Low  $C_{\text{IN}}$  0.45pF**
- **Rail-to-Rail Output**
- $A_V \geq 10$
- Slew Rate:  $+1500\text{V}/\mu\text{s}$ ,  $-1000\text{V}/\mu\text{s}$
- Supply Range: 3.1V to 5.25V
- Quiescent Current: 16.5mA
- Operating Temp Range:  $-40^\circ\text{C}$  to  $125^\circ\text{C}$
- Single in 8-Lead SO-8, 6-Lead TSOT-23 Packages
- Dual in 8-Lead MS8, 3mm  $\times$  3mm 10-Lead DFN 10 Packages

## APPLICATIONS

- Transimpedance Amplifiers
- ADC Drivers
- Photomultiplier Tube Post-Amplifier
- Low  $I_{\text{BIAS}}$  Circuits

## DESCRIPTION

The **LTC<sup>®</sup>6268-10/LTC6269-10** is a single/dual 4GHz FET-input operational amplifier with extremely low input bias current and low input capacitance. It also features low input-referred current noise and voltage noise making it an ideal choice for high speed transimpedance amplifiers, and high-impedance sensor amplifiers. It is a decompensated op amp that is gain-of-10 stable.

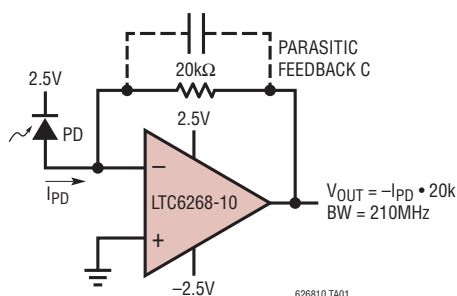
It operates on 3.1V to 5.25V supply and consumes 16.5mA per amplifier. A shutdown feature can be used to lower power consumption when the amplifier is not in use.

The LTC6268-10 single op amp is available in 8-lead SOIC and 6-lead SOT-23 packages. The SOIC package includes two unconnected pins which can be used to create an input pin guard ring to protect against board leakage currents. The LTC6269-10 dual op amp is available in 8-lead MSOP with exposed pad and 3mm  $\times$  3mm 10-lead DFN packages. They are fully specified over the  $-40^\circ\text{C}$  to  $85^\circ\text{C}$  and the  $-40^\circ\text{C}$  to  $125^\circ\text{C}$  temperature ranges.

LT, LT, LTC, LTM, Linear Technology and the Linear logo are registered trademarks of Linear Technology Corporation. All other trademarks are the property of their respective owners.

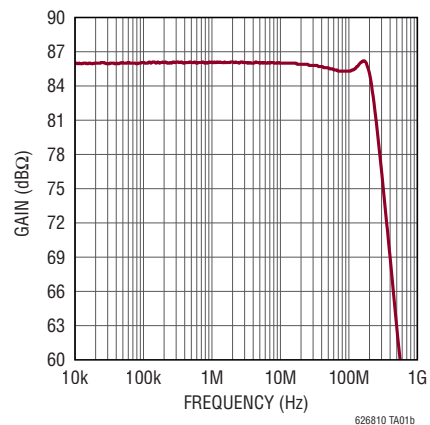
## TYPICAL APPLICATION

**20k $\Omega$  Gain 210MHz Transimpedance Amplifier**



PD = OSI OPTOELECTRONICS, FCI-125G-006

**20k $\Omega$  TIA Frequency Response**



# LTC6268-10/LTC6269-10

## ABSOLUTE MAXIMUM RATINGS

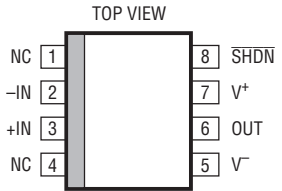
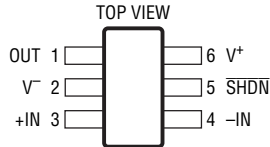
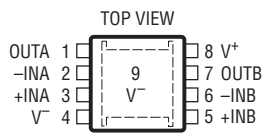
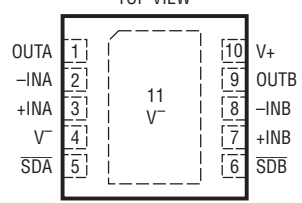
(Note 1)

Supply Voltage $V^+$ to $V^-$ .....	5.5V
Input Voltage .....	$V^- - 0.2V$ to $V^+ + 0.2V$
Input Current (+IN, -IN) (Note 2) .....	$\pm 1mA$
Input Current (SHDN) .....	$\pm 1mA$
Output Current ( $I_{OUT}$ ) (Note 8, 9) .....	135mA
Output Short-Circuit Duration (Note 3) ... Thermally Limited	
Operating Temperature Range	
LTC6268-10I/LTC6269-10I .....	$-40^\circ C$ to $85^\circ C$
LTC6268-10H/LTC6269-10H .....	$-40^\circ C$ to $125^\circ C$

Specified Temperature Range (Note 4)

LTC6268-10I/LTC6269-10I .....	$-40^\circ C$ to $85^\circ C$
LTC6268-10H/LTC6269-10H .....	$-40^\circ C$ to $125^\circ C$
Maximum Junction Temperature .....	$150^\circ C$
Storage Temperature Range .....	$-65^\circ C$ to $150^\circ C$
Lead Temperature S8, S6 and MS8E (Soldering, 10 sec) .....	$300^\circ C$

## PIN CONFIGURATION

<p style="text-align: center;">TOP VIEW</p>  <p style="text-align: center;">S8 PACKAGE 8-LEAD PLASTIC SO <math>T_{JMAX} = 150^\circ C</math>, <math>\theta_{JA} = 120^\circ C/W</math> (NOTE 5)</p>	<p style="text-align: center;">TOP VIEW</p>  <p style="text-align: center;">S6 PACKAGE 6-LEAD PLASTIC TSOT-23 <math>T_{JMAX} = 150^\circ C</math>, <math>\theta_{JA} = 192^\circ C/W</math> (NOTE 5)</p>
<p style="text-align: center;">TOP VIEW</p>  <p style="text-align: center;">MS8E PACKAGE 8-LEAD PLASTIC MSOP <math>T_{JMAX} = 150^\circ C</math>, <math>\theta_{JA} = 40^\circ C/W</math> (NOTE 5) EXPOSED PAD (PIN 9) IS <math>V^-</math>, IT IS RECOMMENDED TO SOLDER TO PCB</p>	<p style="text-align: center;">TOP VIEW</p>  <p style="text-align: center;">DD PACKAGE 10-LEAD (3mm x 3mm) PLASTIC DFN <math>T_{JMAX} = 150^\circ C</math>, <math>\theta_{JA} = 43^\circ C/W</math> (NOTE 5) EXPOSED PAD (PIN 11) IS <math>V^-</math>, IT IS RECOMMENDED TO SOLDER TO PCB</p>

## ORDER INFORMATION

LEAD FREE FINISH	TAPE AND REEL	PART MARKING*	PACKAGE DESCRIPTION	SPECIFIED TEMPERATURE RANGE
LTC6268IS6-10#TRMPBF	LTC6268IS6-10#TRPBF	LTGQT	6-Lead Plastic TSOT-23	-40°C to 85°C
LTC6268HS6-10#TRMPBF	LTC6268HS6-10#TRPBF	LTGQT	6-Lead Plastic TSOT-23	-40°C to 125°C
LTC6268IS8-10#PBF	LTC6268IS8-10#TRPBF	626810	8-Lead Plastic SOIC	-40°C to 85°C
LTC6268HS8-10#PBF	LTC6268HS8-10#TRPBF	626810	8-Lead Plastic SOIC	-40°C to 125°C
LTC6269IMS8E-10#PBF	LTC6269IMS8E-10#TRPBF	LTGRM	8-Lead Plastic MSOP	-40°C to 85°C
LTC6269HMS8E-10#PBF	LTC6269HMS8E-10#TRPBF	LTGRM	8-Lead Plastic MSOP	-40°C to 125°C
LTC6269IDD-10#PBF	LTC6269IDD-10#TRPBF	LGRK	10-Lead Plastic DD	-40°C to 85°C
LTC6269HDD-10#PBF	LTC6269HDD-10#TRPBF	LGRK	10-Lead Plastic DD	-40°C to 125°C

Consult LTC Marketing for parts specified with wider operating temperature ranges. \*The temperature grade is identified by a label on the shipping container.

For more information on lead free part marking, go to: <http://www.linear.com/leadfree/>

For more information on tape and reel specifications, go to: <http://www.linear.com/tapeandreeel/>

## 5.0V ELECTRICAL CHARACTERISTICS

The ● denotes specifications that apply over the full operating temperature range, otherwise specifications are at  $T_A = 25^\circ\text{C}$ ,  $V_{\text{SUPPLY}} = 5.0\text{V}$  ( $V^+ = 5\text{V}$ ,  $V^- = 0\text{V}$ ,  $V_{\text{CM}} = \text{mid-supply}$ ),  $R_L = 1\text{k}\Omega$ ,  $V_{\text{SHDN}}$  is unconnected.

SYMBOL	PARAMETER	CONDITIONS	MIN	TYP	MAX	UNITS
$V_{\text{OS}}$	Input Offset Voltage	$V_{\text{CM}} = 2.75\text{V}$	-0.7 -3	0.2	0.7 3	mV mV
		$V_{\text{CM}} = 4.0\text{V}$	-1.0 -4.5	0.2	1.0 4.5	mV mV
$\text{TC } V_{\text{OS}}$	Input Offset Voltage Drift	$V_{\text{CM}} = 2.75\text{V}$		4		$\mu\text{V}/^\circ\text{C}$
$I_{\text{B}}$	Input Bias Current (Notes 6, 8)	$V_{\text{CM}} = 2.75\text{V}$ LTC6268I-10/LTC6269I-10	-20 -900	$\pm 3$	20 900	fA fA
		LTC6268H-10/LTC6269H-10	-4		4	pA
		$V_{\text{CM}} = 4.0\text{V}$ LTC6268I-10/LTC6269I-10	-20 -900	$\pm 3$	20 900	fA fA
		LTC6268H-10/LTC6269H-10	-4		4	pA
$I_{\text{OS}}$	Input Offset Current (Notes 6, 8)	$V_{\text{CM}} = 2.75\text{V}$ LTC6268I-10/LTC6269I-10	-40 -450	$\pm 6$	40 450	fA fA
		LTC6268H-10/LTC6269H-10	-2		2	pA
$e_{\text{n}}$	Input Voltage Noise Density, $V_{\text{CM}} = 2.75\text{V}$	$f = 1\text{MHz}$		4.0		$\text{nV}/\sqrt{\text{Hz}}$
	Input Voltage Noise Density, $V_{\text{CM}} = 4.0\text{V}$	$f = 1\text{MHz}$		4.0		$\text{nV}/\sqrt{\text{Hz}}$
	Input Referred Noise Voltage	$f = 0.1\text{Hz}$ to $10\text{Hz}$		12.6		$\mu\text{V}_{\text{P-P}}$
$i_{\text{n}}$	Input Current Noise Density, $V_{\text{CM}} = 2.75\text{V}$	$f = 100\text{kHz}$		7		$\text{fA}/\sqrt{\text{Hz}}$
	Input Current Noise Density, $V_{\text{CM}} = 4.0\text{V}$	$f = 100\text{kHz}$		7		$\text{fA}/\sqrt{\text{Hz}}$
$R_{\text{IN}}$	Input Resistance	Differential		>1000		$\text{G}\Omega$
		Common Mode		>1000		$\text{G}\Omega$
$C_{\text{IN}}$	Input Capacitance	Differential (DC to 200MHz)		0.1		pF
		Common Mode (DC to 100MHz)		0.45		pF
CMRR	Common Mode Rejection Ratio	$V_{\text{CM}} = 0.5\text{V}$ to $3.2\text{V}$ (PNP Side)	72 68	85		dB dB
		$V_{\text{CM}} = -0.1\text{V}$ to $4.5\text{V}$	64 52	82		dB dB
IVR	Input Voltage Range	Guaranteed by CMRR	-0.1		4.5	V

626810f

# LTC6268-10/LTC6269-10

## 5.0V ELECTRICAL CHARACTERISTICS

The ● denotes specifications that apply over the full operating temperature range, otherwise specifications are at  $T_A = 25^\circ\text{C}$ ,  $V_{\text{SUPPLY}} = 5.0\text{V}$  ( $V^+ = 5\text{V}$ ,  $V^- = 0\text{V}$ ,  $V_{\text{CM}} = \text{mid-supply}$ ),  $R_L = 1\text{k}\Omega$ ,  $V_{\text{SHDN}}$  is unconnected.

SYMBOL	PARAMETER	CONDITIONS	MIN	TYP	MAX	UNITS
PSRR	Power Supply Rejection Ratio	$V_{\text{CM}} = 1.0\text{V}$ , $V_{\text{SUPPLY}}$ Ranges from 3.1V to 5.25V	● 78 75	95		dB dB
	Supply Voltage Range		● 3.1		5.25	
$A_V$	Open Loop Voltage Gain	$V_{\text{OUT}} = 0.5\text{V}$ to 4.5V	● 125 40	250		V/mV V/mV
		$R_{\text{LOAD}} = 10\text{k}$				
		$R_{\text{LOAD}} = 100$	● 10 2	21		V/mV V/mV
$V_{\text{OL}}$	Output Swing Low (Input Overdrive 30mV) Measured from $V^-$	$I_{\text{SINK}} = 10\text{mA}$	●	80	140 200	mV mV
		$I_{\text{SINK}} = 25\text{mA}$	●	130	200 260	mV mV
$V_{\text{OH}}$	Output Swing High (Input Overdrive 30mV) Measured from $V^+$	$I_{\text{SOURCE}} = 10\text{mA}$	●	70	140 200	mV mV
		$I_{\text{SOURCE}} = 25\text{mA}$	●	160	270 370	mV mV
$I_{\text{SC}}$	Output Short Circuit Current (Note 9)		● 60 40	90		mA mA
$I_{\text{S}}$	Supply Current Per Amplifier		● 15 9	16.5	18 25	mA mA
	Supply Current in Shutdown (Per Amplifier)		●	0.39	0.85 1.5	mA mA
$I_{\text{SHDN}}$	Shutdown Pin Current	$V_{\text{SHDN}} = 0.75\text{V}$	●	-12	2	$\mu\text{A}$
		$V_{\text{SHDN}} = 1.50\text{V}$	●	-12	2	$\mu\text{A}$
$V_{\text{IL}}$	$\text{SHDN}$ Input Low Voltage	Disable	●		0.75	V
$V_{\text{IH}}$	$\text{SHDN}$ Input High Voltage	Enable. If $\text{SHDN}$ is Unconnected, Amp is Enabled	●	1.5		V
$t_{\text{ON}}$	Turn On Time, Delay from $\text{SHDN}$ Toggle to Output Reaching 90% of Target	$\text{SHDN}$ Toggle from 0V to 2V		360		ns
$t_{\text{OFF}}$	Turn Off Time, Delay from $\text{SHDN}$ Toggle to Output High Z	$\text{SHDN}$ Toggle from 2V to 0V		183		ns
GBW	Gain-Bandwidth Product (Note 8)	$f = 10\text{MHz}$	●	3500	4000	MHz
SR+	Slew Rate+	$A_V = 11$ ( $R_F = 1000$ , $R_G = 100$ ) $V_{\text{OUT}} = 0.5\text{V}$ to 4.5V, Measured 20% to 80%, $R_{\text{LOAD}} = 500\Omega$	● 1100 600	1500		V/ $\mu\text{s}$ V/ $\mu\text{s}$
		$A_V = 11$ ( $R_F = 1000$ , $R_G = 100$ ) $V_{\text{OUT}} = 4.5\text{V}$ to 0.5V, Measured 80% to 20%,	● 900 500	1000		V/ $\mu\text{s}$ V/ $\mu\text{s}$
FPBW	Full Power Bandwidth (Note 7)	$4V_{\text{P-P}}$		73		MHz
HD	Harmonic Distortion(HD2/HD3)	$A_V = 10$ , 10MHz. $2V_{\text{P-P}}$ , $V_{\text{CM}} = 2.25\text{V}$ , $R_L = 1\text{k}$ , $R_F = 450\Omega$ , $R_G = 50\Omega$		-91/-96		dB
$I_{\text{LEAK}}$	Output Leakage Current in Shutdown	$V_{\text{SHDN}} = 0\text{V}$ , $V_{\text{OUT}} = 0\text{V}$			400	nA
		$V_{\text{SHDN}} = 0\text{V}$ , $V_{\text{OUT}} = 5\text{V}$			400	nA

626810f

### 3.3V ELECTRICAL CHARACTERISTICS

The ● denotes specifications that apply over the full operating temperature range, otherwise specifications are at  $T_A = 25^\circ\text{C}$ ,  $V_{\text{SUPPLY}} = 3.3\text{V}$  ( $V^+ = 3.3\text{V}$ ,  $V^- = 0\text{V}$ ,  $V_{\text{CM}} = \text{mid-supply}$ ),  $R_L = 1\text{k}\Omega$ ,  $V_{\text{SHDN}}$  is unconnected.

SYMBOL	PARAMETER	CONDITIONS	MIN	TYP	MAX	UNITS	
$V_{\text{OS}}$	Input Offset Voltage	$V_{\text{CM}} = 1.0\text{V}$	-0.7 -3	0.2	0.7 3	mV mV	
		$V_{\text{CM}} = 2.3\text{V}$	-1.0 -4.5	0.2	1.0 4.5	mV mV	
$\text{TC } V_{\text{OS}}$	Input Offset Voltage Drift	$V_{\text{CM}} = 1.0\text{V}$		4		$\mu\text{V}/\text{C}$	
$I_{\text{B}}$	Input Bias Current (Notes 6, 8)	$V_{\text{CM}} = 1.0\text{V}$ LTC6268I-10/LTC6269I-10 LTC6268H-10/LTC6269H-10	● ●	-20 -900 -4	$\pm 3$ 900 4	fA fA pA	
		$V_{\text{CM}} = 2.3\text{V}$ LTC6268I-10/LTC6269I-10 LTC6268H-10/LTC6269H-10	● ●	-20 -900 -4	$\pm 3$ 900 4	fA fA pA	
$I_{\text{OS}}$	Input Offset Current (Notes 6, 8)	$V_{\text{CM}} = 1.0\text{V}$ LTC6268I-10/LTC6269I-10 LTC6268H-10/LTC6269H-10	● ●	-40 -450 -2	$\pm 6$ 450 2	fA fA pA	
$e_{\text{n}}$	Input Voltage Noise Density, $V_{\text{CM}} = 1.0\text{V}$	$f = 1\text{MHz}$		4.0		$\text{nV}/\sqrt{\text{Hz}}$	
	Input Voltage Noise Density, $V_{\text{CM}} = 2.3\text{V}$	$f = 1\text{MHz}$		4.0		$\text{nV}/\sqrt{\text{Hz}}$	
	Input Referred Noise Voltage	$f = 0.1\text{Hz}$ to $10\text{Hz}$		13.5		$\mu\text{V}_{\text{P-P}}$	
$i_{\text{n}}$	Input Current Noise Density, $V_{\text{CM}} = 1.0\text{V}$	$f = 100\text{kHz}$		7		$\text{fA}/\sqrt{\text{Hz}}$	
	Input Current Noise Density, $V_{\text{CM}} = 2.3\text{V}$	$f = 100\text{kHz}$		7		$\text{fA}/\sqrt{\text{Hz}}$	
$R_{\text{IN}}$	Input Resistance	Differential		>1000		$\text{G}\Omega$	
		Common Mode		>1000		$\text{G}\Omega$	
$C_{\text{IN}}$	Input Capacitance	Differential (DC to 200MHz)		0.1		pF	
		Common Mode (DC to 100MHz)		0.45		pF	
CMRR	Common Mode Rejection Ratio	$V_{\text{CM}} = 0.5\text{V}$ to $1.2\text{V}$ (PNP Side)	●	63 60	90	dB dB	
		$V_{\text{CM}} = -0.1\text{V}$ to $2.8\text{V}$ (Full Range)	●	60 50	77	dB dB	
IVR	Input Voltage Range	Guaranteed by CMRR	●	-0.1	2.8	V	
$A_{\text{V}}$	Open Loop Voltage Gain	$V_{\text{OUT}} = 0.5\text{V}$ to $2.8\text{V}$	●	$R_{\text{LOAD}} = 10\text{k}$	80 40	200	V/mV V/mV
		$R_{\text{LOAD}} = 100$		10 2	18	V/mV V/mV	
$V_{\text{OL}}$	Output Swing Low (Input Overdrive 30mV). Measured from $V^-$	$I_{\text{SINK}} = 10\text{mA}$	●		80 140 200	mV mV mV	
		$I_{\text{SINK}} = 25\text{mA}$	●		140 200 260	mV mV mV	
$V_{\text{OH}}$	Output Swing High (Input Overdrive 30mV). Measured from $V^+$	$I_{\text{SOURCE}} = 10\text{mA}$	●		80 140 200	mV mV mV	
		$I_{\text{SOURCE}} = 25\text{mA}$	●		170 270 370	mV mV mV	
$I_{\text{SC}}$	Output Short Circuit Current (Note 9)		●	50 35	80	mA mA	
$I_{\text{S}}$	Supply Current per Amplifier		●	14.5 9	16	17.5 25	mA mA

# LTC6268-10/LTC6269-10

## 3.3V ELECTRICAL CHARACTERISTICS

The ● denotes specifications that apply over the full operating temperature range, otherwise specifications are at  $T_A = 25^\circ\text{C}$ ,  $V_{\text{SUPPLY}} = 3.3\text{V}$  ( $V^+ = 3.3\text{V}$ ,  $V^- = 0\text{V}$ ,  $V_{\text{CM}} = \text{mid-supply}$ )  $R_L = 1\text{k}\Omega$ ,  $V_{\text{SHDN}}$  is unconnected.

SYMBOL	PARAMETER	CONDITIONS	MIN	TYP	MAX	UNITS
	Supply Current in Shutdown (Per Amplifier)			0.23	0.6 1.2	mA mA
$I_{\text{SHDN}}$	Shutdown Pin Current	$V_{\text{SHDN}} = 0.75\text{V}$ $V_{\text{SHDN}} = 1.5\text{V}$	● ●	-12 -12	2 2	$\mu\text{A}$ $\mu\text{A}$
$V_{\text{IL}}$	SHDN Input Low Voltage	Disable	●		0.75	V
$V_{\text{IH}}$	SHDN Input High Voltage	Enable. If SHDN is Unconnected, Amp Is Enabled	●	1.5		V
$t_{\text{ON}}$	Turn On Time, Delay from SHDN Toggle to Output Reaching 90% of Target	SHDN Toggle from 0V to 2V		750		ns
$t_{\text{OFF}}$	Turn Off Time, Delay from SHDN Toggle to Output High Z	SHDN Toggle from 2V to 0V		201		ns
GBW	Gain-Bandwidth Product (Note 8)	$f = 10\text{MHz}$	●	3500	4000	MHz
SR+	Slew Rate+	$A_V = 11$ ( $R_F = 1000$ , $R_G = 100$ ), $V_{\text{OUT}} = 1\text{V}$ to $2.3\text{V}$ , Measured 20% to 80%, $R_{\text{LOAD}} = 500\Omega$	●	800 600	1500	$\text{V}/\mu\text{s}$ $\text{V}/\mu\text{s}$
SR-	Slew Rate-	$A_V = 11$ ( $R_F = 1000$ , $R_G = 100$ ), $V_{\text{OUT}} = 1\text{V}$ to $2.3\text{V}$ , Measured 80% to 20%, $R_{\text{LOAD}} = 500\Omega$	●	600 400	1000	$\text{V}/\mu\text{s}$ $\text{V}/\mu\text{s}$
FPBW	Full Power Bandwidth (Note 7)	$2.3\text{V}_{\text{P-P}}$		105		MHz
HD	Harmonic Distortion(HD2/HD3)	$A = 10$ , $10\text{MHz}$ . $2\text{V}_{\text{P-P}}$ , $V_{\text{CM}} = 1.65\text{V}$ , $R_L = 1\text{k}$ , $R_F = 450\Omega$ , $R_G = 50\Omega$		-67/-78		dB

**Note 1:** Stresses beyond those listed under Absolute Maximum Ratings may cause permanent damage to the device. Exposure to any Absolute Maximum Rating condition for extended periods may affect device reliability and lifetime.

**Note 2:** The inputs are protected by two series connected ESD protection diodes to each power supply. The input current should be limited to less than 1mA. The input voltage should not exceed 200mV beyond the power supply.

**Note 3:** A heat sink may be required to keep the junction temperature below the absolute maximum rating when the output is shorted indefinitely.

**Note 4:** The LTC6268-10/LTC6269-10 is guaranteed to meet specified performance from  $-40^\circ\text{C}$  to  $85^\circ\text{C}$ . The LTC6268-10H/LTC6269-10H is guaranteed to meet specified performance from  $-40^\circ\text{C}$  to  $125^\circ\text{C}$ .

**Note 5:** Thermal resistance varies with the amount of PC board metal connected to the package. The specified values are for short traces connected to the leads.

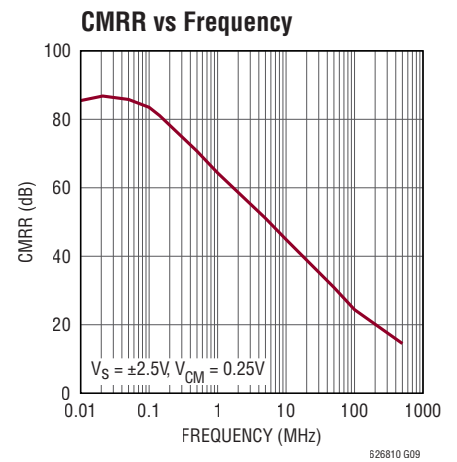
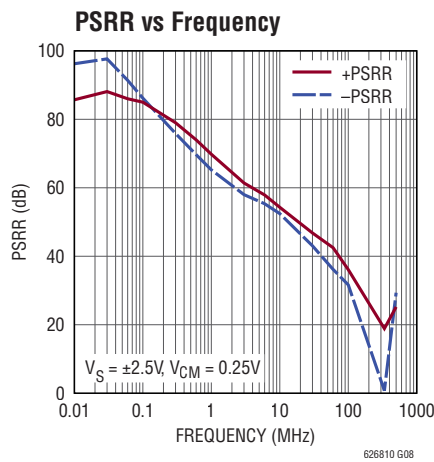
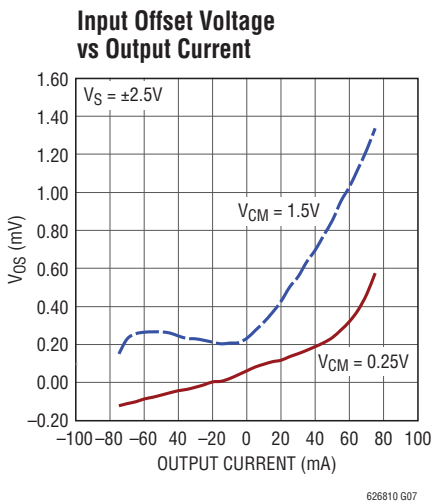
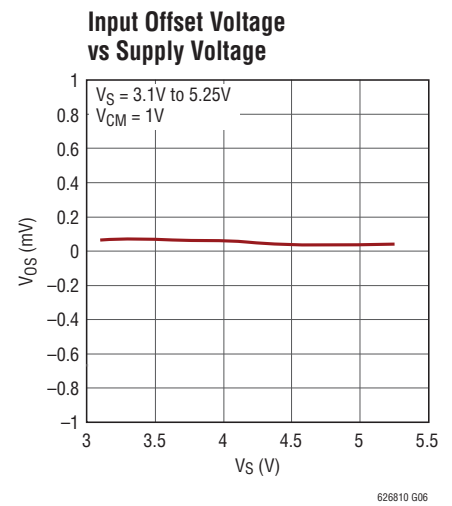
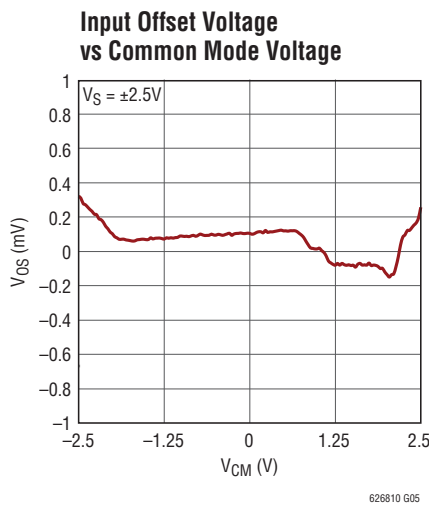
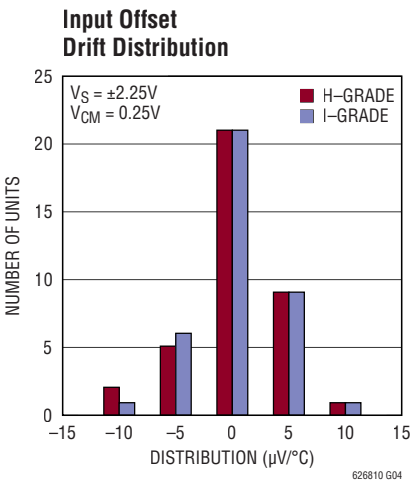
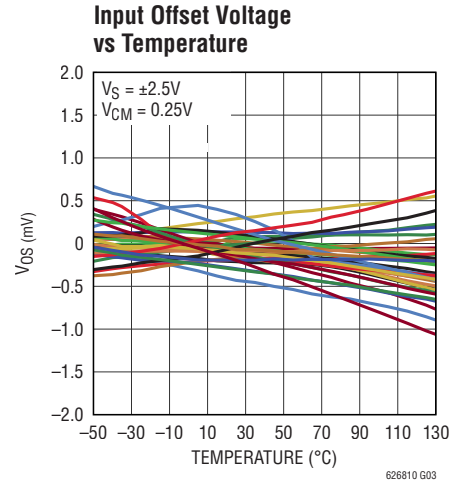
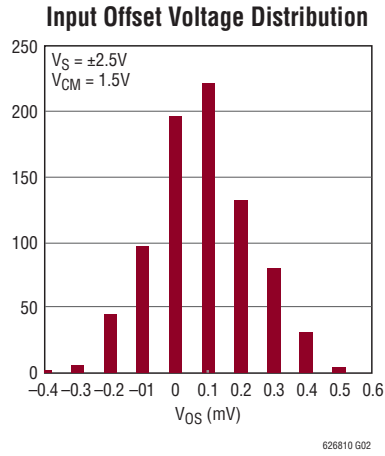
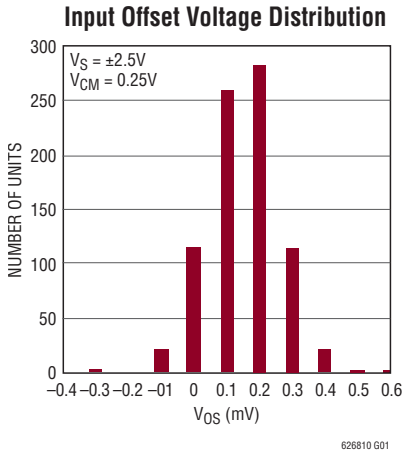
**Note 6:** The input bias current is the average of the currents into the positive and negative input pins. Typical measurement is for S8 package.

**Note 7:** Full Power Bandwidth is determined from distortion performance in a gain-of-10 configuration with  $\text{HD2/HD3} < -40\text{dB}$  (1%) as the criteria for a valid output.

**Note 8:** This parameter is specified by design and/or characterization and is not tested in production.

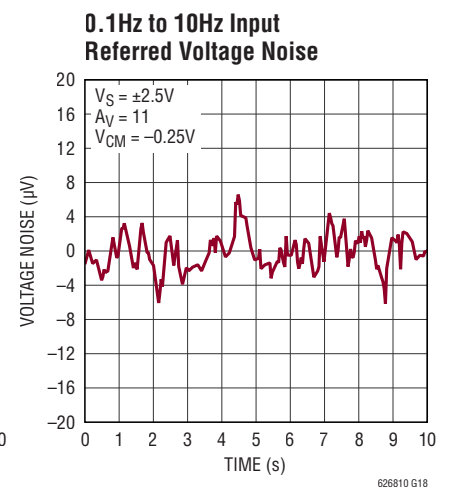
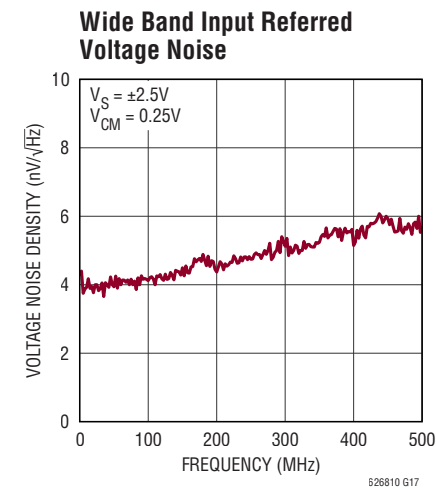
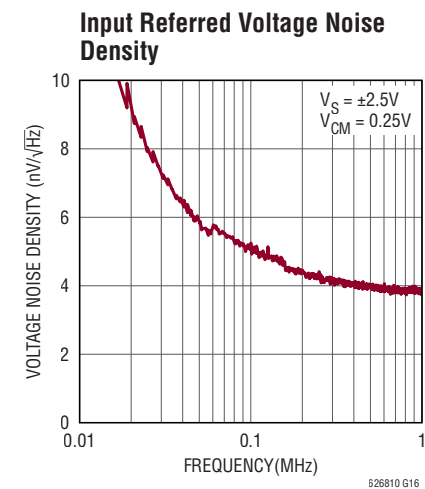
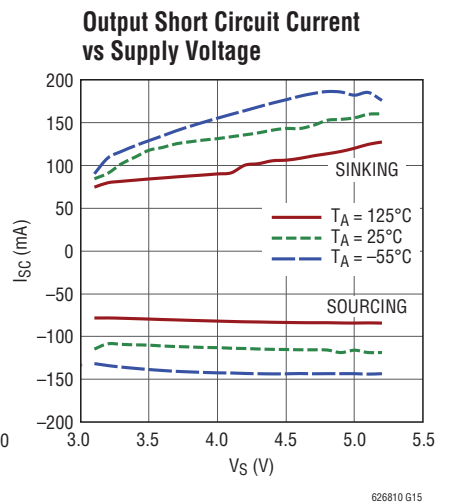
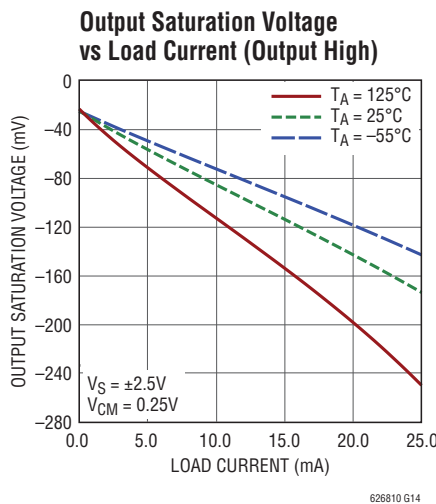
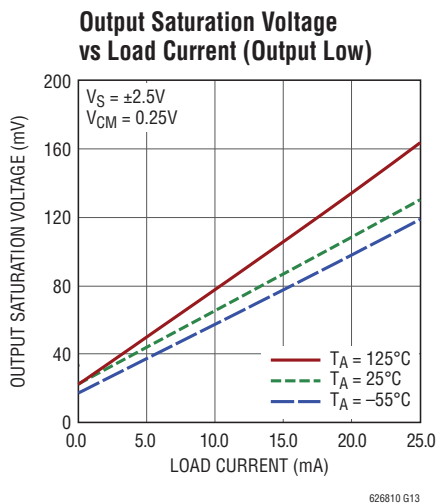
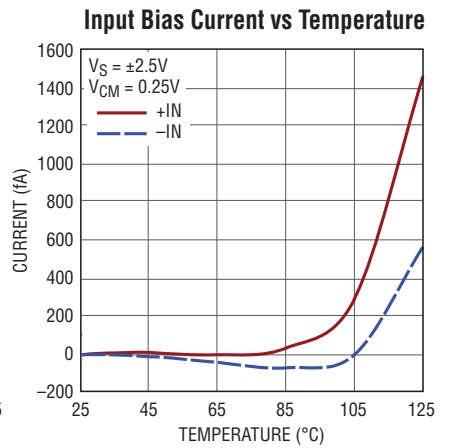
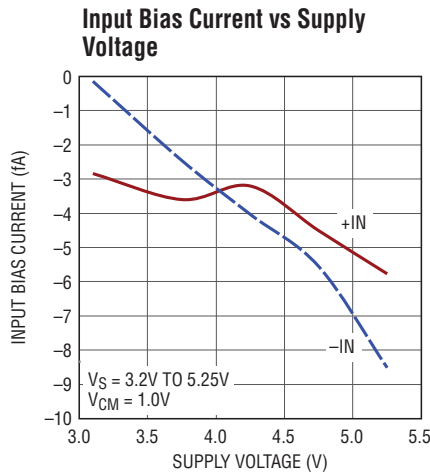
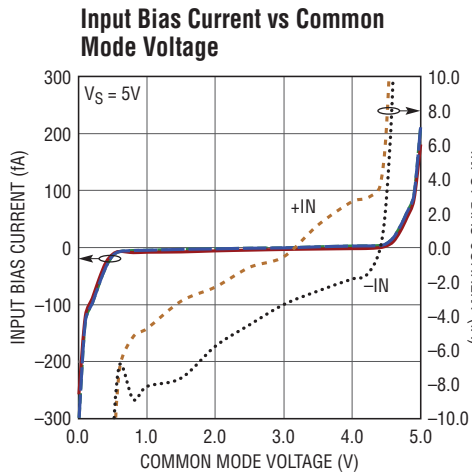
**Note 9:** The LTC6268-10/LTC6269-10 is capable of producing peak output currents in excess of 135mA. Current density limitations within the IC require the continuous current supplied by the output (sourcing or sinking) over the operating lifetime of the part be limited to under 135mA (Absolute Maximum).

**TYPICAL PERFORMANCE CHARACTERISTICS**  $T_A = 25^\circ\text{C}$ , unless otherwise noted.



# LTC6268-10/LTC6269-10

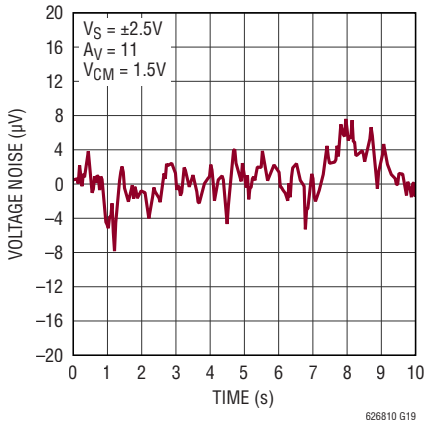
## TYPICAL PERFORMANCE CHARACTERISTICS $T_A = 25^\circ\text{C}$ , unless otherwise noted.



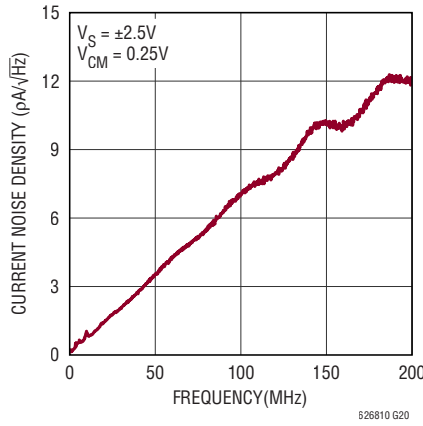
626810f

**TYPICAL PERFORMANCE CHARACTERISTICS**  $T_A = 25^\circ\text{C}$ , unless otherwise noted.

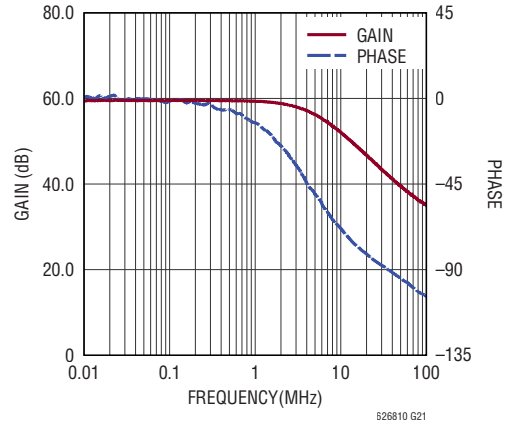
**0.1Hz to 10Hz Input Referred Voltage Noise**



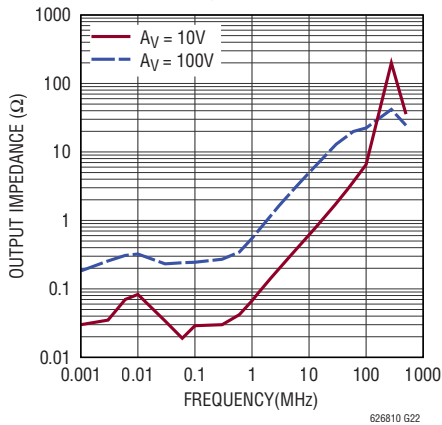
**Input Referred Current Noise**



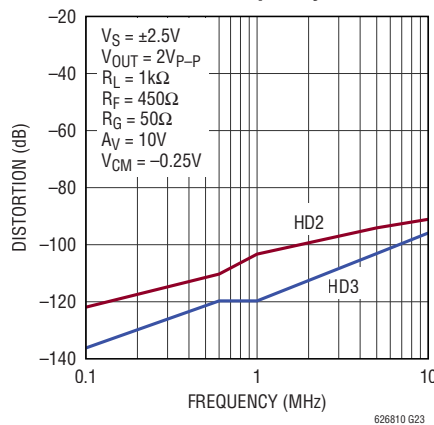
**Gain/Phase vs Frequency**



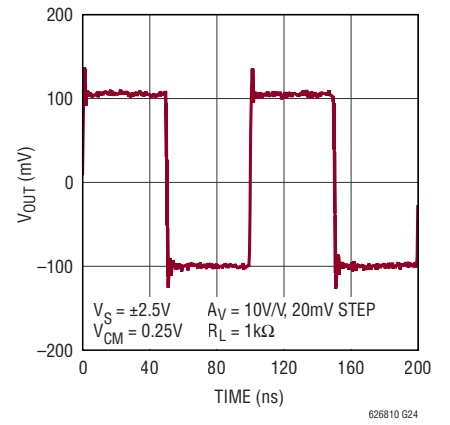
**Output Impedance vs Frequency**



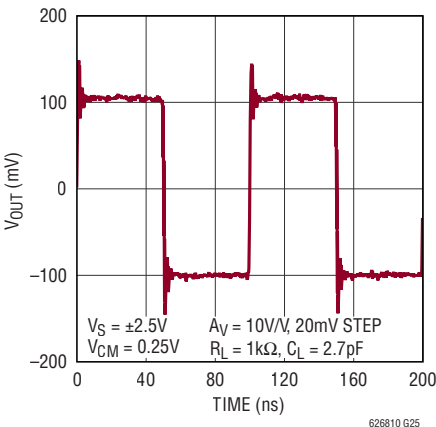
**Harmonic Distortion vs Frequency**



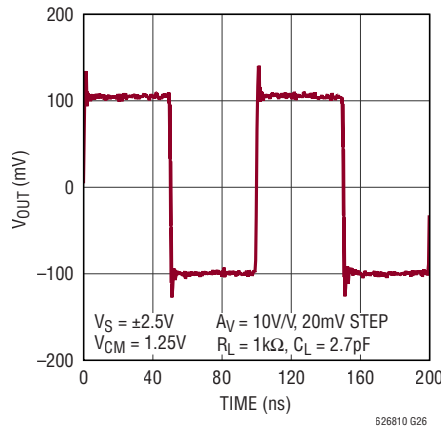
**Small Signal Step Response**



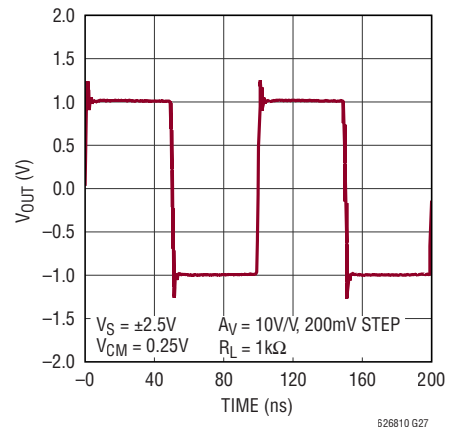
**Small Signal Step Response**



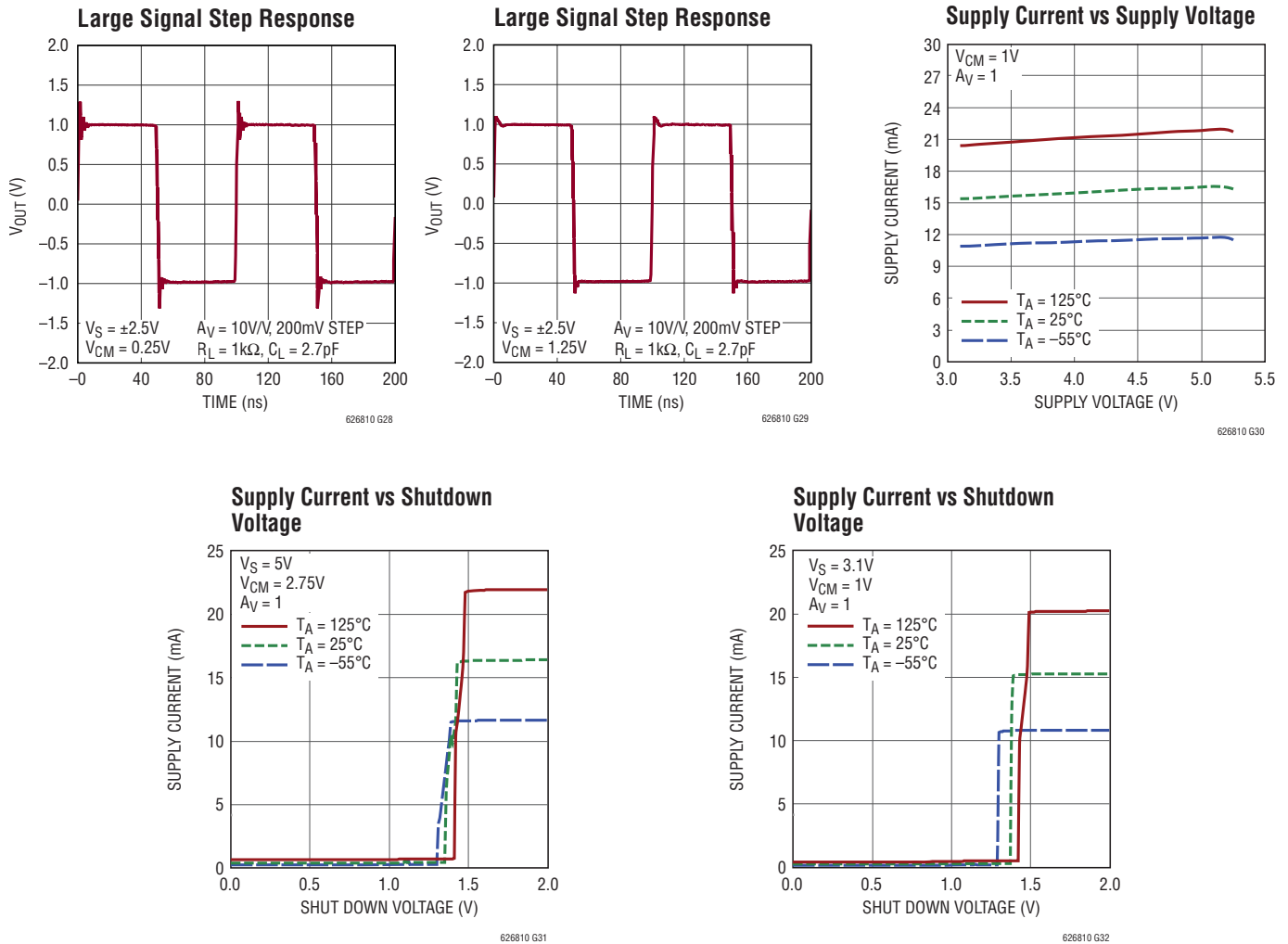
**Small Signal Step Response**



**Large Signal Step Response**



## TYPICAL PERFORMANCE CHARACTERISTICS T<sub>A</sub> = 25°C, unless otherwise noted.



## PIN FUNCTIONS

**-IN:** Inverting Input of the Amplifier. The voltage range of this pin is from  $V^-$  to  $V^+ - 0.5V$ .

**+IN:** Non-Inverting Input. The voltage range of this pin is from  $V^-$  to  $V^+ - 0.5V$ .

**V<sup>+</sup>:** Positive Power Supply. Total supply ( $V^+ - V^-$ ) voltage is from 3.1V to 5.25V. Split supplies are possible as long as the total voltage between  $V^+$  and  $V^-$  is between 3.1V and 5.25V. A bypass capacitor of 0.1 $\mu$ F should be used between  $V^+$  to ground as close to the pin as possible.

**V<sup>-</sup>:** Negative Power Supply. Normally tied to ground, it can also be tied to a voltage other than ground as long

as the voltage difference between  $V^+$  and  $V^-$  is between 3.1V and 5.25V. If it is not connected to ground, bypass it to ground with a capacitor of 0.1 $\mu$ F as close to the pin as possible.

**SHDN, SDA, SDB:** Active Low op amp shutdown, threshold is 0.75V above the negative supply,  $V^-$ . If left unconnected, the amplifier is enabled.

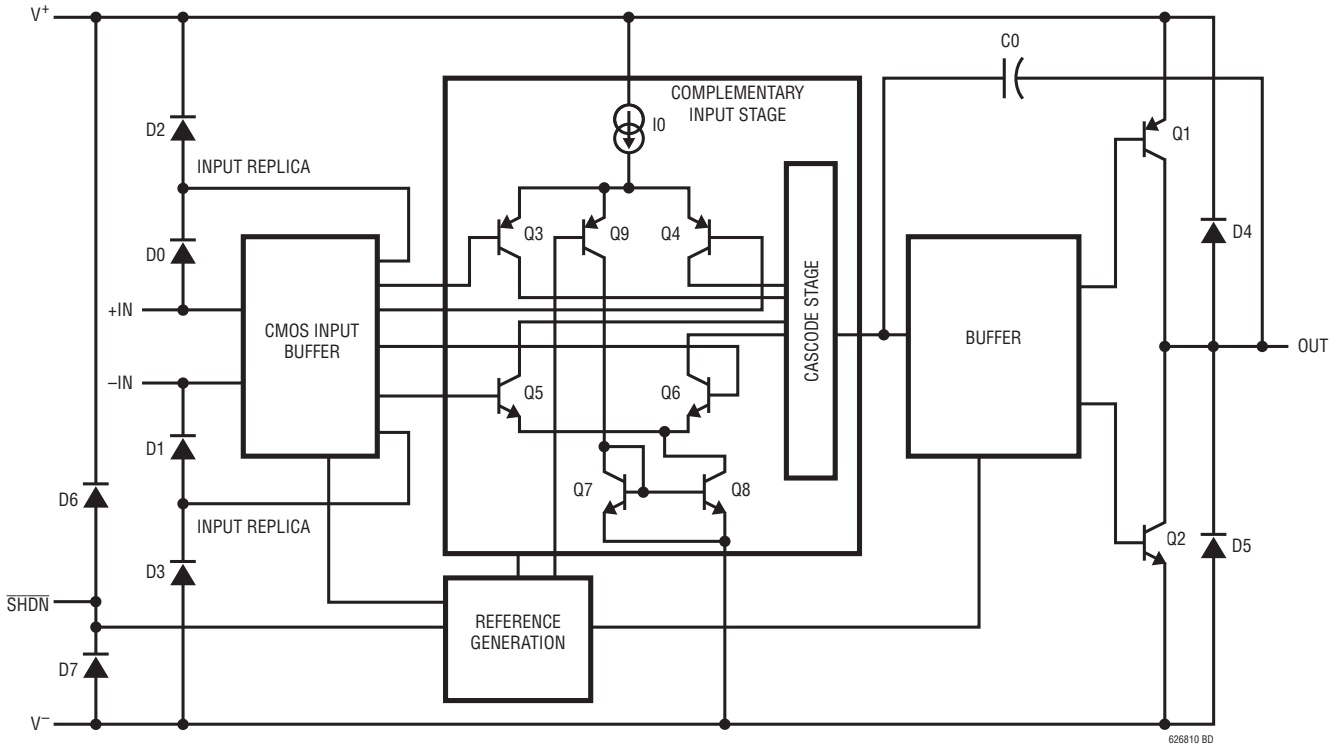
**OUT:** Amplifier Output.

**NC:** Not connected. May be used to create a guard ring around the input to guard against board leakage currents. See Applications Information section for more details.

626810f

**SIMPLIFIED SCHEMATIC**

LTC6268-10 Simplified Schematic Diagram



(ONE POLARITY SHOWN IN INPUT PINS)

# LTC6268-10/LTC6269-10

## OPERATION

The LTC6268-10/LTC6269-10 input signal range is specified from the negative supply to 0.5V below the positive power supply, while the output can swing from rail-to-rail. The schematic above depicts a simplified schematic of the amplifier.

The input pins drive a CMOS buffer stage. The CMOS buffer stage creates replicas of the input voltages to boot strap the protection diodes. In turn, the buffer stage drives a complementary input stage consisting of two differential

amplifiers, active over different ranges of input common mode voltage. The main differential amplifier is active with input common mode voltages from the negative power supply to approximately 1.55V below the positive supply, with the second amplifier active over the remaining range to 0.5V below the positive supply rail. The buffer and output bias stage uses a special compensation technique ensuring stability of the op amp. The common emitter topology of output transistors Q1/Q2 enables the output to swing from rail-to-rail.

## APPLICATIONS INFORMATION

### Noise

To minimize the LTC6268-10's noise over a broad range of applications, careful consideration has been placed on input referred voltage noise ( $e_N$ ), input referred current noise ( $i_N$ ) and input capacitance  $C_{IN}$ .

For a transimpedance amplifier (TIA) application such as shown in Figure 1, all three of these op amp parameters, plus the value of feedback resistance  $R_F$ , contribute to noise behavior in different ways, and external components and traces will add to  $C_{IN}$ . It is important to understand the impact of each parameter independently. Input referred

voltage noise ( $e_N$ ) consists of flicker noise (or 1/f noise), which dominates at lower frequencies, and thermal noise which dominates at higher frequencies. For LTC6268-10, the 1/f corner, or transition between 1/f and thermal noise, is at 40kHz. The  $i_N$  and  $R_F$  contributions to input referred noise current at the minus input are relatively straight forward, while the  $e_N$  contribution is amplified by the noise gain. Because there is no gain resistor, the noise gain is calculated using feedback resistor ( $R_F$ ) in conjunction with impedance of  $C_{IN}$  as  $(1 + 2\pi R_F \cdot C_{IN} \cdot \text{Freq})$ , which increases with frequency. All of the contributions will be limited by the closed loop bandwidth. The equivalent input current noise is shown in Figure 2 and Figure 3, where  $e_N$  represents contribution from input referred voltage noise ( $e_N$ ),  $i_N$  represents contribution from input referred current noise ( $i_N$ ), and  $R_F$  represents contribution from feedback resistor ( $R_F$ ). TIA gain ( $R_F$ ) and capacitance at input ( $C_{IN}$ ) are also shown on each figure. Comparing Figure 2 and Figure 3,  $i_N$  dominates at higher frequencies. At lower frequencies, the  $R_F$  contribution dominates. Since average wide band  $e_N$  is  $4.0\text{nV}/\sqrt{\text{Hz}}$  (see typical performance characteristics),  $R_F$  contribution will become a lesser factor at lower frequencies if  $R_F$  is less than  $860\Omega$  as indicated by the following equation:

$$\frac{e_N/R_F}{\sqrt{4kT/R_F}} \geq 1$$

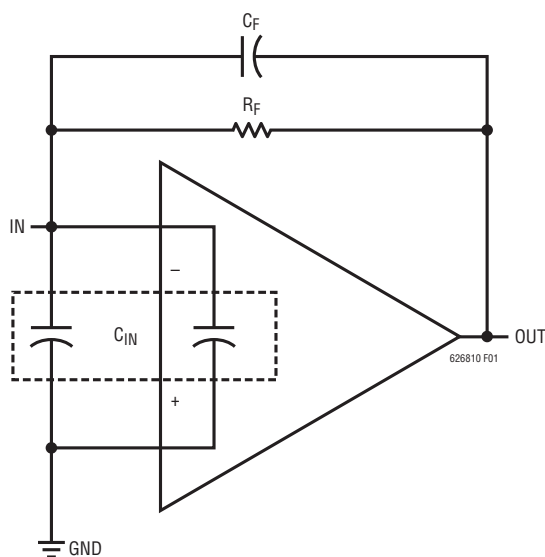


Figure 1. Simplified TIA Schematic

626810f

## APPLICATIONS INFORMATION

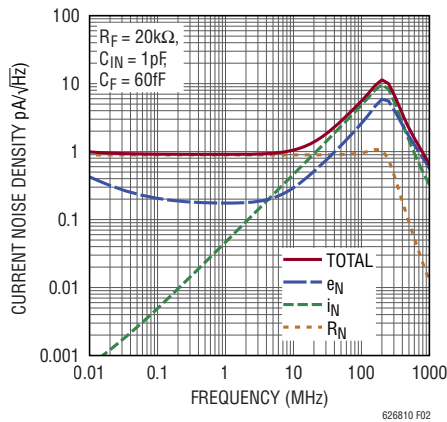


Figure 2

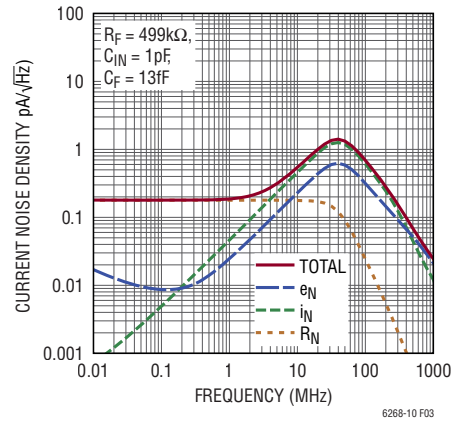


Figure 3

### Optimizing the Bandwidth for TIA Application

The capacitance at the inverting input node can cause amplifier stability problems if left unchecked. When the feedback around the op amp is resistive ( $R_F$ ), a pole will be created with  $R_F \parallel C_{IN}$ . This pole can create excessive phase shift and possibly oscillation. Referring to Figure 1, the response at the output is:

$$\frac{R_F}{1 + \frac{2\zeta s}{\omega} + \frac{s^2}{\omega^2}}$$

Where  $R_F$  is the DC gain of the TIA,  $\omega$  is the natural frequency of the closed loop, which can be expressed as:

$$\omega = \sqrt{\frac{2\pi\text{GBW}}{R_F(C_{IN} + C_F)}}$$

Hence the maximum achievable bandwidth of TIA is:

$$f_{TIA} \text{ (Hz)} = \sqrt{\frac{\text{GBW}}{2\pi R_F(C_{IN})}}$$

$\zeta$  is the damping factor of the loop, which can be expressed as:

$$\zeta = \frac{1}{2} \left( \sqrt{\frac{1}{2\pi\text{GBW} \cdot R_F(C_{IN} + C_F)}} + R_F \left( C_F + \frac{C_{IN} + C_F}{1 + A_0} \right) \cdot \sqrt{\frac{2\pi\text{GBW}}{R_F(C_{IN} + C_F)}} \right)$$

Where  $C_{IN}$  is the total capacitance at the inverting input node of the op amp, GBW is the gain bandwidth of the op amp, and  $A_0$  is the DC open loop gain of the op amp.

The small capacitor  $C_F$  in parallel with  $R_F$  can introduce enough damping to stabilize the loop. By assuming  $C_{IN} \gg C_F$ , the following condition needs to be met for  $C_F$ ,

$$C_F > \sqrt{\frac{C_{IN}}{\pi \cdot \text{GBW} \cdot R_F}}$$

Since LTC6268-10 is a decompensated op amp with gain-of-10 stable, it requires that  $C_{IN}/C_F \geq 10$ . Table 1 shows the minimum and maximum  $C_F$  for  $R_F$  of 20k and 402k and  $C_{IN}$  of 1pF and 5pF.

Table 1. Min/Max  $C_F$

$R_F$	$C_{IN} = 1\text{pF}$	$C_{IN} = 5\text{pF}$
20k $\Omega$	60fF/100fF	140fF/500fF
402k $\Omega$	13fF/100fF	31fF/500fF

## APPLICATIONS INFORMATION

### Achieving Higher Bandwidth with Higher Gain TIAs

Good layout practices are essential to achieving best results from a TIA circuit. The following two examples show drastically different results from an LTC6268-10 in a 402k TIA. (See Figure 4.) The first example is with an 0805 resistor in a basic circuit layout. In a simple layout, without expending a lot of effort to reduce feedback capacitance, the rise time achieved is about 87ns (Figure 5), implying a bandwidth of 4MHz ( $BW = 0.35/t_r$ ). In this case, the bandwidth of the TIA is limited not by the GBW of the LTC6268-10, but rather by the fact that the feedback capacitance is reducing the actual feedback impedance (the TIA gain itself) of the TIA. Basically, it's a resistor bandwidth limitation. The impedance of the 402kΩ is being reduced by its own parasitic capacitance at high frequency. From the 4MHz bandwidth and the 402k low frequency gain, we can estimate the total feedback capacitance as  $C = 1/(2\pi \cdot 4\text{MHz} \cdot 402\text{k}\Omega) = 0.1\text{pF}$ . That's fairly low, but it can be reduced further.

With some extra layout techniques to reduce feedback capacitance, the bandwidth can be increased. Note that

we are increasing the effective “bandwidth” of the 402k resistance. A very powerful method to reduce feedback capacitance is to shield the E field paths that give rise to the capacitance. In this particular case, the method is to place a ground trace between the resistor pads. Such a ground trace shields the output field from getting to the summing node end of the resistor and effectively shunts the field to ground instead. The trace increases the output load capacitance very slightly. See Figure 6 for a pictorial representation.

Figure 7 shows the dramatic increase in bandwidth simply by careful attention to low capacitance methods around the feedback resistance. Bandwidth and rise time went from 4MHz (87ns) to 34MHz (10.3ns), a factor of 8. The ground trace used for LTC6268-10 was much wider than that used in the case of the LTC6268 (see LTC6268 data sheet), extending under the entire resistor dielectric. Assuming all the bandwidth limit is due to feedback capacitance (which isn't fair), we can calculate an upper limit of  $C_f = 1/(2\pi \cdot 402\text{k}\Omega \cdot 34\text{MHz}) = 11.6\text{fF}$ .

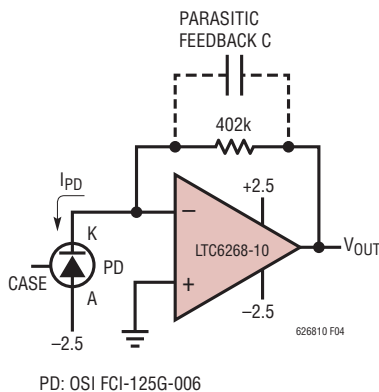


Figure 4. LTC6268-10 and Low Capacitance Photodiode in a 402kΩ TIA

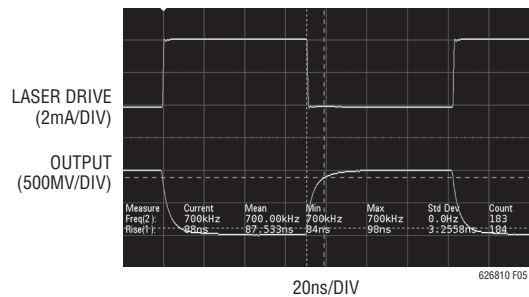
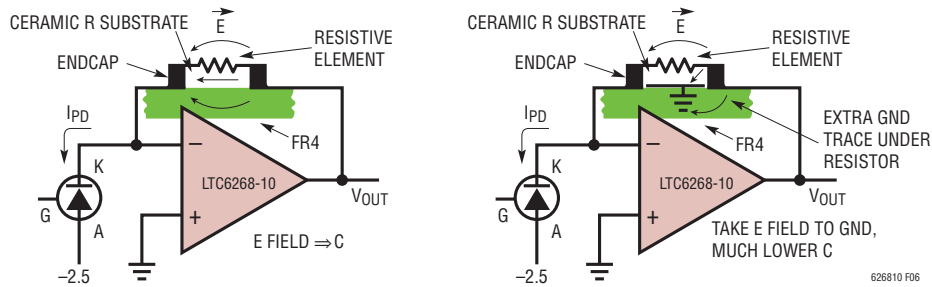


Figure 5. Time Domain Response of 402kΩ TIA without Extra Effort to Reduce Feedback Capacitance. Rise Time Is 87ns and BW Is 4MHz

## APPLICATIONS INFORMATION



**Figure 6. A Normal Layout at Left and a Field-Shunting Layout at Right. Simply Adding a Ground Trace Under the Feedback Resistor Does Much to Shunt Field Away from the Feedback Side and Dumps It to Ground. Note That the Dielectric Constant of Fr4 and Ceramic Is Typically 4, so Most of the Capacitance Is in the Solids and Not Through the Air. Feedback C is Reduced from 100fF at Left to 11.6fF at Right**

### Maintaining Ultralow Input Bias Current

Leakage currents into high impedance signal nodes can easily degrade measurement accuracy of fA signals. High temperature applications are especially susceptible to these issues. For humid environments, surface coating may be necessary to provide a moisture barrier.

There are several factors to consider in a low input bias current circuit. At the femtoamp level, leakage sources can come from unexpected sources including adjacent signals on the PCB, both on the same layer and from internal layers, any form of contamination on the board from the assembly process or the environment, other components on the signal path and even the plastic of the device package. Care taken in the design of the system can mitigate these sources and achieve excellent performance.

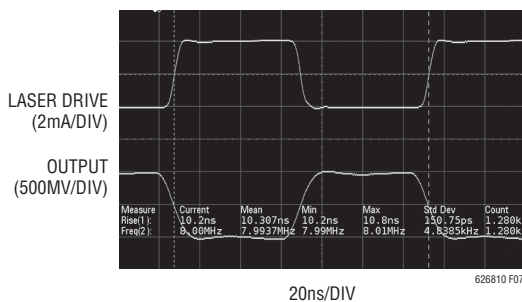


**Figure 7. LTC6268-10 in a 402kΩ TIA with Extra Layout Effort to Reduce Feedback Capacitance Achieves 10.3ns Total System Rise Time, or 34MHz Total System Bandwidth**

The choice of device package should be considered because although each has the same die internally, the pin spacing and adjacent signals influence the input bias current. The LTC6268-10/LTC6269-10 is available in SOIC, MSOP, DFN and SOT-23 packages. Of these, the SOIC has been designed as the best choice for low input bias current. It has the largest lead spacing which increases the impedance of the package plastic and the pinout is such that the two input pins are isolated on the far side of the package from the other signals. The gull-wing leads on this package also allow for better cleaning of the PCB and reduced contamination-induced leakage. The other packages have advantages in size and pin count but do so by reducing the input isolation. Leadless packages such as the DFN offer the minimum size but have the smallest pin spacing and may trap contaminants under the package.

The material used in the construction of the PCB can sometimes influence the leakage characteristics of the design. Exotic materials such as Teflon can be used to improve leakage performance in specific cases but they are generally not necessary if some basic rules are applied in the design of conventional FR4 PCBs. It is important to keep the high impedance signal path as short as possible on the board. A node with high impedance is susceptible to picking up any stray signals in the system so keeping it as short as possible reduces this effect. In some cases, it may be necessary to have a metallic shield over this portion of the circuit. However, metallic shielding increases capacitance. Another technique for avoiding leakage paths is to cut slots in the PCB. High impedance circuits are also

## APPLICATIONS INFORMATION

susceptible to electrostatic as well as electromagnetic effects. The static charge carried by a person walking by the circuit can induce an interference on the order of 100's of femtoamps. A metallic shield can reduce this effect as well.

The layout of a high impedance input node is very important. Other signals should be routed well away from this signal path and there should be no internal power planes under it. The best defense from coupling signals is distance and this includes vertically as well as on the surface. In cases where the space is limited, slotting the board around the high impedance input nodes can provide additional isolation and reduce the effect of contamination. In electrically noisy environments the use of driven guard rings around these nodes can be effective (see Figure 8). Adding any additional components such as filters to the high impedance input node can increase leakage. The leakage current of a ceramic capacitor is orders of magnitude larger than the bias current of this device. Any filtering will need to be done after this first stage in the signal chain.

### Driving Capacitive Load

The layout of the output node is also very important since LTC6268-10/LTC6269-10 is very sensitive to capacitive loading due to the very high gain-bandwidth-product. Appreciable ringing will be observed when capacitive loading is more than 5pF.

### Low Input Offset Voltage

The LTC6268-10 has a maximum offset voltage of  $\pm 2.5\text{mV}$  (PNP region) over temperature. The low offset voltage is essential for precision applications. There are 2 different input stages that are used depending on the input common mode voltage. To increase the versatility of the LTC6268-10, the offset voltages are trimmed for both regions of operation.

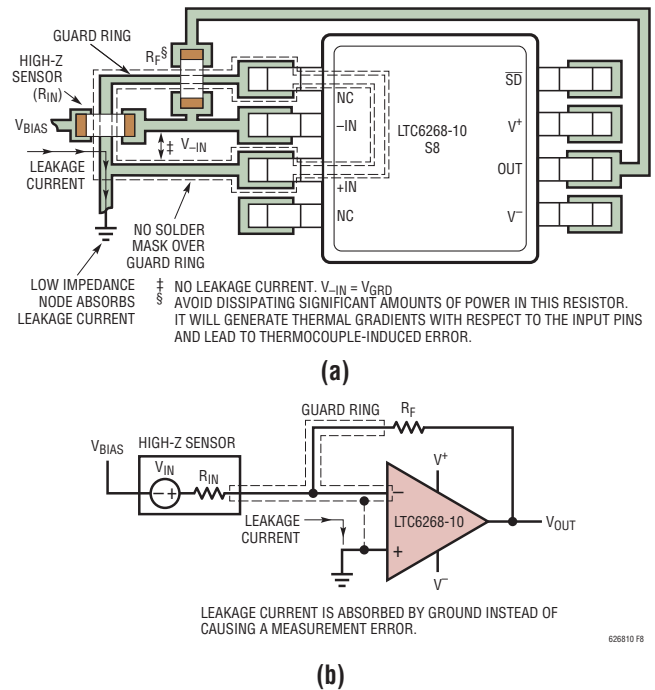


**Figure 8. Example Layout of Inverting Amplifier (or Transimpedance) with Leakage Guard Ring**

### Rail-to-Rail Output

The LTC6268-10 has a rail-to-rail output stage that has excellent output drive capability. It is capable of delivering over  $\pm 40\text{mA}$  of output drive current over temperature. Furthermore, the output can reach within 200mV of either rail while driving  $\pm 10\text{mA}$ . Attention must be paid to keep the junction temperature of the IC below 150°C.

### Input Protection

To prevent breakdown of internal devices in the input stage, the two op amp inputs should NOT be separated by more than 2.0V. To help protect the input stage, internal circuitry will engage automatically if the inputs are separated by  $>2.0\text{V}$  and input currents will begin to flow. In all cases, care should be taken so that these currents remain less than 1mA. Additionally, if only one input is driven, internal circuitry will prevent any breakdown condition under

## APPLICATIONS INFORMATION

transient conditions. The worst-case differential input voltage usually occurs when the +input is driven and the output is accidentally shorted to ground while in a unity gain configuration.

### ESD

ESD Protection devices can be seen in the simplified schematic. The +IN and -IN pins use a sophisticated method of ESD protection that incorporates a total of 4 reverse-biased diodes connected as 2 series diodes to each rail. To maintain extremely low input bias currents, the center node of each of these series diode chains is driven by a buffered copy of the input voltage. This maintains the two diodes connected directly to the input pins at low reverse bias, minimizing leakage current of these ESD diodes to the input pins.

The remaining pins have traditional ESD protection, using reverse-biased ESD diodes connected to each power supply rail. Care should be taken to make sure that the voltages on these pins do not exceed the supply voltages by more than 100mV or these diodes will begin to conduct large amounts of current.

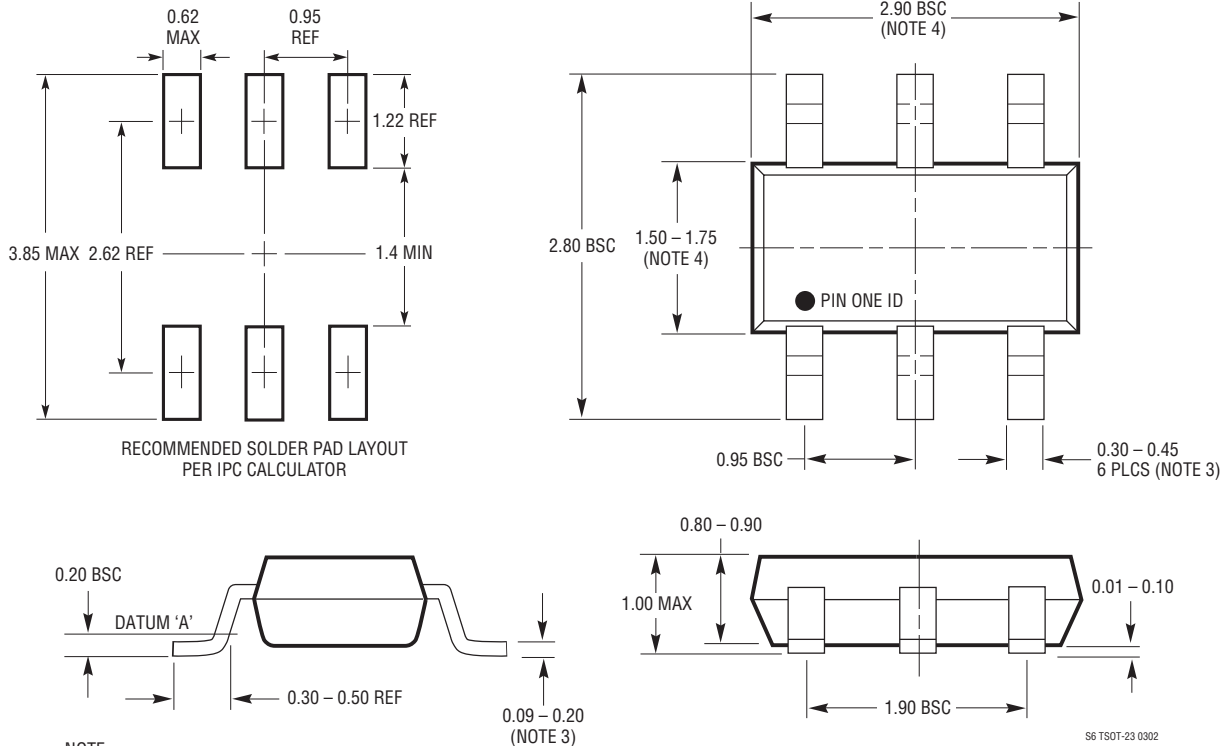
### Shutdown

The LTC6268-10S6, LTC6268-10S8, and LTC6268-10DD have  $\overline{\text{SHDN}}$  pins that can shut down the amplifier to less than 1.2mA supply current per amplifier. The  $\overline{\text{SHDN}}$  pin voltage needs to be within 0.75V of  $V^-$  for the amplifier to shut down. During shutdown, the output will be in a high output resistance state, so the LTC6268-10 is suitable for multiplexer applications. The internal circuitry is kept in a low current active state for fast recovery. When left floating, the  $\overline{\text{SHDN}}$  pin is internally pulled up to the positive supply and the amplifier is enabled.

## PACKAGE DESCRIPTION

Please refer to <http://www.linear.com/designtools/packaging/> for the most recent package drawings.

**S6 Package**  
**6-Lead Plastic TSOT-23**  
 (Reference LTC DWG # 05-08-1636)



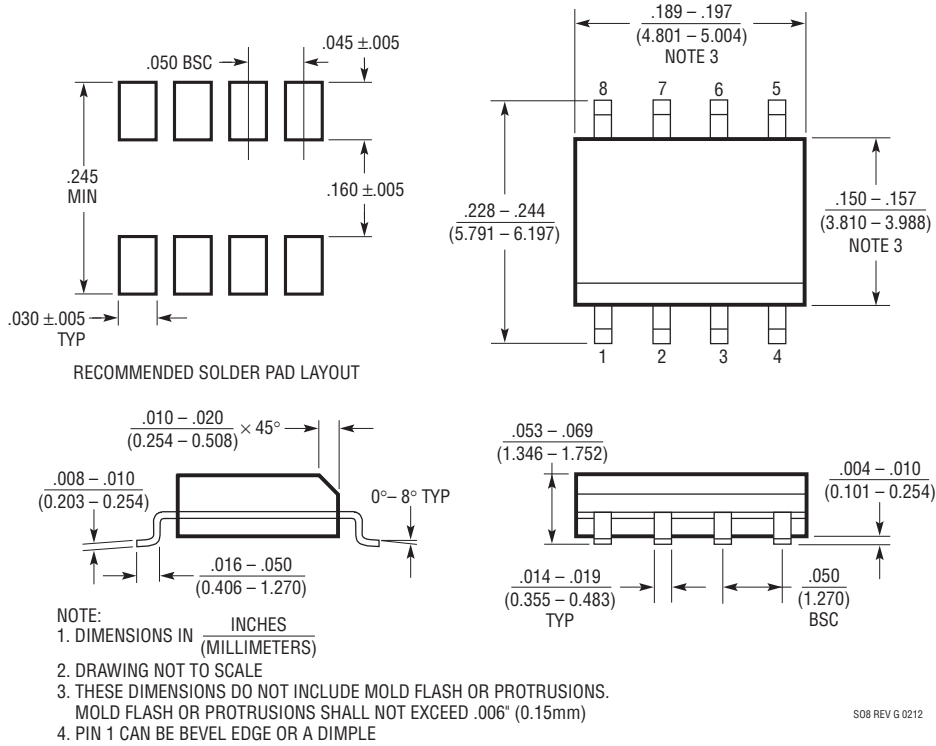
- NOTE:
1. DIMENSIONS ARE IN MILLIMETERS
  2. DRAWING NOT TO SCALE
  3. DIMENSIONS ARE INCLUSIVE OF PLATING
  4. DIMENSIONS ARE EXCLUSIVE OF MOLD FLASH AND METAL BURR
  5. MOLD FLASH SHALL NOT EXCEED 0.254mm
  6. JEDEC PACKAGE REFERENCE IS MO-193

S6 TSOT-23 0302

## PACKAGE DESCRIPTION

Please refer to <http://www.linear.com/designtools/packaging/> for the most recent package drawings.

### S8 Package 8-Lead Plastic Small Outline (Narrow .150 Inch) (Reference LTC DWG # 05-08-1610 Rev G)

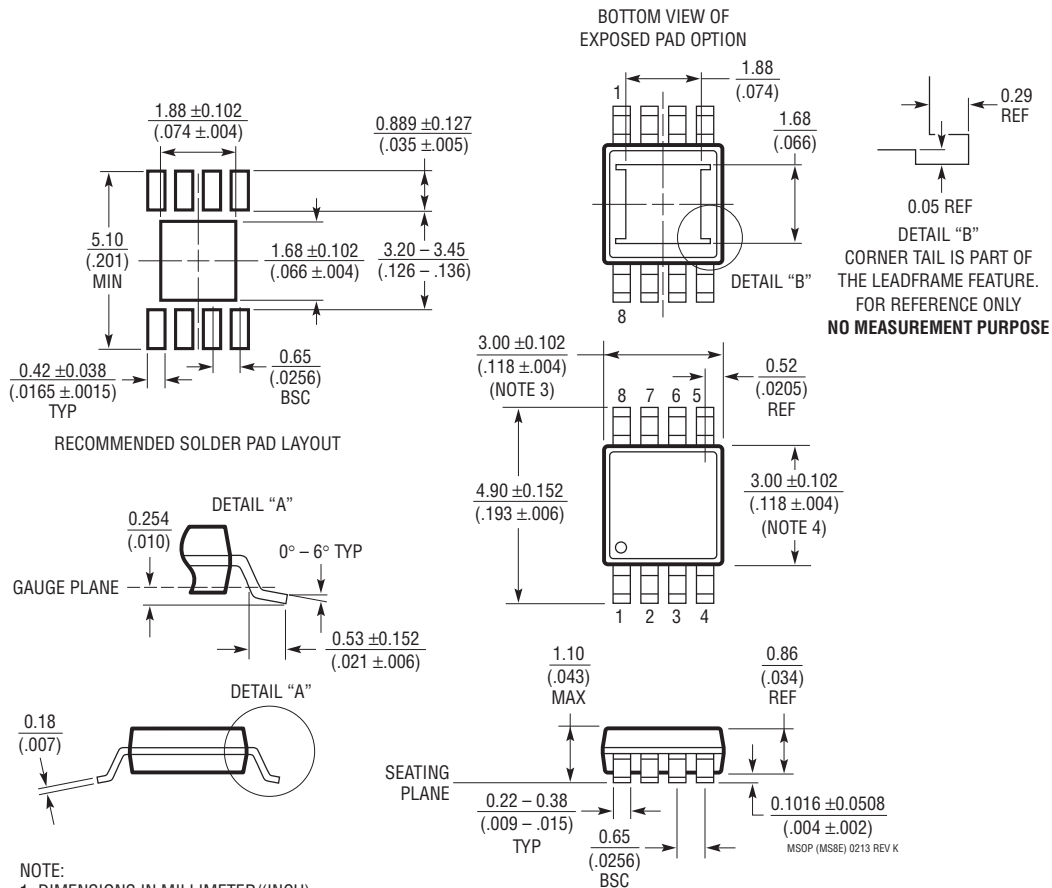


# LTC6268-10/LTC6269-10

## PACKAGE DESCRIPTION

Please refer to <http://www.linear.com/designtools/packaging/> for the most recent package drawings.

### MS8E Package 8-Lead Plastic MSOP, Exposed Die Pad (Reference LTC DWG # 05-08-1662 Rev K)



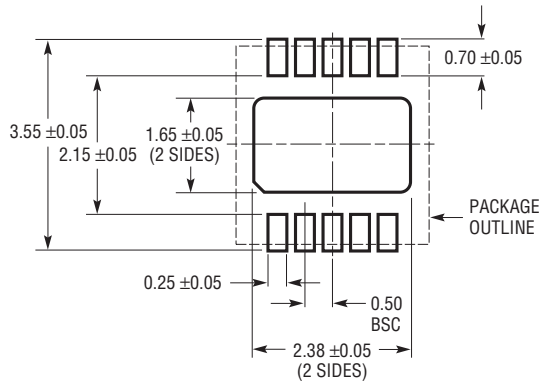
- NOTE:
1. DIMENSIONS IN MILLIMETER/(INCH)
  2. DRAWING NOT TO SCALE
  3. DIMENSION DOES NOT INCLUDE MOLD FLASH, PROTRUSIONS OR GATE BURRS. MOLD FLASH, PROTRUSIONS OR GATE BURRS SHALL NOT EXCEED 0.152mm (.006") PER SIDE
  4. DIMENSION DOES NOT INCLUDE INTERLEAD FLASH OR PROTRUSIONS. INTERLEAD FLASH OR PROTRUSIONS SHALL NOT EXCEED 0.152mm (.006") PER SIDE
  5. LEAD COPLANARITY (BOTTOM OF LEADS AFTER FORMING) SHALL BE 0.102mm (.004") MAX
  6. EXPOSED PAD DIMENSION DOES INCLUDE MOLD FLASH. MOLD FLASH ON E-PAD SHALL NOT EXCEED 0.254mm (.010") PER SIDE.

626810f

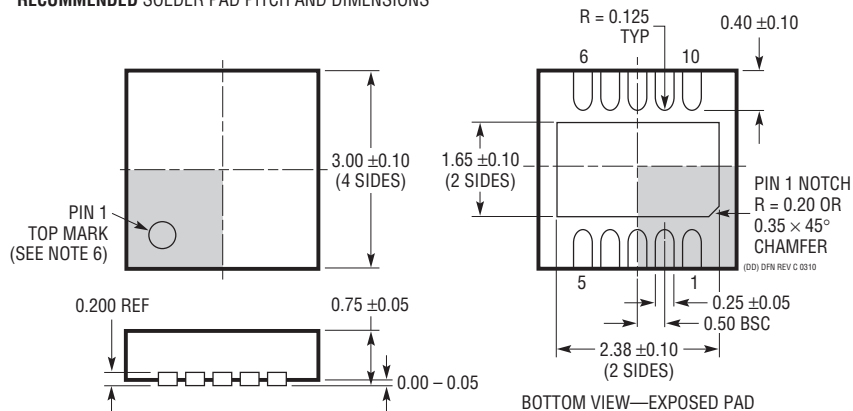
## PACKAGE DESCRIPTION

Please refer to <http://www.linear.com/designtools/packaging/> for the most recent package drawings.

### DD Package 10-Lead Plastic DFN (3mm × 3mm) (Reference LTC DWG # 05-08-1699 Rev C)



#### RECOMMENDED SOLDER PAD PITCH AND DIMENSIONS



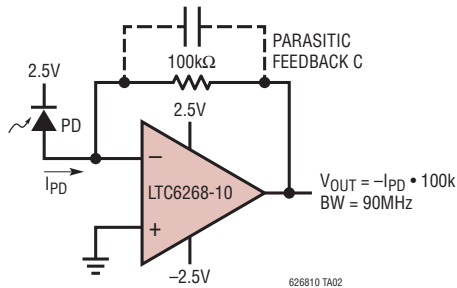
#### NOTE:

1. DRAWING TO BE MADE A JEDEC PACKAGE OUTLINE M0-229 VARIATION OF (WEED-2). CHECK THE LTC WEBSITE DATA SHEET FOR CURRENT STATUS OF VARIATION ASSIGNMENT
2. DRAWING NOT TO SCALE
3. ALL DIMENSIONS ARE IN MILLIMETERS
4. DIMENSIONS OF EXPOSED PAD ON BOTTOM OF PACKAGE DO NOT INCLUDE MOLD FLASH. MOLD FLASH, IF PRESENT, SHALL NOT EXCEED 0.15mm ON ANY SIDE
5. EXPOSED PAD SHALL BE SOLDER PLATED
6. SHADED AREA IS ONLY A REFERENCE FOR PIN 1 LOCATION ON THE TOP AND BOTTOM OF PACKAGE

# LTC6268-10/LTC6269-10

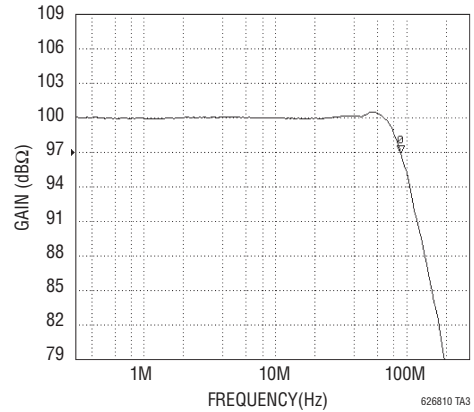
## TYPICAL APPLICATION

### 100kΩ Gain 90MHz Transimpedance Amplifier



PD = OSI OPTOELECTRONICS, FCI-125G-006  
 OUTPUT NOISE = 20mV<sub>r,p</sub> MEASURED ON A 100MHz BW

### 100kΩ TIA Frequency Response



## RELATED PARTS

PART NUMBER	DESCRIPTION	COMMENTS
<b>Op Amps</b>		
<a href="#">LTC6268/LTC6269</a>	500MHz Ultra-Low Bias Current FET Input Op Amp	Unity Gain Stable, Ultra Low Input Bias Current (3fA), 500MHz GBW
<a href="#">LTC6244</a>	Dual 50MHz, Low Noise, Rail-to-Rail, CMOS Op Amp	Unity Gain Stable, 1pA Input Bias Current, 100μV Max Offset.
<a href="#">LTC6240/LTC6241/LTC6242</a>	18MHz, Low Noise, Rail-to-Rail Output, CMOS Op Amp	18MHz GBW, 0.2pA Input Current, 125μV Max Offset.
<a href="#">LTC6252/LTC6253/LTC6254</a>	720MHz, 3.5mA Power Efficient Rail-to-Rail I/O Op Amp	720MHz GBW, Unity Gain Stable, Low Noise
<a href="#">LTC6246/LTC6247/LTC6248</a>	180MHz, 1mA Power Efficient Rail-to-Rail I/O Op Amps	180MHz GBW, Unity Gain Stable, Low Noise
<a href="#">LT1818</a>	400MHz, 2500V/μs, 9mA Single Operational Amplifier	Unity Gain Stable, 6nV/√Hz Unity Gain Stable
<a href="#">LT6236</a>	215MHz, Rail-to-Rail Output, 1.1nV/√Hz, 3.5mA Op Amp Family	350μV Max Offset Voltage, 3V to 12.6V Supply
<a href="#">LT6411</a>	650MHz Differential ADC Driver/Dual Selectable Amplifier	SR 3300V/μs, 6ns 0.1% Settling.
<b>SAR ADC</b>		
<a href="#">LTC2376-18/LTC2377-18/LTC2378-18/LTC2379-18</a>	18-Bit, 250ksps to 1.6Msps, Low Power SAR ADC, 102dB SNR	18mW at 1.6Msps, 3.4μW at 250sps, -126dB THD.

626810f



# Bibliography

- [1] (2016) Basic practical nmr concepts. [Online]. Available: <https://www2.chemistry.msu.edu/facilities/nmr/handouts/DH%20NMR%20Basics.pdf>
- [2] (2016) Lc circuit. LCCircuit.jpg. [Online]. Available: [https://en.wiki2.org/wiki/LC\\_circuit](https://en.wiki2.org/wiki/LC_circuit)
- [3] (2016) Ophir 5085re. [Online]. Available: <http://www.atecorp.com/products/ophir.aspx>
- [4] A. Bakshi and U. Bakshi, *Electrical Circuit Analysis*. Technical Publications, 2008.
- [5] M. Billeter, G. Nijim, B. Yalvac, and A. Sahakian, “Laboratory Demonstration of Spatial Encoding in MRI,” *American Society for Engineering University*, 2006.
- [6] chegg.com. (2016) Helmholtz coil. helmholtzcoil.jpg. [Online]. Available: <http://www.chegg.com/homework-help/questions-and-answers/helmholtz-coils-two-identical-circular-coils-radius-r-number-turns-n-separated-distance-eq-q>
- [7] N. Dogan, “Development of halbach magnet for portable nmr device,” *Journal of Physics: Conference Series*, 2009.
- [8] M.-H. Education. (2000) Chapter 13: Spectroscopy. ProtonswBofield.jpg. [Online]. Available: <http://www.mhhe.com/physsci/chemistry/carey/student/olc/ch13nmr.html>
- [9] Gyroscope.com. (2016) Circular halbach array. halbachmagnet.jpg. [Online]. Available: <http://www.gyroscope.com/d.asp?product=CIRCULARHALBACH>
- [10] R. Hashemi, W. Bradley, and C. Lisanti, *MRI: The Basics*. Lippincott Williams and Wilkins, 2004.
- [11] S. Jie, Q. Liu, and Y. Gengying, “Home-built magnetic resonance imaging system(0.3T) with a complete digital spectrometer,” *Review of Scientific Instruments*, 2005.
- [12] J. Kirsch, “A pulse NMR experiment for an undergraduate physics laboratory,” *Physics Department, Massachusetts Institute of Technology, Cambridge MA*, Unknown.

- [13] I. Lowe and C. Tarr, "A fast recovery probe and receiver for pulsed nuclear magnetic resonance spectroscopy," *Review of Scientific Instruments*, pp. 320–322, 1968.
- [14] B. Manz, A. Coy, R. Dykstra, C. Eccles, M. Hunter, B. Parkinson, and P. Callaghan, "A mobile one-sided NMR sensor with a homogeneous magnetic field: The NMR Mole," *Journal of Magnetic Resonance*, vol. 183, no. 1, p. 2531, 2006.
- [15] E. Media. (2016) Q and bandwidth of a resonant circuit. [Online]. Available: <http://www.allaboutcircuits.com/textbook/alternating-current/chpt-6/q-and-bandwidth-resonant-circuit/>
- [16] J. Mispelter, M. Lupu, and A. Briguët, *NMR Probeheads for Biophysical and Biomedical Experiments*. Imperial College Press, 2006.
- [17] G. Moresi and R. Magin, "Miniature Permanent Magnet for Table-top NMR," *Journal of Magnetic Resonance*, vol. 19B, no. 1, p. 3543, 2003.
- [18] G. Pohost, G. Elgavish, and W. Evanochko, "Nuclear Magnetic Resonance Imaging: With or Without Nuclear?" *Journal of the American College of Cardiology*, vol. 7, no. 3, pp. 709–710, 1986.
- [19] O. RF. (2005) Ophir 5085re power amplifier.
- [20] I. Rosu. (2016) Understanding noise figure. [Online]. Available: <http://www.qsl.net/va3iul/Noise/Understanding%20Noise%20Figure.pdf>
- [21] A. Sahakian, C. Hayes, and B. Yalvac, "An Inexpensive Laboratory Module to Teach Principles of NMR/MRI," *American Society for Engineering Education Annual Conference and Exposition*, 2005.
- [22] H. Schild. (1990) Mri made easy. Protonsrfpulse.jpg. [Online]. Available: <http://image.slidesharecdn.com/mribrainimran-150107105636-conversion-gate01/95/mri-brain-basics-and-radiological-anatomy-10-638.jpg?cb=1420629033>
- [23] T. Sleator, "Pulsed nuclear magnetic resonance and spin echo," *Environmental Physics*, 2008.
- [24] S. Technologies. (2015) Radioprocessor g owners manual. [Online]. Available: [www.spincore.com](http://www.spincore.com)
- [25] s. Wright, D. Brown, J. Porter, D. Spence, E. Esperza, D. Cole, and R. Huson, "A desktop magnetic resonance imaging system," *Magnetic Resonance Materials in Physic Biology and Medicine*, vol. 13, pp. 177–185, 2002.